

# Constitutive equations for metals with an application to the extrusion of lead

**Citation for published version (APA):**

Wijngaarden, van, H. (1988). *Constitutive equations for metals with an application to the extrusion of lead*. [Phd Thesis 1 (Research TU/e / Graduation TU/e), Mechanical Engineering]. Technische Universiteit Eindhoven. <https://doi.org/10.6100/IR282369>

**DOI:**

[10.6100/IR282369](https://doi.org/10.6100/IR282369)

**Document status and date:**

Published: 01/01/1988

**Document Version:**

Publisher's PDF, also known as Version of Record (includes final page, issue and volume numbers)

**Please check the document version of this publication:**

- A submitted manuscript is the version of the article upon submission and before peer-review. There can be important differences between the submitted version and the official published version of record. People interested in the research are advised to contact the author for the final version of the publication, or visit the DOI to the publisher's website.
- The final author version and the galley proof are versions of the publication after peer review.
- The final published version features the final layout of the paper including the volume, issue and page numbers.

[Link to publication](#)

**General rights**

Copyright and moral rights for the publications made accessible in the public portal are retained by the authors and/or other copyright owners and it is a condition of accessing publications that users recognise and abide by the legal requirements associated with these rights.

- Users may download and print one copy of any publication from the public portal for the purpose of private study or research.
- You may not further distribute the material or use it for any profit-making activity or commercial gain
- You may freely distribute the URL identifying the publication in the public portal.

If the publication is distributed under the terms of Article 25fa of the Dutch Copyright Act, indicated by the "Taverne" license above, please follow below link for the End User Agreement:

[www.tue.nl/taverne](http://www.tue.nl/taverne)

**Take down policy**

If you believe that this document breaches copyright please contact us at:

[openaccess@tue.nl](mailto:openaccess@tue.nl)

providing details and we will investigate your claim.

**CONSTITUTIVE EQUATIONS FOR METALS**  
**WITH AN APPLICATION TO THE**  
**EXTRUSION OF LEAD**

Hans van Wijngaarden



# **CONSTITUTIVE RELATIONS FOR METALS WITH AN APPLICATION TO THE EXTRUSION OF LEAD**

PROEFSCHRIFT

ter verkrijging van de graad van doctor aan de Technische Universiteit Eindhoven, op  
gezag van de rector magnificus, prof.dr. F.N. Hooge, voor een commissie aangewezen  
door het college van dekanen in het openbaar te verdedigen op dinsdag 26 januari  
1988 te 16.00 uur

door

HANS VAN WIJNGAARDEN

geboren te Arnhem

Dit proefschrift is goedgekeurd door de promotoren:

Prof.dr.ir. J.D. Janssen

en

Prof.ir. F. Doorschot

Co-promotor: dr.ir. F.E. Veldpaus

Het onderzoek voor dit proefschrift werd grotendeels uitgevoerd in het Natuurkundig Laboratorium van de N.V. Philips Gloeilampen te Eindhoven.

voor Monique

# Table of Contents

<b>Abstract</b> .....	<b>1</b>
<b>General Introduction</b> .....	<b>2</b>
<b>1 Fundamental laws and constitutive principles</b> .....	<b>4</b>
1.1 Introduction .....	4
1.2 Some kinematical quantities .....	4
1.3 The fundamental laws .....	6
1.4 Some constitutive principles .....	9
1.5 Further simplifications .....	11
<b>2 Hidden variables</b> .....	<b>13</b>
2.1 Introduction .....	13
2.2 The consequences of the introduction of hidden variables .....	13
2.3 Isotropy .....	16
2.4 Elasticity and simple visco-elasticity .....	18
2.5 One hidden scalar .....	19
2.6 Generalized visco-elastic material behaviour .....	21
2.7 Elastic-plastic models with hardening .....	25
2.8 Materials of type N .....	29
2.9 Some final remarks .....	31
<b>3 The decomposition of constitutive equations</b> .....	<b>32</b>
3.1 Introduction .....	32
3.2 The decomposition of the deformation rate tensor .....	33
3.3 Rate type constitutive equations for elastic bodies .....	37
3.4 Some properties of elastic rate type relationships .....	40
3.5 The Oldroyd model .....	42
3.6 The Maxwell model .....	44
3.7 The Kelvin model .....	45
<b>4 The determination of material properties</b> .....	<b>48</b>
4.1 Introduction .....	48
4.2 The tension test .....	50

4.3 The torsion-tension test .....	59
4.4 The compression test .....	69
<b>5 The extrusion of lead .....</b>	<b>75</b>
5.1 Introduction .....	75
5.2 Thermocompression bonding .....	76
5.3 A model for thermocompression .....	77
5.4 The solution procedure .....	81
5.5 Preliminary results .....	86
<b>6 Discussion .....</b>	<b>92</b>
<b>References .....</b>	<b>94</b>
<b>Appendix A .....</b>	<b>98</b>
<b>Appendix B .....</b>	<b>100</b>
<b>Appendix C .....</b>	<b>102</b>
<b>Appendix D .....</b>	<b>104</b>
<b>Appendix E .....</b>	<b>106</b>
<b>Appendix F .....</b>	<b>109</b>
<b>Appendix G .....</b>	<b>111</b>
<b>Appendix H .....</b>	<b>113</b>
<b>Samenvatting .....</b>	<b>115</b>
<b>Curriculum vitae .....</b>	<b>116</b>
<b>Nawoord .....</b>	<b>117</b>

## List of Illustrations

Figure 1.	The simple shear test	47
Figure 2.	The tension test	49
Figure 3.	Necking of an aluminium bar	49
Figure 4.	The necking zone of a cylindrical bar	51
Figure 5.	Correction factor	52
Figure 6.	Several stages of a finite element analysis of the necking of	54
Figure 7.	The stress components in the necking zone ( $z = 0$ )	55
Figure 8.	Stress-strain curves	56
Figure 9.	Predicted shapes of the necking zone	56
Figure 10.	Cross-section of the experimental set-up of Galenkamp	57
Figure 11.	Photo of the set-up of Galenkamp	58
Figure 12.	Results of a tension test for an aluminium bar	59
Figure 13.	The torsion-tension test	60
Figure 14.	Photo of three torsion bars	62
Figure 15.	Results obtained from two torsion tests of lead	63
Figure 16.	Results obtained from two torsion tests of copper	64
Figure 17.	Elongation during a torsion test of two copper bars	65
Figure 18.	Shortening during a torsion test of two lead bars	66
Figure 19.	Results obtained from two torsion tests of lead	67
Figure 20.	Photo of the experimental set-up for torsion tests	68
Figure 21.	The compression test	68
Figure 22.	Results obtained from four compression tests of lead	70
Figure 23.	Results obtained from two compression tests of lead	72
Figure 24.	Results obtained from two compression tests of lead	73
Figure 25.	Results obtained from two compression tests of lead	74
Figure 26.	A thermocompression bond of lead (right) and aluminium (left)	77
Figure 27.	Compression and unloading of a ring	78
Figure 28.	Cross section of the upper half of the ring	79
Figure 29.	Several stress-strain rate curves	80
Figure 30.	Several elements with their nodal points for the velocity	83
Figure 31.	Compression of a ring with a rectangular cross-section	83
Figure 32.	Numerical and analytical results of the compression of a ring	84



Figure 33. Numerical and analytical results of the compression of a ring . . . . .	85
Figure 34. Convergence for different material properties . . . . .	86
Figure 35. :Deformation pattern at different height reductions for different . . . . .	88
Figure 36. Compression force for different material properties . . . . .	89
Figure 37. Axial stress during several stages of the compression phase . . . . .	89
Figure 38. Vector plots during several stages of the compression phase . . . . .	90
Figure 39. Axial stress during several stages of the unloading phase . . . . .	91

## **Abstract**

This thesis deals with constitutive equations for metals. Two theories with which the relationship between stresses and strains can be obtained are discussed. The first theory concerns the introduction of hidden variables. Special attention is given to the constraints that follow from the Clausius-Duhem inequality. The latter is also known as the second law of thermodynamics. Relationships for metals that are derived from this theory are models for metals, which are referred to as work and strain hardening materials and materials of type N. The second theory discusses the decomposition of stresses and strain rates. Special consideration is given to the relationship between stress rates and the elastic part of the deformation rate. It is proven that only a special class of stress rates can be used for this purpose. A comparison is made between the models obtained with both theories. Next two special cases that follow from the second theory are discussed: the Maxwell model for elastic-plastic materials and the Kelvin model for kinematic hardening materials. Three experimental set-ups with which material properties can be obtained are described: the tension test, including necking, a combined torsion-tension test, with special attention for pure torsion, and the compression test. Some experimental results are given. Finally, the set-up of a computer program for the extrusion of lead is discussed. A numerical method that can be used to solve all kind of constitutive equations for metals is described. Some results which have been recently obtained with this program are presented.

## General Introduction

In this thesis, the constitutive equations of metals are discussed. With regard to these equations, special attention is given to the relationships between stresses on the one hand and deformations and deformation rates on the other.

At the beginning of this century, the Levy-Von Mises relationships were put forward for this purpose. These relationships suggest that the stress is proportional to the deformation rate and that the proportionality factor may depend on the deformation and the deformation rate. In fact these relationships are a special case of the so-called Newton relationships for fluids. Hill (1950) gave an extension to this model. He considered the total deformation to consist of an elastic and a plastic part. The relationships he obtained are often referred to as the Prantl-Reuss relationships. Since then only minor changes have been proposed with respect to this model. Prager (1956), for instance, looked at non-isotropic hardening phenomena.

However, these relationships did not obey what is known as the principle of objectivity, which states that the constitutive relationships are not influenced by rigid body rotations. In order to overcome this problem, the so-called objective stress rates were introduced; these can be regarded as a kind of time derivative of the stress tensor. This objective stress rate was assumed to be proportional to the elastic part of the deformation rate. Also in the case of non-isotropic hardening the objective rates were introduced. In specific deformation patterns some of the new models, which obeyed the principle of objectivity, predicted a very strange stress response. These results led to an intense discussion in literature, as to which objective rate should be used.

The first 3 chapters of this thesis discuss two theories, with which constitutive relationships of metals can be obtained. The first theory contains the introduction of so-called hidden tensors, as discussed by De Groot in 1951. Some objective objective rates can be obtained directly from this theory. The other theory is actually similar to the way Hill (1950) obtained his relationships, because the starting point for this theory is the decomposition of the deformation rate into an elastic and a plastic (or viscous) part. It will be seen that the objective rate of the stress tensor, which is related to the

elastic part of the deformation rate, derives from the fact, that this relationship must be elastic in thermodynamical sense.

Apart from the two general theories about constitutive equations for metals, experiments have to be done to obtain the special material properties for each single metal. Three different experiments will be discussed, each with its own limitations. The tension test can be used for so-called strain hardening metals. An extension to the usual measurement techniques will be discussed, with which data from this test can be obtained during necking. However, this extension can only be used at room temperature. The torsion test can be used for all kind of metals at every temperature, but only at rather low strain rates. This limitation can be overcome by applying the compression test which, in turn, is only suitable for metals that show little any history dependent material behaviour.

Finally some of these theories are applied to the extrusion of lead. Within Philips thermocompression is used as a bonding technique. If lead is the bonding metal, then a difference in thermal expansion of the two bonded substrates can be tolerated, because of the creep and relaxation capability of lead. Lead is therefore a very attractive metal for bonding. To give an insight into the mechanical behaviour of the process an analysis has been made of the two stages, in which the bond is made: the compression and the unloading stage. The mechanical model is solved by using a finite element technique. Instead of using the displacements as variables in the numerical analysis, as is usual for plastic deformation processes, the velocities and pressures are the variables, for which a solution must be obtained. The solution technique is similar to that used in fluid dynamics.

# 1 Fundamental laws and constitutive principles

## 1.1 Introduction

The main quantities used in this work together with their notation, will be introduced in this chapter. First, some of the kinematical quantities in continuum mechanics will be discussed. Then, before introducing the fundamental balance laws in the field of thermomechanics, so-called state, constitutive and external variables will be defined, in terms of which the fundamental laws and the second law of thermodynamics are formulated. At the end of the subparagraph the second law will be discussed with special regard to the Clausius-Duhem inequality.

In subparagraph 1.2 some widely accepted constitutive principles are discussed, in particular the principle of objectivity and its consequences of this principle. This leads to a general expression for the constitutive equation.

In the last subparagraph two principles are discussed, from which classes of constitutive behaviour can be deduced. These principles concern the introduction of so-called hidden tensors and the decomposition of the stress and strain rate.

## 1.2 Some kinematical quantities

In continuum mechanics a real body is considered to consist of an infinite set of material points. Each of these points can be uniquely identified by a column  $\xi$  of three material coordinates, one for each dimension. Let  $x(\xi, t)$  be the current (i.e. at time  $t$ ) position vector of some point with identification column  $\xi$ , measured with respect to a fixed origin. It is assumed in the continuum's theory, that  $x(\xi, t)$  is continuous and can be differentiated with respect to  $\xi$  as well as to  $t$ .

The velocity vector  $u(\xi, t)$  can be obtained by differentiating  $x(\xi, t)$  with respect to time:

$$u(\xi, t) = \dot{x}(\xi, t) = \frac{\partial x(\xi, t)}{\partial t} \quad (1.2.1)$$

In the sequel the notion 'rate of a quantity' is used to denote the time derivative of that quantity for constant value of  $\xi$ . So, the velocity is the rate of the position.

The deformation of a body is a relative notion and has to be looked at with respect to a well-known reference condition of the body. Let this condition have occurred at time  $t_0$ . The position vector at this time  $t_0$ , i.e. the reference position vector, is denoted by the capital letter  $X$ :

$$X = X(\xi) = x(\xi, t_0) \quad (1.2.2)$$

From this relationship it can be seen that the current position vector  $x$  can also be regarded as a function of the reference position vector  $X$ :

$$x = x(X, t) \quad (1.2.3)$$

The deformation of the body with respect to the reference condition is characterized by the deformation tensor  $F$ :

$$F = F(X, t) = \frac{\partial x(X, t)}{\partial X} \quad (1.2.4)$$

The deformation tensor is regular and its determinant  $J = \det(F)$  is positive and equal to the current volume per unit reference volume.  $F$  can therefore be uniquely decomposed, according to:

$$F = R \cdot U = V \cdot R \quad (1.2.5)$$

where  $R$  is a rotation tensor,  $U$  and  $V$  are symmetrical, positive definite tensors, which are called the right and left elongation tensor respectively:

$$R^{-1} = R^T; \quad \det(R) = 1; \quad U = U^T; \quad V = V^T \quad (1.2.6)$$

The right and left Cauchy (or Green) strain tensor  $C$  and  $B$  are defined by:

$$C = F^T \cdot F = U^2; \quad B = F \cdot F^T = V^2 \quad (1.2.7)$$

The rate of deformation is given by  $\dot{F} \cdot F^{-1}$  and is independent of the reference situation. The rate is decomposed in the deformation rate tensor  $D$  and the spin tensor  $\Omega$ :

$$D + \Omega = \dot{F} \cdot F^{-1} = (\nabla u)^T \quad (1.2.8)$$

where  $\nabla$  is the current gradient operator. Furthermore,  $D$  is a symmetric tensor and  $\Omega$  an skew-symmetric tensor:

$$\mathbf{D} = \mathbf{D}^T, \Omega = -\Omega^T \quad (1.2.9)$$

From the definition of  $\mathbf{J}$  and  $\mathbf{D}$  it can be deduced that:

$$\text{tr}(\mathbf{D}) = \mathbf{I}:\mathbf{D} = \frac{\dot{J}}{J} \quad (1.2.10)$$

### 1.3 The fundamental laws

The state of a body in thermomechanics is known if the density  $\rho$ , the position vector  $\mathbf{x}$  and the absolute temperature  $\theta$  are known for the whole interval under consideration. In each state the so-called balance equations have to be fulfilled. These balance equations form a set of eight equations, being the balance equations of mass, of momentum, of moment of momentum, and of energy. The latter is known as the first law of thermodynamics. However, these balance equations are not formulated in terms of the density, position vector and temperature only, but also in terms of some other variables.

All the variables, in the balance equations and the second law of thermodynamics, which is discussed later, can be separated into three groups:

- the state variables

$\rho$  the density

$\mathbf{x}$  the position vector

$\theta$  the absolute temperature

- the constitutive variables

$\eta$  the entropy

$\psi$  the free energy

$\mathbf{h}$  the heat flow vector

$\sigma$  the Cauchy stress tensor

- the external variables

$r$  the specific heat production

$\underline{b}$  the specific load vector

The state variables determine the state of a body. The constitutive variables are determined entirely by the current and past values of the state variables. Let  $\hat{c}$  represent some constitutive variable and let  $\Xi$  be the set of all  $\xi$ , which identify the body. This constitutive variable is then mathematically given by a constitutive equation of the type:

$$\hat{c}(\xi, t) = \hat{c}(\rho(\xi, \tau), \chi(\xi, \tau), \theta(\xi, \tau); \tau \leq t; \xi \in \Xi) \quad (1.3.1)$$

The fact that the constitutive variables can be expressed in terms of the internal variables, is known as the principle of determinism. In the next section other principles will be discussed, which lead to simplifications of relationship 1.3.1.

The internal energy  $e$  is often introduced as a constitutive variable. This variable depends on the free energy, the entropy and the temperature in the following way:

$$e = \psi + \theta \cdot \eta \quad (1.3.2)$$

It will not be considered as a separate variable as it can be expressed in terms of others.

The constitutive variables will be regarded as primitive variables. Their descriptions in terms of the state variables, i.e. the constitutive equations, are unique for every distinct material and specify the physical properties of the material. The physical interpretation of the constitutive variables will not be discussed here, but can be found in, for instance, Fast (1962) and Muller (1985).

The external variables are independent variables, which enter the balance equations. In most parts of this work it is assumed that their influence can be neglected.

In thermomechanics the variables mentioned have to obey a set of so-called balance equations. These equations are:

- the balance equation of mass

$$\frac{\dot{\rho}}{\rho} + \nabla \cdot \underline{u} = 0 \quad (1.3.3)$$

- the balance equations of momentum

$$\nabla \cdot \underline{\sigma} + \rho \cdot \underline{b} = \rho \cdot \dot{\underline{u}} \quad (1.3.4)$$

- the balance equations of moment of momentum



$$\boldsymbol{\sigma} = \boldsymbol{\sigma}^T \quad (1.3.5)$$

- the balance equation of energy

$$\rho \cdot \dot{e} = - \nabla \cdot \mathbf{h} + \boldsymbol{\sigma} : \mathbf{D} + \rho \cdot r \quad (1.3.6)$$

The latter equation is better known as the first law of thermodynamics. The second law of thermodynamics is not represented by a balance equation, but by an inequality. This inequality represents the idea that every thermodynamical process has a direction, which means that not every conceivable state of a body can be achieved from the current state. In a more formal way, it is stated that the entropy production has to be positive. This leads to (Muller, 1985):

$$\rho \cdot (\dot{\psi} + \dot{\theta} \cdot \eta) - \boldsymbol{\sigma} : \mathbf{D} + \frac{1}{\rho} \cdot \mathbf{h} \cdot \nabla \cdot \theta \leq 0 \quad (1.3.7)$$

Equation 1.3.5 and inequality 1.3.7 can be regarded as restrictions on the constitutive equations 1.3.2. The remaining equations 1.3.3, 1.3.4 and 1.3.6 form a set of five equations for the unknown state variables. Equation 1.3.3 can immediately be solved by time integration, resulting in:

$$\frac{\rho_0}{\rho} = J = \det(\mathbf{F}) \quad (1.3.8)$$

This means that the density can be expressed in terms of the position vector  $x$  and that the general constitutive equation 1.3.1 can be simplified to:

$$\hat{c}(\boldsymbol{\zeta}, t) = \hat{c}(x(\boldsymbol{\zeta}, \tau), \theta(\boldsymbol{\zeta}, \tau); \tau \leq t; \boldsymbol{\zeta} \in \Xi) \quad (1.3.9)$$

A second simplification is based on the assumption that the inequality 1.3.7 can be decomposed into two parts:

$$\rho \cdot (\dot{\psi} + \dot{\theta} \cdot \eta) - \boldsymbol{\sigma} : \mathbf{D} \leq 0 \quad (1.3.10)$$

$$\mathbf{h} \cdot \mathbf{g} \leq 0 \quad (1.3.11)$$

where  $\mathbf{g}$  represents the gradient of the temperature:

$$\mathbf{g} = \nabla \cdot \theta \quad (1.3.12)$$

Inequality 1.3.10 is referred to as the Clausius-Duhem inequality.

## 1.4 Some constitutive principles.

In this subparagraph some widely accepted constitutive principles, concerning the constitutive equations, will be discussed. First some principles and their consequences will just be mentioned. Special attention will be given to the principle of objectivity, because some consequences of this principle will be extensively discussed in this thesis.

The acceptance of the principles of local action, of invariance of Galilei-translations and of invariance under a shift of the origin of time, yields the conclusion that the entropy  $\eta$ , the free energy  $\psi$ , the heat flow vector  $h$  and the stress tensor  $\sigma$  are completely determined by the history of the strain tensor  $F$ , of the temperature  $\theta$ , and of the temperature gradient  $g$ . Details of these principles can be found in Eringen (1967) or in Muller (1985). Relationship 1.3.9 for a constitutive quantity  $\hat{c}$  can therefore be reduced to:

$$\hat{c}(\xi, t) = \hat{c}(F(\xi, \tau), \theta(\xi, \tau), g(\xi, \tau); \tau \leq t) \quad (1.4.1)$$

Usually the dependence of the material coordinates  $\xi$  is not explicitly denoted and hence the constitutive equations are written as:

$$\hat{c}(t) = \hat{c}(F(\tau), \theta(\tau), g(\tau); \tau \leq t) \quad (1.4.2)$$

Prior to the introduction of the principle of objectivity the idea of objective and invariant variables will be discussed. Let  $x$  be the position vector of a certain material point, and let  $\bar{x}$  be the position vector of this point after a rigid body rotation. Then the relationship between  $x$  and  $\bar{x}$  is given by:

$$\bar{x} = Q \cdot x \quad (1.4.3)$$

where  $Q$  is a rotation tensor, which can only depend on time.

Let  $p$  and  $\bar{p}$  represent some quantity respectively before and after the rigid body rotation. Then the invariance and objectivity of this quantity can be defined by the following scheme:

	invariant	objective
scalar	$\bar{p} = p$	$\bar{p} = p$
vector	$\bar{p} = \underline{p}$	$\bar{p} = Q \cdot p$

$$\text{tensor } \bar{P} = P \quad \bar{P} = Q^T.P.Q$$

In Appendix A most of the previously introduced variables are divided into objective, invariant and other variables, with the following result:

-Objective variables:

$$\text{scalar } \eta, \psi, \theta, J$$

$$\text{vector } h, g, \underline{x}$$

$$\text{tensor } \sigma, \mathbf{B}, \mathbf{D}$$

-Invariant variables

$$\text{scalar } \eta, \psi, \theta, J$$

$$\text{vector } \underline{X}$$

$$\text{tensor } \mathbf{C}$$

The principle of objectivity states that only objective quantities can be related to objective quantities, and invariant quantities to invariant quantities. In the next paragraph constitutive relationships between invariant quantities will be discussed. An invariant stress tensor and invariant heat flow vector must therefore be introduced.

The invariant stress tensor  $\bar{\mathbf{S}}$  is simultaneously introduced with an invariant deformation rate tensor  $\dot{\bar{\mathbf{C}}}$ . They are defined by:

$$\bar{\mathbf{S}} = J.A^{-1}.\sigma.A^{-T} \quad (1.4.4)$$

$$\dot{\bar{\mathbf{C}}} = \mathbf{A}^T.D.A \quad ; \quad \dot{\bar{\mathbf{C}}}(t_0) = 0 \quad (1.4.5)$$

$$\mathbf{A}(t) = \mathbf{F}(t).\bar{\mathbf{A}}(\mathbf{U}(\tau), \tau \leq t) \quad (1.4.6)$$

where  $\bar{\mathbf{A}}$  is an invariant tensor. In Appendix A the invariancy of  $\bar{\mathbf{S}}$  and  $\dot{\bar{\mathbf{C}}}$  is shown and some commonly used choices of the tensor  $\mathbf{A}$  are discussed.

The invariant heat flow vector  $\bar{h}$  is defined together with an invariant temperature gradient vector  $\bar{g}$ :

$$\bar{h} = \mathbf{A}^{-1}.h \quad ; \quad \bar{g} = \mathbf{A}^T.g \quad (1.4.7)$$

The principle of objectivity states that for the invariant constitutive quantities the general relationship 1.4.2 reduces to:

$$\psi(t) = \psi(\bar{\mathbf{C}}(\tau), \theta(\tau), \bar{\mathbf{g}}(\tau); \tau \leq t) \quad (1.4.8)$$

$$\eta(t) = \eta(\bar{\mathbf{C}}(\tau), \theta(\tau), \bar{\mathbf{g}}(\tau); \tau \leq t) \quad (1.4.9)$$

$$\bar{\mathbf{h}}(t) = \bar{\mathbf{h}}(\bar{\mathbf{C}}(\tau), \theta(\tau), \bar{\mathbf{g}}(\tau); \tau \leq t) \quad (1.4.10)$$

$$\bar{\mathbf{S}}(t) = \bar{\mathbf{S}}(\bar{\mathbf{C}}(\tau), \theta(\tau), \bar{\mathbf{g}}(\tau); \tau \leq t) \quad (1.4.11)$$

An example of a constitutive equation, which obeys the principle of objectivity is Fourier's law. This law assumes that the heat flow is a linear function of the temperature gradient:

$$\bar{\mathbf{h}} = -\bar{\mathbf{K}} \cdot \bar{\mathbf{g}} \quad (1.4.12)$$

where  $\bar{\mathbf{K}}$  is an invariant and symmetric tensor. In terms of the objective heat flow and temperature gradient vectors this relationship becomes:

$$\underline{\mathbf{h}} = -\mathbf{A} \cdot \bar{\mathbf{K}} \cdot \mathbf{A}^T \cdot \underline{\mathbf{g}} = -\mathbf{K} \cdot \underline{\mathbf{g}} \quad (1.4.13)$$

where  $\mathbf{K}$  is objective. From inequality 1.3.11 it follows that  $\mathbf{K}$  is positive definite. Often it is assumed that  $\mathbf{K}$  reduces to:

$$\mathbf{K} = k \cdot \mathbf{I} \quad ; \quad k > 0 \quad (1.4.14)$$

where  $k$  is the thermal conductivity.

In this thesis, the main interest is the constitutive relationship for the stresses. As the entropy and the free energy enter the Clausius-Duhem inequality, they have to be taken into account as well. For the heat flow, it is assumed that Fourier's law holds.

## 1.5 Further simplifications

In the next two chapters the consequences of two well-known methods for simplifying the general constitutive equations, are discussed and compared.

The first method is achieved by assuming that the current value of constitutive quantities only depends on the current value of a number of variables, including so-called hidden variables. The rate of these hidden variables depends on the same variables as the constitutive quantities. In this way, the history of the body under consideration can be taken into account. This is the subject of the next chapter.

The second method is based on the decomposition of the Cauchy stress tensor  $\sigma$  and the decomposition of the deformation rate tensor  $\mathbf{D}$  into an elastic, or reversible, part and an irreversible part. This method is especially popular in the field of metal plasticity. It is discussed in more detail in chapter 3.

## 2 Hidden variables

### 2.1 Introduction

In this chapter the constitutive equations 1.4.8, 1.4.9 and 1.4.11 will be reformulated in current variables only. These current variables are the already introduced strain and strain rate tensors  $\bar{\mathbf{C}}$  and  $\dot{\bar{\mathbf{C}}}$ , the temperature  $\theta$  and the temperature gradient  $\bar{\mathbf{g}}$ , but there is also a set of so-called hidden variables. These variables can have a physical meaning, but their main property is, that their evolution in time is described by the current variables themselves.

In the next two subparagraphs the consequences of the introduction of hidden variables will be analysed, taking into account the second law of thermodynamics (the Clausius-Duhem inequality) and isotropy. Some possible simplifications will be discussed. In the rest of the chapter some well-known classes of constitutive behaviour, such as viscous and elastic behaviour will be discussed. These classes are obtained by introducing no hidden variables, one hidden scalar and, finally, one hidden tensor.

In the last two subparagraphs of this chapter one hidden scalar and one hidden tensor with a clear physical meaning will be introduced. This will lead to two constitutive relationships for metals.

### 2.2 The consequences of the introduction of hidden variables

As discussed in the previous subparagraph some assumptions will be made concerning the constitutive relationships 1.4.8, 1.4.9 and 1.4.11. The first assumption is that the constitutive relationships only depend on the current values of certain variables, such as the pseudo strain and strain rate tensors  $\bar{\mathbf{C}}$  and  $\dot{\bar{\mathbf{C}}}$ , the temperature  $\theta$ , the temperature gradient  $\bar{\mathbf{g}}$  and finally some hidden, independent variables. Such variables can

be scalar and vectorial and tensorial quantities, which means that the hidden variables can be defined by:

$$\begin{aligned} q_1, \dots, q_s & : \text{scalar variables} \\ \underline{q}_1, \dots, \underline{q}_v & : \text{vectorial variables} \\ \mathbf{Q}_1, \dots, \mathbf{Q}_t & : \text{tensorial variables} \end{aligned}$$

For reasons of compactness of notation, these hidden variables are regarded as the components of a column  $\tilde{J}$ :

$$\tilde{J} = (q_1, \dots, q_s, \underline{q}_1, \dots, \underline{q}_v, \mathbf{Q}_1, \dots, \mathbf{Q}_t)^T \quad (2.2.1)$$

It then follows that the constitutive relationships can be formulated by:

$$\hat{c} = \hat{c}(\bar{\mathbf{C}}, \dot{\bar{\mathbf{C}}}, \theta, \bar{\mathbf{g}}, \tilde{J}) \quad (2.2.2)$$

All the quantities in this relationship depend on time but, for the sake of brevity this is not mentioned in 2.2.2 .

As already stated, the constitutive variables are, in general, a function of the current and past states of the body. This means that the hidden variables in 2.2.2 must take into account the influence of the past states on the current value of the constitutive variables. This leads to the second assumption: the rate of the hidden variables is determined by exactly the same variables, as in the case of the constitutive variables. In mathematical form, this assumption leads to:

$$\dot{\tilde{J}} = \tilde{J}(\bar{\mathbf{C}}, \dot{\bar{\mathbf{C}}}, \theta, \bar{\mathbf{g}}, \tilde{J}) \quad (2.2.3)$$

The consequences of these two assumptions with respect to the Clausius-Duhem inequality and isotropy, will be investigated. If  $\sigma$  and  $\mathbf{D}$ , in inequality 1.3.10, are replaced by the invariant stress and strain rate tensor  $\bar{\mathbf{S}}$  and  $\dot{\bar{\mathbf{C}}}$ , this inequality becomes:

$$\rho_0(\dot{\psi} + \dot{\theta}\eta) - \bar{\mathbf{S}}:\dot{\bar{\mathbf{C}}} \leq 0 \quad (2.2.4)$$

With a constitutive relationship of the type 2.2.2 the rate of  $\psi$  is given by:

$$\dot{\psi} = \frac{\partial \psi}{\partial \bar{\mathbf{C}}}:\dot{\bar{\mathbf{C}}} + \frac{\partial \psi}{\partial \dot{\bar{\mathbf{C}}}}:\ddot{\bar{\mathbf{C}}} + \frac{\partial \psi}{\partial \theta}\dot{\theta} + \frac{\partial \psi}{\partial \bar{\mathbf{g}}}\cdot\dot{\bar{\mathbf{g}}} + \tilde{X} \times \dot{\tilde{J}} \quad (2.2.5)$$

where  $\tilde{X} \times \dot{\tilde{J}}$  is a formal notation for the contribution to  $\dot{\psi}$ , due to the hidden variables  $\tilde{J}$ . This implies that  $\tilde{X}$  follows from the requirement that:

$$\psi(\dots, \tilde{J} + d\tilde{J}) - \psi(\dots, \tilde{J}) = \tilde{X} \times d\tilde{J} \quad (2.2.6)$$

for each infinitesimally small column  $d\tilde{J}$ . Within this relationship for  $\psi$ , the evaluation relationship 2.2.3 and the fact, that the hidden variables,  $\bar{\mathbf{C}}$ ,  $\dot{\bar{\mathbf{C}}}$  and  $\bar{\mathbf{g}}$  form a set of independent parameters, the Clausius-Duhem inequality 2.2.4 leads to:

$$\left( \frac{\partial \psi}{\partial \bar{\mathbf{C}}} - \frac{1}{\rho_0} \cdot \bar{\mathbf{S}} \right) : \dot{\bar{\mathbf{C}}} + \tilde{X} \times \dot{\tilde{J}} \leq 0 \quad (2.2.7)$$

$$\frac{\partial \psi}{\partial \dot{\bar{\mathbf{C}}}} = 0 \quad (2.2.8)$$

$$\frac{\partial \psi}{\partial \theta} = -\eta \quad (2.2.9)$$

$$\frac{\partial \psi}{\partial \bar{\mathbf{g}}} = 0 \quad (2.2.10)$$

All the choices that will be considered for  $\tilde{J}$  are independent of the strain rate tensor  $\dot{\bar{\mathbf{C}}}$ . In that case, it directly follows from 2.2.7 that 2.2.7 can be split into the following two parts:

$$\left( \frac{\partial \psi}{\partial \bar{\mathbf{C}}} - \frac{1}{\rho_0} \cdot \bar{\mathbf{S}} \right) : \dot{\bar{\mathbf{C}}} \leq 0 \quad (2.2.11)$$

$$\tilde{X} \times \dot{\tilde{J}} \leq 0 \quad (2.2.12)$$

In order to fulfil inequality 2.2.11 it seems obvious to make the following assumption for the constitutive relationship of the stress  $\bar{\mathbf{S}}$ :

$$\bar{\mathbf{S}} = \rho_0 \cdot \frac{\partial \psi}{\partial \bar{\mathbf{C}}} + {}^4\mathbf{M} : \dot{\bar{\mathbf{C}}} \quad (2.2.13)$$

where the fourth order tensor  ${}^4\mathbf{M}$  is a semi-positive definite fourth order tensor which may depend on the state and hidden variables. This tensor is usually simplified to  $\mu \cdot \mathbf{I}$ . Then relationship 2.2.13 becomes:

$$\bar{\mathbf{S}} = \rho_0 \cdot \frac{\partial \psi}{\partial \bar{\mathbf{C}}} + \mu \cdot \dot{\bar{\mathbf{C}}} \quad ; \quad \mu \geq 0 \quad (2.2.14)$$

The scalar  $\mu$  is called the viscosity which, for most materials, depends on the state and hidden variables.



Another widely accepted assumption has been described in De Groot (1951) and De Groot and Mazur (1962). In order to fulfil the inequality 2.2.12, the authors argued that it seems logical to assume that:

$$\dot{\tilde{J}} + \tilde{L}(\tilde{X}) = 0 \quad (2.2.15)$$

where  $\tilde{L}$  is a linear, semi-positive definite operator on  $\tilde{X}$ .

Another well-known assumption is that the operator  $\tilde{L}$  is symmetrical, i.e.:

$$\tilde{L}(\tilde{A}) \times \tilde{B} = \tilde{A} \times \tilde{L}(\tilde{B}) \quad \text{for } \forall \tilde{A}, \tilde{B} \quad (2.2.16)$$

The assumptions 2.2.15 and 2.2.16 have often been discussed in literature. As already mentioned, equation 2.2.15 is widely accepted. This is not the case for the so-called Onsager relationships 2.2.16, as can be seen in Truesdell (1968). De Groot, however, gave some arguments for the symmetry of the operator  $\tilde{L}$ , derived from statistical thermodynamics (De Groot and Mazur, 1962).

## 2.3 Isotropy

A special class of materials are the so-called isotropic materials. The constitutive behaviour of these materials is equal for every direction. Most materials are considered to be isotropic.

For isotropic scalar functions the following theorem can be employed. The proof of this theorem can be found in Muller (1985), for instance.

Let  $f$  be an isotropic scalar function of some tensors  $\mathbf{A}$  and  $\mathbf{B}$ , some vectors  $\mathbf{a}$  and  $\mathbf{b}$  and some scalars  $a$  and  $b$ :

$$f = f(\mathbf{A}, \mathbf{B}, \mathbf{a}, \mathbf{b}, a, b) \quad (2.3.1)$$

Then, because of the isotropy,  $f$  can only be a function of invariant characteristics of the variables:

$$f = f(I:\mathbf{A}, I:\mathbf{B}, I:\mathbf{A}^2, \mathbf{A}:\mathbf{B}, I:\mathbf{B}^2, I:\mathbf{A}^3, \mathbf{A}^2:\mathbf{B}, \mathbf{A}:\mathbf{B}^2, I:\mathbf{B}^3, a.a, a.b, b.b, a, b) \quad (2.3.2)$$

This theorem says, for instance, that  $f$  can't just depend on one single component of the tensor  $\mathbf{A}$  or  $\mathbf{B}$ , or on combinations like  $\mathbf{a}.\mathbf{B}.\mathbf{a}$ . Similar results are found if  $f$  depends on more than two tensors or vectors.

Previously it was argued that the free energy  $\psi$  is a function of  $\bar{\mathbf{C}}$ ,  $\theta$  and  $\tilde{\mathbf{J}}$ , where the hidden variables in the column  $\tilde{\mathbf{J}}$  are scalar, vectorial and tensorial quantities. In the sequel it will be assumed that  $\psi$  is an isotropic function of  $\bar{\mathbf{C}}$ ,  $\theta$  and  $\tilde{\mathbf{J}}$  and only some special cases are considered.

If there is only one hidden vectorial variable  $\underline{q}$ , then this hidden vector can be replaced by a hidden scalar, which can be interpreted as the length of the vector  $\underline{q}$ . This is a direct consequence of the theorem 2.3.2. Hence the case of one single hidden vector is not taken into account in this chapter.

Far-reaching consequences of isotropy can be derived for the case, in which the free energy is quadratically expanded, as was suggested by De Groot (1951). Theorem 2.3.2 then gives:

$$\begin{aligned} \psi = & \psi_0 + \frac{1}{2} \bar{\mathbf{C}} : {}^4\mathbf{E} : \bar{\mathbf{C}} + \alpha \theta I : \bar{\mathbf{C}} + I : \bar{\mathbf{C}} \sum_{i=1}^s (\beta_i q_i) + \sum_{i=1}^t (\bar{\mathbf{C}} : {}^4\mathbf{N}^i : \mathbf{Q}^i) + \frac{1}{2} \gamma \theta^2 + \\ & + \theta \sum_{i=1}^s (\delta_i q_i) + \theta \sum_{i=1}^t (\varepsilon_i I : \mathbf{Q}_i) + \frac{1}{2} \sum_{i,j=1}^s (\zeta_{ij} q_i q_j) + \sum_{i,j=1}^{s,t} (\kappa_{ij} q_i I : \mathbf{Q}_j) + \\ & + \frac{1}{2} \sum_{i,j=1}^t (\mathbf{Q}_i : {}^4\mathbf{B}_{ij} : \mathbf{Q}_j) + \frac{1}{2} \sum_{i,j=1}^v (v_{ij} q_i \cdot q_j) \end{aligned} \quad (2.3.3)$$

where  $\alpha, \beta_i, \gamma, \delta_i, \varepsilon_i, \zeta_{ij}, \kappa_{ij}$  and  $v_{ij}$  are constant, and where all fourth order tensors, like  ${}^4\mathbf{E}$ ,  ${}^4\mathbf{N}_i$  and  ${}^4\mathbf{B}_{ij}$ , are of the type:

$${}^4\mathbf{P} = p_1 {}^4\mathbf{I} + p_2 I I; \quad p_1 \text{ and } p_2 \text{ are constant} \quad (2.3.4)$$

The relationships 2.2.14 and 2.2.9 for the stress  $\bar{\mathbf{S}}$  and the entropy  $\eta$  become:

$$\bar{\mathbf{S}} = \rho \alpha {}^4\mathbf{E} : \bar{\mathbf{C}} + \alpha \theta I + \sum_{i=1}^s (\beta_i q_i) + \sum_{i=1}^t ({}^4\mathbf{N}_i : \mathbf{Q}_i) + \mu \dot{\bar{\mathbf{C}}} \quad (2.3.5)$$

$$\eta = -\alpha I : \bar{\mathbf{C}} - \gamma \theta - \sum_{i=1}^s (\delta_i q_i) - \sum_{i=1}^t (\varepsilon_i I : \mathbf{Q}_i) \quad (2.3.6)$$

One of the striking results is that in these relationships for the stress and entropy no hidden vectors enter.

As already mentioned in the first section of this chapter, only a few simple cases will be considered in the following subparagraphs by introducing no hidden variables, one hidden scalar, one hidden tensor and finally one hidden scalar and tensor. Special attention will be given to the relationships in 2.2.14, the so-called stress-strain relationships.

## 2.4 Elasticity and simple visco-elasticity

In this subparagraph the case will be considered, in which the free energy doesn't depend on any single hidden variable. The general expression for the free energy then becomes:

$$\psi = \psi(\bar{\mathbf{C}}, \theta) \quad (2.4.1)$$

and for isotropic materials this relationship reduces to:

$$\psi = \psi(I:\bar{\mathbf{C}}, I:\bar{\mathbf{C}}^2, I:\bar{\mathbf{C}}^3, \theta) = \psi(I_1, I_2, I_3, \theta) \quad (2.4.2)$$

The stress-strain relationships can be easily obtained by substitution of 2.4.2 in 2.2.14:

$$\begin{aligned} \bar{\mathbf{S}} &= \alpha_0 \mathbf{I} + \alpha_1 \bar{\mathbf{C}} + \alpha_2 \bar{\mathbf{C}}^2 + \mu \dot{\bar{\mathbf{C}}} \\ \alpha_0 &= \rho_0 \frac{\partial \psi}{\partial I_1}; \quad \alpha_1 = 2\rho_0 \frac{\partial \psi}{\partial I_2}; \quad \alpha_2 = 3\rho_0 \frac{\partial \psi}{\partial I_3} \end{aligned} \quad (2.4.3)$$

Materials with constitutive equations of this kind are called simple visco-elastic materials. If  $\mu = 0$ , i.e. no viscosity, the material is called pseudo-elastic. Then the stress-strain relationship reduces to:

$$\bar{\mathbf{S}} = \alpha_0 \mathbf{I} + \alpha_1 \bar{\mathbf{C}} + \alpha_2 \bar{\mathbf{C}}^2 \quad (2.4.4)$$

and the rate of the free energy is given by:

$$\dot{\psi} = \frac{1}{\rho_0} \bar{\mathbf{S}} : \dot{\bar{\mathbf{C}}} + \frac{\partial \psi}{\partial \theta} \dot{\theta} = \frac{1}{\rho} \boldsymbol{\sigma} : \mathbf{D} - \eta \dot{\theta} \quad (2.4.5)$$

Hence, in the isothermal case, the added mechanical power equals the rate of the free energy. This result is discussed in Appendix B.

A material is called elastic if it is pseudo-elastic and if the free energy depends on  $\theta$  and on the Cauchy strain tensor  $\mathbf{C}$ , introduced in section 1.2. From this definition it is

deduced in Appendix B that the Cauchy stress tensor  $\sigma$  will be a quadratical function of the objective Cauchy strain tensor  $\mathbf{B}$ :

$$\sigma = a_0 \mathbf{I} + a_1 \mathbf{B} + a_2 \mathbf{B}^2 \quad (2.4.6)$$

A final result, obtained in Appendix B, and used in the next chapter, is that the eigenvalues  $\sigma_i$  of the stress tensor (i.e. the main stresses) for an elastic material are given by:

$$J\sigma_i = \rho_0 \frac{\partial \psi}{\partial e_i} ; \quad e_i = \ln(\lambda_i) \quad (2.4.7)$$

where  $\lambda_1^2$ ,  $\lambda_2^2$  and  $\lambda_3^2$  are the eigenvalues of  $\mathbf{B}$ .

## 2.5 One hidden scalar

The simplest extension in the concept of hidden variables to the simple visco-elastic model, is the introduction of one hidden scalar  $q$ :

$$\psi = \psi(\bar{\mathbf{C}}, \theta, q) \quad (2.5.1)$$

According to 2.2.14 and 2.2.15 the stress-strain relationships are given by:

$$\bar{\mathbf{S}} = \rho_0 \frac{\partial \psi}{\partial \bar{\mathbf{C}}} + \mu \dot{\bar{\mathbf{C}}} ; \quad \mu \geq 0 \quad (2.5.2)$$

$$\dot{q} + l \frac{\partial \psi}{\partial q} = 0 ; \quad l \geq 0 \quad (2.5.3)$$

where  $l$  is a scalar quantity. As an example, the isotropic, isothermal, quadratic expansion of the free energy is considered. Then, 2.3.3 reduces to:

$$\psi = \psi_0 + \frac{1}{2} \bar{\mathbf{C}} : {}^4\mathbf{E} : \bar{\mathbf{C}} + \beta q l : \bar{\mathbf{C}} + \frac{1}{2} \zeta q^2 \quad (2.5.4)$$

where  ${}^4\mathbf{E} = E_1 \mathbf{I} + E_2 \mathbf{II}$  because of 2.3.4, while  $\psi_0$ ,  $E_1$ ,  $E_2$ ,  $\beta$  and  $\zeta$  are constant. Substitution in 2.5.1 and 2.5.2 gives:

$$\bar{\mathbf{S}} = \rho_0 (E_2 l : \bar{\mathbf{C}} + \beta q) \mathbf{I} + \rho_0 E_1 \bar{\mathbf{C}} + \mu \dot{\bar{\mathbf{C}}} \quad (2.5.5)$$

$$\dot{q} + l \zeta q + l \beta l : \bar{\mathbf{C}} = 0 \quad (2.5.6)$$

Equation 2.5.5 can be decomposed into a relationship for the trace of  $\bar{\mathbf{S}}$  and a relationship for the deviatoric part  $\bar{\mathbf{S}}^d$  of  $\bar{\mathbf{S}}$ :

$$\bar{\mathbf{S}}^d = \rho_0 E_1 \bar{\mathbf{C}}^d + \mu (\dot{\bar{\mathbf{C}}})^d \quad (2.5.7)$$

$$\text{tr}(\bar{\mathbf{S}}) = 3\rho_0 \beta q + \rho_0 (E_1 + 3E_2) I: \bar{\mathbf{C}} + \mu I: \dot{\bar{\mathbf{C}}} \quad (2.5.8)$$

It can be seen from 2.5.7 that  $\bar{\mathbf{S}}^d$  doesn't depend on the hidden scalar  $q$ . Furthermore, it can be seen, that 2.5.6 and 2.5.8 form a set of two linear equations, relating  $q$  and the trace of  $\bar{\mathbf{S}}$  to the trace of  $\bar{\mathbf{C}}$  and  $\dot{\bar{\mathbf{C}}}$ . With the definition of  $\dot{\bar{\mathbf{C}}}$  in 1.4.5 it follows that:

$$I: \dot{\bar{\mathbf{C}}} = \mathbf{D}: (\mathbf{A} \cdot \mathbf{A}^T) \quad (2.5.9)$$

In the special case, in which  $\mathbf{A}$  is a rotation tensor, this relationship reduces to:

$$I: \dot{\bar{\mathbf{C}}} = I: \mathbf{D} = \frac{\dot{J}}{J} \quad \text{so} \quad I: \bar{\mathbf{C}} = \ln(J) \quad (2.5.10)$$

In this case the definition of  $\bar{\mathbf{S}}$  in 1.4.4 results in:

$$\text{tr}(\bar{\mathbf{S}}) = J \boldsymbol{\sigma}: \mathbf{A}^{-T} \cdot \mathbf{A}^{-1} = J I: \boldsymbol{\sigma} = -3J p_h \quad (2.5.11)$$

where  $p_h = -\frac{1}{3} I: \boldsymbol{\sigma}$  is the hydrostatic pressure. Substitution of 2.5.10 and 2.5.11 in 2.5.8 and 2.5.6 yields:

$$p_h = -\rho \beta q - \rho \left( \frac{1}{3} E_1 + E_2 \right) \ln(J) - \frac{1}{3} \mu \frac{\dot{J}}{J} \quad (2.5.12)$$

$$\dot{q} + I \zeta q + I \beta \ln(J) = 0 \quad (2.5.13)$$

From these equations it can be seen that by eliminating  $q$  from these equations a relationship remains between the hydrostatic pressure and the relative volume change  $J$ . So, in this case, the introduction of one hidden scalar leads to what is normally called a p-V relationship.

Another well-known special case of 2.5.7, 2.5.8 and 2.5.9 is obtained, if the scalar factor  $\beta$  becomes infinite. Then the equations reduce to  $I: \dot{\bar{\mathbf{C}}} = 0$ . A trivial interpretation of this relationship is possible if  $\mathbf{A}$  is a rotation tensor, since it then follows from 2.5.10 that  $\text{tr}(\mathbf{D}) = 0$  and  $J = 1$ , which is the requirement for a material that is incompressible.

Usually incompressibility, is accounted for in a different way, which is also applicable when  $\mathbf{A}$  is not a rotation tensor. In that case, the requirement of incompressibility is considered as a restriction, which can be expressed mathematically by:

$$\frac{\dot{J}}{J} = \text{tr}(\mathbf{D}) = 0 \quad \text{so} \quad \dot{\bar{\mathbf{C}}}: (\mathbf{A}^{-1} \cdot \mathbf{A}^{-T}) = 0 \quad (2.5.14)$$

In the application of the second law of thermodynamics, this restriction can be taken into account by using a Lagrange multiplier  $p$ . The Clausius-Duhem inequality is then replaced by:

$$\rho_0 (\dot{\psi} + \dot{\theta}\eta) - \bar{\mathbf{S}}:\dot{\bar{\mathbf{C}}} - p(\mathbf{A}^{-1} \cdot \mathbf{A}^{-T}):\dot{\bar{\mathbf{C}}} \leq 0 \quad (2.5.15)$$

and it is easy to see that the stress-strain relationship 2.2.14 becomes:

$$\bar{\mathbf{S}} = -p\mathbf{A}^{-1} \cdot \mathbf{A}^{-T} + \rho_0 \frac{\partial \psi}{\partial \bar{\mathbf{C}}} + \mu \dot{\bar{\mathbf{C}}} \quad (2.5.16)$$

Substituting relationship 1.4.4 into this result, the following expression is obtained for the objective stress tensor  $\sigma$ :

$$\sigma = -p\mathbf{I} + \mathbf{A}(\rho_0 \frac{\partial \psi}{\partial \bar{\mathbf{C}}} + \mu \dot{\bar{\mathbf{C}}})\mathbf{A}^T \quad (2.5.17)$$

It can be seen from this result that the requirement of incompressibility leads to the addition of  $-p\mathbf{I}$  to the Cauchy stress tensor. For this reason incompressibility is taken into account in the following by separating the Cauchy tensor in:

$$\sigma = -p\mathbf{I} + \tau \quad (2.5.18)$$

where a constitutive relationship is given for  $\tau$ .

From the results of this subparagraph it can be seen that the introduction of one hidden scalar variable can lead to a well-known material behaviour, although no physical meaning had previously been given to that hidden variable.

## 2.6 Generalized visco-elastic material behaviour

The obvious extension to the previous subparagraph is the introduction of one hidden tensorial variable  $\mathbf{Q}$ . The free energy is given in this case by:

$$\psi = \psi(\bar{\mathbf{C}}, \theta, \mathbf{Q}) \quad (2.6.1)$$

If only the case is considered, in which the free energy is an isotropic, quadratic function, as in 2.3.3, it follows that:

$$\bar{\mathbf{S}} = {}^4\mathbf{E}:\bar{\mathbf{C}} + {}^4\mathbf{N}:\mathbf{Q} + \alpha\theta\mathbf{I} + \mu\dot{\bar{\mathbf{C}}} \quad (2.6.2)$$

$$\dot{\mathbf{Q}} + {}^4\mathbf{L}:({}^4\mathbf{N}:\bar{\mathbf{C}} + {}^4\mathbf{B}:\mathbf{Q} + \varepsilon\theta\mathbf{I}) = 0 \quad (2.6.3)$$

where  ${}^4\mathbf{E}$ ,  ${}^4\mathbf{N}$  and  ${}^4\mathbf{B}$  are constant fourth order tensors and where it is assumed that  ${}^4\mathbf{L}$  is symmetric (Onsager relations) and positive definite (Clausius-Duhem). For the time being it is also assumed that  ${}^4\mathbf{L}$  is constant. Then  $\mathbf{Q}$  can be solved from 2.6.3 (see Appendix C), which leads to :

$$\mathbf{Q} = - \sum_{i=1}^6 {}^4\mathbf{V}_i : \int_0^t ({}^4\mathbf{N}:\bar{\mathbf{C}}(\tau) + \varepsilon\theta(\tau)\mathbf{I}) e^{-\lambda_i(t-\tau)} d\tau \quad (2.6.4)$$

where the fourth order tensor  ${}^4\mathbf{V}$  and the scalars  $\lambda_i (i = 1, \dots, 6)$  are determined by:

$${}^4\mathbf{V}_i = \mathbf{V}_i \mathbf{V}_i ; \quad (\lambda_i^{-1} {}^4\mathbf{L} + {}^4\mathbf{B}) : \mathbf{V}_i = 0 ; \quad \mathbf{V}_i : {}^4\mathbf{L} : \mathbf{V}_i = 1 \quad (2.6.5)$$

From 2.6.4 it can be seen that  $\mathbf{Q}$  is a history dependent strain tensor with a correction term for the temperature. This means that  $\bar{\mathbf{S}}$  depends not only on the current state of the body but also on the total history.

Schapery (1964) made an extension of this model by introducing a reduced time  $\chi$ . He assumed that  ${}^4\mathbf{L}$  can be written as:

$${}^4\mathbf{L} = \nu {}^4\bar{\mathbf{L}} ; \quad \nu > 0 \quad (2.6.6)$$

where  ${}^4\bar{\mathbf{L}}$  is positive definite, symmetric and constant, while  $\nu$  can be a function of the internal variables, except of  $\bar{\mathbf{C}}$  (2.2.12). Then the reduced time  $\chi$  is defined by:

$$\chi = \int_0^t \nu d\tau \quad (2.6.7)$$

and using this variable, the evolution equation 2.6.3 becomes:

$$\frac{d\mathbf{Q}}{d\chi} + {}^4\bar{\mathbf{L}} : ({}^4\mathbf{B}:\mathbf{Q} + {}^4\mathbf{N}:\bar{\mathbf{C}} + \varepsilon\theta\mathbf{I}) = 0 \quad (2.6.8)$$

This equation can also be solved for  $\mathbf{Q}$ , resulting in:

$$\mathbf{Q} = - \sum_{i=1}^6 {}^4\mathbf{V}_i : \int_0^t ({}^4\mathbf{N} : \dot{\bar{\mathbf{C}}}(\tau) + \varepsilon \theta(\tau) \mathbf{I}) v(\tau) e^{-\lambda_i(t-\tau)} d\tau \quad (2.6.9)$$

By substitution of this result in the stress-strain equation 2.6.2 a so-called integral model for the stresses is obtained. If  ${}^4\mathbf{N}$  is regular, a so-called differential model can be obtained. From 2.6.2 it follows that:

$$\mathbf{Q} = -{}^4\mathbf{N} : (\dot{\bar{\mathbf{S}}} - {}^4\mathbf{E} : \dot{\bar{\mathbf{C}}} - \mu \ddot{\bar{\mathbf{C}}} - \alpha \dot{\theta} \mathbf{I} + \theta \mathbf{Z}) \quad (2.6.10)$$

and this result can be used to eliminate  $\mathbf{Q}$  from the evolution equation 2.6.3, yielding:

$$\dot{\bar{\mathbf{S}}} + {}^4\mathbf{X} : \dot{\bar{\mathbf{S}}} = \mu \ddot{\bar{\mathbf{C}}} + {}^4\mathbf{Y}_1 : \dot{\bar{\mathbf{C}}} + {}^4\mathbf{Y}_2 : \bar{\mathbf{C}} + \alpha \dot{\theta} \mathbf{I} + \theta \mathbf{Z} \quad (2.6.11)$$

where the fourth order tensors  ${}^4\mathbf{X}$ ,  ${}^4\mathbf{Y}_1$  and  ${}^4\mathbf{Y}_2$  and the second order tensor  $\mathbf{Z}$  are given by:

$${}^4\mathbf{X} = {}^4\mathbf{N} : {}^4\mathbf{L} : {}^4\mathbf{B} : -{}^4\mathbf{N} \quad (2.6.12)$$

$${}^4\mathbf{Y}_1 = \dot{\mu} {}^4\mathbf{I} + \mu {}^4\mathbf{X} + {}^4\mathbf{E} \quad (2.6.13)$$

$${}^4\mathbf{Y}_2 = {}^4\mathbf{X} : {}^4\mathbf{E} - {}^4\mathbf{N} : {}^4\mathbf{L} : {}^4\mathbf{N} \quad (2.6.14)$$

$$\mathbf{Z} = \alpha {}^4\mathbf{X} : \mathbf{I} - \varepsilon {}^4\mathbf{N} : {}^4\mathbf{L} : \mathbf{I} \quad (2.6.15)$$

The models obtained are still very complicated and are usually simplified by making further assumptions. In order to obtain relationships which are well-known from literature, the following simplification will be considered: it is assumed that the fourth tensors  ${}^4\mathbf{B}$ ,  ${}^4\mathbf{N}$ ,  ${}^4\mathbf{E}$  and  ${}^4\mathbf{L}$  satisfy the requirements:

$${}^4\mathbf{N} = {}^4\mathbf{B} = {}^4\mathbf{E} = E_1 {}^4\mathbf{I} + E_2 \mathbf{II} \quad (2.6.16)$$

$${}^4\mathbf{N} : {}^4\mathbf{L} = \frac{E_1}{\lambda} {}^4\mathbf{I} \rightarrow {}^4\mathbf{L} = \frac{1}{\lambda} {}^4\mathbf{I} - \frac{E_2}{\lambda(E_1 + 3E_2)} \mathbf{II} \quad (2.6.17)$$

with positive scalars  $E_1$  and  $\lambda$  and non-negative  $E_2$ . Substitution of 2.6.17 into 2.6.11 results in:

$$\begin{aligned} \frac{1}{E_1} \dot{\bar{\mathbf{S}}} + \frac{1}{\lambda} \dot{\bar{\mathbf{S}}} &= \frac{\mu}{E_1} \ddot{\bar{\mathbf{C}}} + \left(1 + \frac{\mu}{\lambda} + \frac{\dot{\mu}}{E_1}\right) \dot{\bar{\mathbf{C}}} + \\ &+ \left(\frac{E_2}{E_1} \text{tr}(\ddot{\bar{\mathbf{C}}}) + \frac{\alpha - \varepsilon}{\lambda} \theta + \frac{\alpha}{E_1} \dot{\theta}\right) \mathbf{I} \end{aligned} \quad (2.6.18)$$



This equation can be reformulated in terms of the Cauchy stress tensor  $\sigma$  and the deformation rate tensor  $\mathbf{D}$  by using the definition of the invariant tensors  $\bar{\mathbf{S}}$  and  $\bar{\mathbf{C}}$ , defined in section 1.4. A lengthy but straightforward derivation yields:

$$\begin{aligned} \frac{1}{E_1} \overset{\Delta}{\sigma} + \left( -\frac{1}{E_1} \text{tr}(\mathbf{D}) + \frac{1}{\lambda} \right) \sigma = \frac{1}{J} \mathbf{A} \cdot \mathbf{A}^T \left( \frac{\mu}{E_1} \overset{\nabla}{\mathbf{D}} + \left( 1 + \frac{\mu}{\lambda} + \frac{\dot{\mu}}{E_1} \right) \mathbf{D} \right) \cdot \mathbf{A} \cdot \mathbf{A}^T + \\ + \frac{1}{J} \left( \frac{E_2}{E_1} \mathbf{D} : (\mathbf{A} \cdot \mathbf{A}^T) + \frac{\alpha - \varepsilon}{\lambda} \theta + \frac{\alpha}{E_1} \dot{\theta} \right) \mathbf{A} \cdot \mathbf{A}^T \end{aligned} \quad (2.6.19)$$

The objective rates  $\overset{\Delta}{\sigma}$  and  $\overset{\nabla}{\mathbf{D}}$  of respectively  $\sigma$  and  $\mathbf{D}$  are defined by:

$$\overset{\Delta}{\sigma} = \dot{\sigma} - (\dot{\mathbf{A}} \cdot \mathbf{A}^{-1}) \cdot \sigma - \sigma \cdot (\dot{\mathbf{A}} \cdot \mathbf{A}^{-1})^T \quad (2.6.20)$$

$$\overset{\nabla}{\mathbf{D}} = \dot{\mathbf{D}} + (\dot{\mathbf{A}} \cdot \mathbf{A}^{-1})^T \cdot \mathbf{D} + \mathbf{D} \cdot (\dot{\mathbf{A}} \cdot \mathbf{A}^{-1}) \quad (2.6.21)$$

Now the tensor  $\mathbf{A}$  is chosen to be a rotation tensor, in such a way that  $\mathbf{A}$  still satisfies the requirement 1.4.6. In that case the tensor  $\dot{\mathbf{A}} \cdot \mathbf{A}^{-1}$  is skew-symmetrical:

$$\dot{\mathbf{A}} \cdot \mathbf{A}^{-1} = -(\dot{\mathbf{A}} \cdot \mathbf{A}^{-1})^T = -\mathbf{A}^{-T} \cdot \dot{\mathbf{A}}^T \quad (2.6.22)$$

and the objective rates  $\overset{\Delta}{\mathbf{G}}$  and  $\overset{\nabla}{\mathbf{G}}$  of a tensor  $\mathbf{G}$  are identical:

$$\overset{\Delta}{\mathbf{G}} = \overset{\nabla}{\mathbf{G}} = \dot{\mathbf{G}} - \dot{\mathbf{A}} \cdot \mathbf{A}^{-1} \cdot \mathbf{G} + \mathbf{G} \cdot \dot{\mathbf{A}} \cdot \mathbf{A}^{-1} \quad (2.6.23)$$

Based on the following choices for  $\mathbf{H}$ ;, very well-known rates of this type are the Jaumann rate:

$$\dot{\mathbf{A}} \cdot \mathbf{A}^{-1} = \Omega = \frac{1}{2} (\dot{\mathbf{F}} \cdot \mathbf{F}^{-1} - \mathbf{F}^{-T} \cdot \dot{\mathbf{F}}^T) \quad (2.6.24)$$

and the Dienes rate:

$$\dot{\mathbf{A}} \cdot \mathbf{A}^{-1} = \dot{\mathbf{R}} \cdot \mathbf{R}^T \quad \text{and so} \quad \dot{\mathbf{A}} = \mathbf{A} \cdot \dot{\mathbf{R}} \cdot \mathbf{R}^T \quad (2.6.25)$$

In literature other objective rates are often used in which  $\mathbf{A}$  is not a rotation tensor. Some of these rates will be discussed in the next chapter.

If  $\mathbf{A}$  is a rotation tensor, then the constitutive equation 2.6.19 reduces to:

$$\begin{aligned} \frac{1}{E_1} \overset{\nabla}{\sigma} + \left( \frac{1}{E_1} \text{tr}(\mathbf{D}) + \frac{1}{\lambda} \right) \sigma = \frac{1}{J} \left( \frac{\mu}{E_1} \overset{\nabla}{\mathbf{D}} + \left( 1 + \frac{\mu}{\lambda} + \frac{\dot{\mu}}{E_1} \right) \mathbf{D} + \right. \\ \left. + \left( \frac{E_2}{E_1} \text{tr}(\mathbf{D}) + \frac{\alpha - \varepsilon}{\lambda} \theta + \frac{\alpha}{E_1} \dot{\theta} \right) \mathbf{I} \right) \end{aligned} \quad (2.6.26)$$

where  $\overset{\nabla}{\sigma}$  and  $\overset{\nabla}{\mathbf{D}}$  follow from 2.6.22 and 2.6.23 by replacing  $\mathbf{G}$  by  $\sigma$  and  $\mathbf{D}$  respectively. The model represented by 2.6.26 is an extension of the 'so-called Oldroyd model that is described by, for instance, Crochet, Davies and Walters (1984). These authors only considered the case in which the material is incompressible and the temperatures is not taken into account. Then the model reduces to:

$$\sigma = -p\mathbf{I} + \tau \quad ; \quad \text{tr}(\mathbf{D}) = 0 \quad (2.6.27)$$

$$\frac{1}{E_1} \overset{\nabla}{\tau} + \frac{1}{\lambda} \tau = \frac{\mu}{E_1} \overset{\nabla}{\mathbf{D}} + \left( 1 + \frac{\mu}{\lambda} + \frac{\dot{\mu}}{E_1} \right) \mathbf{D} \quad (2.6.28)$$

For  $\mu = 0$  this model reduces to the so-called Maxwell model. The relationship between  $\tau$  and  $\mathbf{D}$  then becomes:

$$\frac{1}{E_1} \overset{\nabla}{\tau} + \frac{1}{\lambda} \tau = \mathbf{D} \quad (2.6.29)$$

## 2.7 Elastic-plastic models with hardening

The models in this subparagraph are based on the assumption that the free energy  $\psi$  depends not only on the total strain tensor  $\bar{\mathbf{C}}$  and the temperature  $\theta$  but also on a hidden scalar variable  $q$  and a hidden tensorial variable  $\mathbf{Q}$ :

$$\psi = \psi(\bar{\mathbf{C}}, \theta, \mathbf{Q}, q) \quad (2.7.1)$$

With respect to  $\mathbf{Q}$ , it is assumed that this tensor represents the plastic part of the total deformation. This interpretation of  $\mathbf{Q}$  means that  $\psi$  will not depend on  $\bar{\mathbf{C}}$  and  $\mathbf{Q}$  separately, but on the difference  $\bar{\mathbf{C}} - \mathbf{Q}$  of these tensors:

$$\psi = \psi(\bar{\mathbf{C}} - \mathbf{Q}, \theta, q) \quad (2.7.2)$$

From this relationship and 2.2.14, it immediately follows that:

$$\bar{\mathbf{S}} = \rho_0 \frac{\partial \psi}{\partial \bar{\mathbf{C}}} + \mu \dot{\bar{\mathbf{C}}} = -\rho_0 \frac{\partial \psi}{\partial \mathbf{Q}} + \mu \dot{\bar{\mathbf{C}}} \quad (2.7.3)$$

and hence the Clausius-Duhem inequality 2.2.7 becomes:

$$-\dot{\pi} - \mu \dot{\bar{\mathbf{C}}} : (\dot{\bar{\mathbf{C}}} - \dot{\bar{\mathbf{Q}}}) + \rho_0 \frac{\partial \psi}{\partial q} \dot{q} \leq 0 \quad (2.7.4)$$

Here,  $\pi$  is the so-called plastic work, defined by:

$$\pi = \int_0^t \bar{\mathbf{S}} : \dot{\bar{\mathbf{Q}}} dt \quad (2.7.5)$$

The third assumption in this section is that the viscosity may be neglected, which means that  $\mu = 0$ . As a consequence of this assumption the stress tensor  $\bar{\mathbf{S}}$  will be a function of  $\bar{\mathbf{C}} - \bar{\mathbf{Q}}$ ,  $\theta$  and  $q$ :

$$\bar{\mathbf{S}} = \rho_0 \frac{\partial \psi}{\partial \bar{\mathbf{C}}} = \bar{\mathbf{S}}(\bar{\mathbf{C}} - \bar{\mathbf{Q}}, \theta, q) \quad (2.7.6)$$

Furthermore, the Clausius-Duhem inequality reduces to:

$$-\dot{\pi} + \rho_0 \frac{\partial \psi}{\partial q} \dot{q} \leq 0 \quad (2.7.7)$$

As already stated before in section 2.2, the completion of this model requires the specification of the evolution equations 2.2.15 for  $\dot{q}$  and  $\dot{\bar{\mathbf{Q}}}$ . According to 2.2.15 and the definition of  $\tilde{\chi}$  in 2.2.6,  $\dot{q}$  and  $\dot{\bar{\mathbf{Q}}}$  must be specified as a function of  $\bar{\mathbf{C}} - \bar{\mathbf{Q}}$ ,  $\theta$  and  $q$ . Because of 2.6.6 this requirement is fulfilled when  $\dot{q}$  and  $\dot{\bar{\mathbf{Q}}}$  are specified in terms of  $\bar{\mathbf{S}}$ ,  $\theta$  and  $q$ . With respect to  $\dot{\bar{\mathbf{Q}}}$ , it is assumed that there exists a function  $\phi = \phi(\bar{\mathbf{S}}, \theta, q)$ , such that:

$$\dot{\bar{\mathbf{Q}}} = \frac{\partial \phi}{\partial \bar{\mathbf{S}}} \quad (2.7.8)$$

This function  $\phi$  is called the plastic potential and the relationship 2.7.8 is known as the flow rule. For isotropic materials it is common practice to assume that the plastic potential only depends on the second invariant  $\bar{\mathbf{S}}^d : \bar{\mathbf{S}}^d$  of the deviatoric stress tensor  $\bar{\mathbf{S}}^d = \bar{\mathbf{S}} - \frac{1}{3} \text{tr}(\bar{\mathbf{S}}) \mathbf{I}$ :

$$\phi = \phi(H, \theta, q) \quad ; \quad H = \sqrt{\frac{3}{2} \bar{\mathbf{S}}^d : \bar{\mathbf{S}}^d} \quad (2.7.9)$$

Then the flow rule turns out to be given by:

$$\dot{\bar{\mathbf{Q}}} = \frac{3}{2} \frac{1}{H} \frac{\partial \phi}{\partial H} \mathbf{S}^d \quad (2.7.10)$$

In practice it is often assumed that the free energy is quadratic in the strain tensor  $\bar{\mathbf{C}} - \mathbf{Q}$  and that  $\psi$  is given by:

$$\psi = \frac{1}{2} (\bar{\mathbf{C}} - \mathbf{Q}) : {}^4\mathbf{E} : (\bar{\mathbf{C}} - \mathbf{Q}) + g(\theta, q) \quad ; \quad {}^4\mathbf{E} = E_1 {}^4\mathbf{I} + E_2 \mathbf{II} \quad (2.7.11)$$

It follows from 2.7.6 and 2.7.10 that:

$$\frac{1}{\rho_0} \dot{\bar{\mathbf{S}}} + \frac{3}{2} \frac{1}{H} \frac{\partial \phi}{\partial H} {}^4\mathbf{E} : \bar{\mathbf{S}}^\sigma = {}^4\mathbf{E} : \dot{\bar{\mathbf{C}}} \quad (2.7.12)$$

This Maxwell model is a very well-known constitutive relationship for elastic-plastic materials. It can be brought into an even better known form, by using  $\bar{\mathbf{S}} = \mathbf{J} \cdot \mathbf{A}^{-1} \cdot \boldsymbol{\sigma} \cdot \mathbf{A}^{-T}$  and  $\dot{\bar{\mathbf{C}}} = \mathbf{A}^T \cdot \mathbf{D} \cdot \mathbf{A}$ , and by considering the case where  $\mathbf{A}$  is a rotation tensor, i.e.  $\mathbf{A}^T \cdot \mathbf{A} = \mathbf{I}$ . With the notation of section 2.6 it can be easily seen that the constitutive relationship 2.7.12 becomes:

$$\frac{1}{\rho_0} (\overset{\nabla}{\boldsymbol{\sigma}} + \text{tr}(\mathbf{D})\boldsymbol{\sigma}) + \frac{3}{2} \frac{1}{H} \frac{\partial \phi}{\partial H} {}^4\mathbf{E} : \boldsymbol{\sigma}^\sigma = \frac{1}{J} {}^4\mathbf{E} : \mathbf{D} \quad (2.7.13)$$

Here  $\overset{\nabla}{\boldsymbol{\sigma}}$  is the Jaumann rate when  $\mathbf{A}$  satisfies 2.6.24, or the Dienes rate when  $\mathbf{A}$  satisfies 2.6.25. Constitutive equations of this type are commonly used in the field of plasticity (see for example, Nagtegaal and De Jong (1980)).

Until now no statements have been made concerning the hidden variable  $q$ . This variable will bring in the phenomenon 'hardening', which can be observed for metals. With respect to this variable two cases will be considered in this section: work hardening and strain hardening. In the first case it will be assumed that  $q$  equals the plastic work  $\pi$ , which has been defined in 2.7.5:

$$q = \pi \quad (2.7.14)$$

This choice for  $q$  implies that  $\psi$  and  $\bar{\mathbf{S}}$  become functions of  $\bar{\mathbf{C}} - \mathbf{Q}$ ,  $\theta$  and  $\pi$ :

$$\psi = \psi(\bar{\mathbf{C}} - \mathbf{Q}, \theta, \pi) \quad ; \quad \bar{\mathbf{S}} = \rho_0 \frac{\partial \psi}{\partial \bar{\mathbf{C}}} = \bar{\mathbf{S}}(\bar{\mathbf{C}} - \mathbf{Q}, \theta, \pi) \quad (2.7.15)$$

Besides, the inequality 2.7.7 now becomes:

$$(1 - h_\pi) \dot{\pi} \geq 0 \quad (2.7.16)$$

where  $h_\pi$  is the so-called work hardening function:

$$h_\pi = \rho_0 \frac{\partial \psi}{\partial \pi} \quad (2.7.17)$$

From the definition 2.7.5 of  $\pi$  it can be seen that:

$$\dot{\pi} = \bar{\mathbf{S}} : \dot{\mathbf{Q}} = \bar{\mathbf{S}} : \frac{\partial \phi}{\partial \bar{\mathbf{S}}} = H \frac{\partial \phi}{\partial H} \quad (2.7.18)$$

and 2.7.16 reduces to:

$$(1 - h_\pi) \frac{\partial \phi}{\partial H} \geq 0 \quad (2.7.19)$$

With the choice for the hidden variable  $q$  the constitutive model is completely determined as soon as the plastic potential  $\phi = \phi(\bar{\mathbf{S}}, \pi, \theta)$  is specified. From 2.7.12 and 2.7.19 it follows that in fact only the partial derivative of  $\phi$  to  $H$  must be determined. This function can easily be determined experimentally by using relationship 2.7.18. A material with a constitutive model of this kind is called an elastic-plastic material with work hardening.

In the second case, it is assumed that  $q$  equals the so-called equivalent plastic strain  $\bar{\varepsilon}$ . This strain is defined by:

$$\bar{\varepsilon} = \int_0^t \sqrt{\frac{2}{3} \dot{\mathbf{Q}} : \dot{\mathbf{Q}}} \, d\tau \quad (2.7.20)$$

Then  $\psi$  and  $\bar{\mathbf{S}}$  become:

$$\psi = \psi(\bar{\mathbf{C}} - \mathbf{Q}, \theta, \bar{\varepsilon}) \quad ; \quad \bar{\mathbf{S}} = \bar{\mathbf{S}}(\bar{\mathbf{C}} - \mathbf{Q}, \theta, \bar{\varepsilon}) \quad (2.7.21)$$

From the definitions of  $\pi$  and  $\bar{\varepsilon}$  it follows that:

$$\dot{\bar{\varepsilon}} = \left| \frac{\partial \phi}{\partial H} \right| = \frac{1}{H} |\dot{\pi}| \quad (2.7.22)$$

and furthermore that the inequality 2.7.7 becomes:

$$\frac{\dot{\pi}}{|\dot{\pi}|} - \frac{h_{\bar{\varepsilon}}}{H} \geq 0 \quad (2.7.23)$$

Here,  $h_{\bar{\varepsilon}}$  is the so-called strain hardening function, defined by:

$$h_{\bar{\varepsilon}} = \rho_0 \frac{\partial \psi}{\partial \bar{\varepsilon}} \quad (2.7.24)$$

In this constitutive model  $\psi$  or the partial derivative of  $\psi$  to  $H$  still has to be determined. Again this can easily be done experimentally with relationship 2.7.22. A material with

a constitutive model of this kind is called an elastic-plastic material with strain hardening. These models are commonly used in the field of plasticity.

## 2.8 Materials of type N

In the previous subparagraph the hidden scalar variable  $q$  was chosen to be either the plastic work or the plastic strain. This means that in both cases  $q$  was defined by giving it a physical meaning. In the other subparagraphs of this chapter, however,  $q$  was defined by prescribing its rate  $\dot{q}$ . This is also done in this subparagraph, but in such a way that the rate of  $q$  obeys a certain normality rule, as did the plastic strain rate  $\dot{\mathbf{Q}}$  in the previous section.

The first assumption for materials of type N are that relationships 2.7.2 and 2.7.6 hold for these materials:

$$\psi = \psi(\bar{\mathbf{C}} - \mathbf{Q}, \theta, q) \quad ; \quad \bar{\mathbf{S}} = \rho_0 \frac{\partial \psi}{\partial \bar{\mathbf{C}}} = \bar{\mathbf{S}}(\bar{\mathbf{C}} - \mathbf{Q}, \theta, q) \quad (2.8.1)$$

The second assumption is that there exists a plastic potential  $\phi = \phi(\bar{\mathbf{S}}, h, \theta)$ , such that (see Kim and Oden (1984) and (1985)):

$$\dot{\mathbf{Q}} = \frac{\partial \phi}{\partial \bar{\mathbf{S}}} \quad ; \quad \dot{q} = \frac{\partial \phi}{\partial h} \quad (2.8.2)$$

where  $h$  is called the hardening function, that is defined by:

$$h = \rho_0 \frac{\partial \psi}{\partial q} \quad (2.8.3)$$

In this subparagraph the same simplifications will be considered for  $\psi$  and  $\phi$  as considered in relationships 2.7.9 and 2.7.12:

$$\psi = \frac{1}{2} (\bar{\mathbf{C}} - \mathbf{Q}) : {}^4\mathbf{E} : (\bar{\mathbf{C}} - \mathbf{Q}) + g(\theta, q) \quad ; \quad \phi = \phi(H, h, \theta) \quad (2.8.4)$$

This means that the same constitutive relationship is obtained as in relationship 2.7.12. The Clausius-Duhem inequality 2.7.7 is reduced to:

$$\left( H \frac{\partial \phi}{\partial H} - h \frac{\partial \phi}{\partial h} \right) \geq 0 \quad (2.8.5)$$

Kim and Oden (1984 and 1985) suggested the following choices for  $\psi$  and  $\phi$

$$\psi = \frac{1}{2}(\bar{\mathbf{C}} - \mathbf{Q}) : {}^4\mathbf{E} : (\bar{\mathbf{C}} - \mathbf{Q}) - h_1 q - \frac{1}{m}(h_1 - h_0)e^{-mq} \quad (2.8.6)$$

$$\phi = D_0 \sum_{i=0}^{\infty} (-1)^i \frac{B^i}{i! (2ni - 1)} \left(\frac{h}{H}\right)^{2ni-1} \quad (2.8.7)$$

Substituting this equation into 2.7.12, the following constitutive relationship is obtained:

$$-{}^4\mathbf{E} : \dot{\bar{\mathbf{S}}} - \frac{3D_0}{2hH} e^{-B(\frac{h}{H})^{2n}} \mathbf{S}^d = \dot{\bar{\mathbf{C}}} \quad (2.8.8)$$

This constitutive model was first proposed by Bodner and Partom (1975). Kim and Oden (1985) developed a numerical solution strategy for this model in the case, where the Dienes rate is used (see 2.7.13). The variables  $h$  and  $q$  follow from 2.8.2 and 2.8.3:

$$h = \rho_0 \frac{\partial \psi}{\partial q} = -\rho_0 (h_1 + (h_0 - h_1)e^{-mq}) \quad (2.8.9)$$

$$\dot{q} = \frac{\partial \phi}{\partial h} = -\frac{\dot{\pi}}{h} = \frac{HD_0}{h^2} e^{-B(\frac{h}{H})^{2n}} \quad (2.8.10)$$

Finally it can be easily deduced that this model obeys the Clausius-Duhem inequality 2.8.5.

One may wonder whether the work and strain hardening materials, that discussed in the previous section, can be of type N. For work hardening materials relationship 2.7.18 must hold and for materials of type N relationship 2.8.2 must hold. A combination of these requirements leads to :

$$\dot{q} = \dot{\pi} = H \frac{\partial \phi}{\partial H} = \frac{\partial \phi}{\partial h} \quad (2.8.11)$$

This requirement can be satisfied, if the plastic potential can be expressed as follows:

$$\phi = \phi(He^h, \theta) \quad (2.8.12)$$

If the inverse of the relationship for  $\dot{\pi}$  in 2.8.11 exists and if relationship 2.8.4 holds, this result means that the stress  $H$  can be expressed as follows in terms of the plastic work  $\pi$  and the plastic work rate  $\dot{\pi}$ :

$$H = f_1(\pi, \theta) f_2(\dot{\pi}, \theta) \quad (2.8.13)$$

A similar result can be obtained for strain hardening materials. Relationships 2.7.22 and 2.8.2 give:

$$\dot{\bar{\epsilon}} = \frac{\partial \phi}{\partial H} = \frac{\partial \phi}{\partial h} \quad (2.8.14)$$

From this requirement it follows that  $\phi$  must be a function of  $H + h$ :

$$\phi = \phi(H + h, \theta) \quad (2.8.15)$$

and that the stress  $H$  can be expressed by an addition of two functions, which depend on the plastic strain and the plastic strain rate respectively:

$$H = f_1(\bar{\epsilon}, \theta) + f_2(\dot{\bar{\epsilon}}, \theta) \quad (2.8.16)$$

## 2.9 Some final remarks

In this chapter visco-elastic and elastic-plastic models have been considered. The bases were the definition of a pseudo strain tensor  $\bar{\mathbf{C}}$ , with corresponding stress tensor  $\bar{\mathbf{S}}$ , and the theory of the hidden variables in thermodynamics. It has been shown that with this theory Oldroyd and Maxwell models were obtained, where the objective rate for the Cauchy stress can be the Jaumann or the Dienes rate. This means that these models are thermodynamically speaking completely acceptable.

The use of these objective rates has been the point of much discussion in literature. In the next chapter, objective rates will be discussed in more detail. From other starting points similar visco-elastic models will be obtained, although mostly with the use of other objective rates.

The models obtained in this chapter can be considered as definitions of classes of material behaviour. Experiments must determine whether a certain material fits such a model.



## 3 The decomposition of constitutive equations

### 3.1 Introduction

As already discussed in the last subparagraph of chapter 1, a very common way of deriving constitutive equations is by decomposing the Cauchy stress tensor  $\sigma$  and the deformation rate tensor  $D$ . It is then assumed that:

- The Cauchy stress tensor  $\sigma$  can be decomposed into two parts:

$$\sigma = \sigma_1 + \sigma_2 \quad (3.1.1)$$

For incompressible materials the Cauchy stress tensor is decomposed into three parts:

$$\sigma = -pI + \tau = -pI + \tau_1 + \tau_2 \quad (3.1.2)$$

The Cauchy stress is a constitutive quantity, which is in fact defined in terms of the state variables. This means that the decomposition only adds two constitutive quantities to the list in subparagraph 1.3 and these quantities are also to be defined in terms of the state variables. The total stress or one of the decomposed parts is denoted by  $\sigma_{(i)}$  in 3.1.1 and by  $\tau_{(i)}$  in 3.1.2 respectively.

- The deformation rate tensor  $D$  consists of an elastic and a viscous or plastic part:

$$D = D_e + D_v \quad (3.1.3)$$

Interpreting the decomposition of the deformation rate tensor is a problem since  $D$  is a well-defined kinematical quantity. Several interpretations have been given in literature. Some of them will be discussed in subparagraph 3.1, and their usefulness assessed.

- For the viscous part of the deformation the deviatoric part of  $\sigma_{(i)}$  is proportional to  $D_v$ :

$$\sigma_{(i)}^d = \eta D_v \quad (3.1.4)$$

and for the elastic part an objective rate  $\overset{\nabla}{\sigma}_{(t)}$  of  $\sigma_{(t)}$  is proportional to  $\mathbf{D}_e$  :

$$\overset{\nabla}{\sigma}_{(t)} = {}^4\mathbf{E}:\mathbf{D}_e \quad (3.1.5)$$

For incompressible materials these relationships become:

$$\tau_{(t)} = \eta\mathbf{D}_v \quad \text{and} \quad \overset{\nabla}{\tau}_{(t)} = {}^4\mathbf{E}:\mathbf{D}_e \quad (3.1.6)$$

An other important problem is to decide which objective rate  $\overset{\nabla}{\sigma}$  can or should be used. This problem is discussed in subparagraph 3.3, where the definition of elasticity from subparagraph 2.4 is the starting point.

## 3.2 The decomposition of the deformation rate tensor

Additive decomposition of the deformation rate tensor  $\mathbf{D}$  in an elastic part  $\mathbf{D}_e$  and a viscous part  $\mathbf{D}_v$  yields:

$$\mathbf{D} = \mathbf{D}_e + \mathbf{D}_v \quad (3.2.1)$$

Since  $\mathbf{D}$  is objective,  $\mathbf{D}_e$  is proportional to the objective stress rate and  $\mathbf{D}_v$  is proportional to the deviatoric part of the Cauchy stress, it is required that both  $\mathbf{D}_e$  and  $\mathbf{D}_v$  are objective:

$$\bar{\mathbf{D}}_e = \mathbf{Q}:\mathbf{D}_e:\mathbf{Q}^T \quad ; \quad \bar{\mathbf{D}}_v = \mathbf{Q}:\mathbf{D}_v:\mathbf{Q}^T \quad (3.2.2)$$

Here, the rotation tensor  $\mathbf{Q}$  represents an arbitrary rigid body rotation in the current state and  $\bar{\mathbf{D}}_e$  and  $\bar{\mathbf{D}}_v$  are the elastic and viscous deformation rate tensors in the rotated current state.

In literature many definitions of either  $\mathbf{D}_e$  or  $\mathbf{D}_v$  are proposed, each with its own kinematical interpretation. The other tensor, i.e.  $\mathbf{D}_v$  or  $\mathbf{D}_e$ , then follows from 3.2.1. In the sequel, some definitions, of which some are commonly used, are considered in more detail, with special attention to the objectivity of the resulting tensors  $\mathbf{D}_e$  and  $\mathbf{D}_v$ . Each definition, resulting in non-objective tensors  $\mathbf{D}_e$  and  $\mathbf{D}_v$ , is considered to be unacceptable.

To define  $\mathbf{D}_v$  and  $\mathbf{D}_e$  usually a so-called unloaded state  $S_0$  is introduced. This is generally an imaginary state in which the body is seen as a set of uncoupled, unstressed

infinitesimally small material elements, and which can be attained from the current state  $S$ , by relaxing the stresses on each of the material elements. For each element it is assumed that the deformation from  $S$ , with respect to  $S_v$ , is purely elastic and is uniquely defined up to a rigid rotation. Let  $x$  be the position vector of a material point in the current state  $S$ , and let  $x_v$  be the position vector of the same material point in the unloaded state  $S_v$ , then is the deformation tensor  $F_e$  of the state  $S$ , with respect to the unloaded state  $S_v$ , defined by:

$$F_e = \frac{\partial x}{\partial x_v} \quad (3.2.3)$$

and let  $V_e$  be the Cauchy strain tensor in the polar decomposition of  $F_e$ :

$$F_e = V_e R_e ; \quad R_e R_e^T = I ; \quad \det(R_e) = 1 \quad (3.2.4)$$

Then  $V_e$  is uniquely determined by the elastic unloading from  $S$  to  $S_v$ , while the definition of the rotation tensor  $R_e$  is still completely free, as the unloaded state was defined up to a rigid rotation.

The deformation tensor of the unloaded state  $S_v$  with respect to the reference state  $S_0$  is denoted by  $F_v$ . Then, the deformation tensor  $F$  of  $S$ , with respect to  $S_0$  and the tensors  $F_e$  and  $F_v$ , are related by:

$$F = F_e F_v = V_e R_e F_v \quad (3.2.5)$$

If the body, in current state, undergoes a rigid rotation  $Q$ , the tensor  $F$  transforms according to:

$$\bar{F} = Q F \quad (3.2.6)$$

The transformation rule for  $R_e$  is not only derived from the rigid body rotation  $Q$  of the current state, but also from an independent rigid body rotation  $Q_v$  of the unloaded state, because the unloaded state was uniquely defined up to a rigid body rotation. From 3.2.5 and 3.2.6 it can be easily seen that the transformation rules for  $V_e$ ,  $R_e$  and  $F_v$  will be given by:

$$\bar{V}_e = Q V_e Q^T ; \quad \bar{R}_e = Q R_e Q_v^T , \quad \bar{F}_v = Q_v F_v \quad (3.2.7)$$

Nemet-Nasser (1979,1982) proposed to define the viscous deformation rate tensor  $D_v$  by:

$$D_v = \frac{1}{2} (\dot{F}_v F^{-1} + (\dot{F}_v F^{-1})^T) \quad (3.2.8)$$

With the transformation rules 3.2.6 and 3.2.7 for  $F$  and  $F_v$ , the transformation rule for  $D_v$  is given by:

$$\begin{aligned} \bar{D}_v = & \mathbf{Q} \cdot \mathbf{D}_v \cdot \mathbf{Q}^T + \frac{1}{2} \mathbf{Q} \cdot (\mathbf{Q}^T \cdot \dot{\mathbf{Q}}_v \cdot \mathbf{F}_v \cdot \mathbf{F}^{-1} + (\mathbf{Q}^T \cdot \dot{\mathbf{Q}}_v \cdot \mathbf{F}_v \cdot \mathbf{F}^{-1})^T) \cdot \mathbf{Q}^T + \\ & \frac{1}{2} \mathbf{Q} \cdot ((\mathbf{Q}^T \cdot \mathbf{Q}_v - \mathbf{I}) \cdot \dot{\mathbf{F}}_v \cdot \mathbf{F}^{-1} + ((\mathbf{Q}^T \cdot \mathbf{Q}_v - \mathbf{I}) \cdot \dot{\mathbf{F}}_v \cdot \mathbf{F}^{-1})^T) \cdot \mathbf{Q}^T \end{aligned} \quad (3.2.9)$$

Comparison of this result with the objectivity requirement 3.2.2, yields that  $\mathbf{Q}_v$  has to satisfy:

$$\mathbf{Q}^T \cdot \mathbf{Q}_v = \mathbf{I} \quad \text{and} \quad \mathbf{Q}^T \cdot \dot{\mathbf{Q}}_v = 0 \quad \text{for } \forall \mathbf{Q} \quad (3.2.10)$$

This means that  $\mathbf{Q}$  should be constant, a requirement that can't be satisfied. Hence, using the definition 3.2.8 according to Nemet-Nasser, there is no choice for  $\mathbf{Q}_v$ , and therefore no definition of  $\mathbf{R}_e$ , for which  $\mathbf{D}_v$  is objective. This means that Nemet-Nasser's definition of the viscous deformation rate tensor  $\mathbf{D}_v$  is unacceptable.

Lee (1969,1981) proposed a definition for both  $\mathbf{D}_e$  and  $\mathbf{D}_v$ :

$$\mathbf{D}_e = \frac{1}{2} (\dot{\mathbf{F}}_e \cdot \mathbf{F}_e^{-1} + (\dot{\mathbf{F}}_e \cdot \mathbf{F}_e^{-1})^T) ; \quad \mathbf{D}_v = \frac{1}{2} (\dot{\mathbf{F}}_v \cdot \mathbf{F}_v^{-1} + (\dot{\mathbf{F}}_v \cdot \mathbf{F}_v^{-1})^T) \quad (3.2.11)$$

However the sum of these proposed tensors is not equal to  $\mathbf{D}$ , which means that 3.2.1 is not satisfied. This can be corrected by a slight modification of the definition of  $\mathbf{D}_v$ , and by maintaining the definition of  $\mathbf{D}_e$ . After this modification,  $\mathbf{D}_v$  is given by:

$$\mathbf{D}_v = \mathbf{D} - \mathbf{D}_e = \frac{1}{2} (\mathbf{F}_e \cdot \dot{\mathbf{F}}_v \cdot \mathbf{F}_v^{-1} \cdot \mathbf{F}_e^{-1} + (\mathbf{F}_e \cdot \dot{\mathbf{F}}_v \cdot \mathbf{F}_v^{-1} \cdot \mathbf{F}_e^{-1})^T) \quad (3.2.12)$$

A lengthy but straight-forward calculation now yields:

$$\bar{D}_v = \mathbf{Q} \cdot \mathbf{D}_v \cdot \mathbf{Q}^T + \frac{1}{2} \mathbf{Q} \cdot (\mathbf{F}_e \cdot \mathbf{Q}_v^T \cdot \dot{\mathbf{Q}}_v \cdot \mathbf{F}_e^{-1} + (\mathbf{F}_e \cdot \mathbf{Q}_v^T \cdot \dot{\mathbf{Q}}_v \cdot \mathbf{F}_e^{-1})^T) \cdot \mathbf{Q}^T \quad (3.2.13)$$

and this means that  $\mathbf{D}_v$  is objective, only if  $\mathbf{Q}_v^T \cdot \dot{\mathbf{Q}}_v = 0$ , which means that  $\mathbf{Q}_v$  is constant. Since  $\mathbf{Q}_v = \mathbf{I}$  in the reference state, it can be seen that  $\mathbf{D}_v$  is objective if and only if  $\mathbf{Q}_v = \mathbf{I}$ . In this case, the transformation rules for  $\mathbf{F}_e$ ,  $\mathbf{F}_v$  and  $\mathbf{R}_e$  become:

$$\bar{\mathbf{F}}_e = \mathbf{Q} \cdot \mathbf{F}_e ; \quad \bar{\mathbf{F}}_v = \mathbf{F}_v ; \quad \bar{\mathbf{R}}_e = \mathbf{Q} \cdot \mathbf{R}_e \quad (3.2.14)$$

This is the case if the unloaded state  $S$ , is invariant for all rigid body rotations of the current state. It can therefore be concluded that the modified definition 3.2.12 of Lee for  $\mathbf{D}_v$  is acceptable, if the rotation tensor  $\mathbf{Q}_v$  equals the identity tensor  $\mathbf{I}$ . This conclusion is in complete agreement with Besseling (1968) and Van der Heyden and Besseling (1984), who referred to the invariant unloaded state as the natural reference state.

As a third example, the definition of  $\mathbf{D}_v$ , according to Kim and Oden (1985), is considered. Starting from the polar decomposition of  $\mathbf{F}$ ,

$$\mathbf{F} = \mathbf{R} \cdot \mathbf{U} ; \mathbf{R} \cdot \mathbf{R}^T = \mathbf{I} ; \det(\mathbf{R}) = 1 \quad (3.2.15)$$

they defined  $\mathbf{D}_v$  by:

$$\mathbf{D}_v = \frac{1}{2} \mathbf{R} \cdot (\dot{\mathbf{K}}_v \cdot \mathbf{U}^{-1} + (\dot{\mathbf{K}}_v \cdot \mathbf{U}^{-1})^T) \cdot \mathbf{R}^T \quad (3.2.16)$$

where  $\mathbf{K}_v$  is given by:

$$\mathbf{K}_v = \mathbf{R}^T \cdot \mathbf{F}_v \quad (3.2.17)$$

In general, it is noted that  $\mathbf{K}_v$  is not the elongation tensor  $\mathbf{U}_v$  from the polar decomposition of  $\mathbf{F}_v$  and, furthermore, that  $\mathbf{K}_v$  is not a symmetrical tensor. In this case it can be shown that:

$$\bar{\mathbf{D}}_v = \mathbf{D}_v + \frac{1}{2} \mathbf{Q} \cdot \mathbf{R} \cdot ((\bar{\mathbf{K}}_v - \dot{\mathbf{K}}_v) \cdot \mathbf{U}^{-1} + ((\bar{\mathbf{K}}_v - \dot{\mathbf{K}}_v) \cdot \mathbf{U}^{-1})^T) \cdot \mathbf{R}^T \cdot \mathbf{Q}^T \quad (3.2.18)$$

where  $\bar{\mathbf{K}}_v = \mathbf{R}^T \cdot \mathbf{Q}^T \cdot \mathbf{Q}_v \cdot \mathbf{R} \cdot \mathbf{K}_v$ .

This result implies that  $\mathbf{D}_v$  is objective if and only if  $\bar{\mathbf{K}}_v = \mathbf{K}_v$ , a requirement, which can only be met if  $\mathbf{Q}_v = \mathbf{Q}$  for all  $\mathbf{Q}$ . From 3.2.7, it can be seen that the definition of  $\mathbf{D}_v$ , according to Kim and Oden, is acceptable if and only if the definition of the tensors  $\mathbf{F}_e$ ,  $\mathbf{F}_v$  and  $\mathbf{R}_e$  involve the transformation rules for these tensors being given by:

$$\bar{\mathbf{F}}_e = \mathbf{Q} \cdot \mathbf{F}_e \cdot \mathbf{Q}^T ; \bar{\mathbf{F}}_v = \mathbf{Q} \cdot \mathbf{F}_v ; \bar{\mathbf{R}}_e = \mathbf{Q} \cdot \mathbf{R}_e \cdot \mathbf{Q}^T \quad (3.2.19)$$

This means that the unloaded state  $S_v$  will not be invariant for rigid body rotations of the current state S: if the current state undergoes a rigid rotation  $\mathbf{Q}$ , the unloaded state has to undergo the same rigid rotation  $\mathbf{Q}$ .

Finally a slight modification is considered, with respect to Kim and Oden's definition. The elongation tensor  $\mathbf{U}_v$  from the polar decomposition  $\mathbf{F}_v$  is introduced for this purpose:

$$\mathbf{U}_v = \mathbf{R}_v^T \cdot \mathbf{F}_v \quad (3.2.20)$$

where  $\mathbf{U}_v$  is a symmetric, positive-definite tensor. The transformation rules for the tensors  $\mathbf{U}_v$  and  $\mathbf{R}_v$  follow from the definition of  $\mathbf{F}_v$  in 3.2.5 and from the transformation rules in 3.2.7:

$$\bar{\mathbf{R}}_v = \mathbf{Q}_v \cdot \mathbf{R}_v ; \bar{\mathbf{U}}_v = \mathbf{U}_v \quad (3.2.21)$$

For  $\mathbf{D}_v$  a definition similar to that in 3.2.16 is used:

$$\mathbf{D}_v = \frac{1}{2} \mathbf{R} \cdot (\dot{\mathbf{U}}_v \mathbf{U}^{-1} + (\dot{\mathbf{U}}_v \mathbf{U}^{-1})^T) \cdot \mathbf{R}^T \quad (3.2.22)$$

From this definition, and the fact that  $\mathbf{U}_v$  and  $\mathbf{U}$  are invariant tensors, it can easily be seen that:

$$\bar{\mathbf{D}}_v = \mathbf{Q} \cdot \mathbf{D}_v \cdot \mathbf{Q}^T \quad (3.2.23)$$

This means that the rigid body rotations of the unloaded state  $S_v$  can be chosen completely independently of the rigid body rotations of the original state  $S$ .

### 3.3 Rate type constitutive equations for elastic bodies

The ultimate aim of the decomposition  $\mathbf{D} = \mathbf{D}_e + \mathbf{D}_v$  is to formulate constitutive equations for certain classes of material behaviour. An essential step in this approach

is the specification of the elastic part of the constitutive equation  $\overset{\nabla}{\boldsymbol{\sigma}} = {}^4\mathbf{L} : \mathbf{D}_e$ , which re-

lates an objective stress rate  $\overset{\nabla}{\boldsymbol{\sigma}}$  of the Cauchy stress to the elastic part of the deformation rate tensor  $\mathbf{D}_e$ . Some of the possible definitions for  $\mathbf{D}_e$  were discussed in subparagraph 3.2. The objective rate and the proportionality tensor  ${}^4\mathbf{L}$  still have to be

specified. The purpose of this subparagraph is to analyse which  $\overset{\nabla}{\boldsymbol{\sigma}}$  is acceptable for a

given  ${}^4\mathbf{L}$  in such a way that the rate type equation  $\overset{\nabla}{\boldsymbol{\sigma}} = {}^4\mathbf{L} : \mathbf{D}_e$  results in a correct description of elastic behaviour, as defined in subparagraph 2.4. For this purpose  $\mathbf{D}_e$  can be replaced by  $\mathbf{D}$ .

Only isotropic elastic behaviour will be considered in this subparagraph. The tensor  ${}^4\mathbf{L}$  is then given by:

$${}^4\mathbf{L} = \mu_1 {}^4\mathbf{I} + \mu_2 \mathbf{I} \mathbf{I} \quad (3.3.1)$$

where  $\mu_1$  and  $\mu_2$  may be functions of the invariants of the strain tensor  $\mathbf{B} = \mathbf{F} \cdot \mathbf{F}^T$ . Besides this, for elastic behaviour, the Cauchy stress tensor  $\boldsymbol{\sigma}$  is related to the strain tensor by (see 2.4.6):

$$\boldsymbol{\sigma} = a_0 \mathbf{I} + a_1 \mathbf{B} + a_2 \mathbf{B}^2 \quad (3.3.2)$$

where  $a_0$ ,  $a_1$  and  $a_2$  may be functions of the invariants of  $\mathbf{B}$ .

In subparagraph 2.6, two alternative objective rates were introduced (see 2.6.20 and 2.6.21):

$$\overset{\Delta}{\sigma} = \dot{\sigma} - (\dot{\mathbf{A}} \cdot \mathbf{A}^{-1}) \cdot \sigma - \sigma \cdot (\dot{\mathbf{A}} \cdot \mathbf{A}^{-1})^T \quad (3.3.3)$$

$$\overset{\nabla}{\sigma} = \dot{\sigma} + (\dot{\mathbf{A}} \cdot \mathbf{A}^{-1})^T \cdot \sigma + \sigma \cdot (\dot{\mathbf{A}} \cdot \mathbf{A}^{-1}) \quad (3.3.4)$$

where the tensor  $\mathbf{A}$  is introduced in subparagraph 1.4. From 1.4.6, it can easily be seen that both these objective rates can be replaced by:

$$\overset{\nabla}{\sigma} = \dot{\sigma} - (\Omega + \mathbf{H}) \cdot \sigma - \sigma \cdot (\Omega + \mathbf{H})^T \quad (3.3.5)$$

where  $\mathbf{H}$  is an objective tensor. Two commonly used objective rates, the Jaumann and Dienes rate, were introduced in subparagraph 2.6. Two other very well-known rates can be obtained for the following choices of  $\mathbf{H}$

$$\begin{aligned} \mathbf{H} &= \mathbf{D} - \frac{1}{2} \text{tr}(\mathbf{D}) \mathbf{I} && \text{Truesdell rate} \\ \mathbf{H} &= -\mathbf{D} - \frac{1}{2} \text{tr}(\mathbf{D}) \mathbf{I} && \text{Cotter-Rivlin rate} \end{aligned} \quad (3.3.6)$$

Substitution of  ${}^4\mathbf{L}$  according to 3.3.1 and of  $\overset{\nabla}{\sigma}$  according to 3.3.5 in the rate type equation  $\overset{\nabla}{\sigma} = {}^4\mathbf{L} : \mathbf{D}$  yields:

$$\dot{\sigma} - (\Omega + \mathbf{H}) \cdot \sigma - \sigma \cdot (\Omega + \mathbf{H})^T = \mu_1 \mathbf{D} + \mu_2 \text{tr}(\mathbf{D}) \mathbf{I} \quad (3.3.7)$$

The problem to be analysed in this subparagraph can now be formulated as: which choices for  $\mathbf{H}$  are acceptable, if it is required that the rate type constitutive equation 3.3.7 results in a stress-strain relationship of the kind 3.3.2.

From 3.3.2 it can be seen that  $\sigma$  and  $\mathbf{B}$  have the same orthonormal eigenvectors  $n_1, n_2$  and  $n_3$ . If the associated eigenvalues of  $\sigma$  and  $\mathbf{B}$  are denoted by  $\sigma_1, \sigma_2$  and  $\sigma_3$  and respectively by  $\lambda_1^2, \lambda_2^2$  and  $\lambda_3^2$ , it follows that:

$$\sigma = \sum_{i=1}^3 \sigma_i n_i n_i ; \quad \mathbf{B} = \sum_{i=1}^3 \lambda_i^2 n_i n_i \quad (3.3.8)$$

Furthermore, it follows from 3.3.2 that the eigenvalues of  $\sigma$  can be expressed in terms of the eigenvalues of  $\mathbf{B}$ :

$$\sigma_i = \sigma_i(e_1, e_2, e_3) ; \quad e_i = \ln(\lambda_i) \quad \text{for } i = 1, 2, 3 \quad (3.3.9)$$

It can also be shown that  $n_i \mathbf{D} \cdot n_i = \dot{e}_i$  for  $i = 1, 2, 3$ . With these results it can be derived from 3.3.7 that:

$$2H_{ij}\sigma_i = \sum_{j=1}^3 \left( \frac{\partial \sigma_i}{\partial e_j} - \mu_1 \delta_{ij} - \mu_2 \right) \dot{e}_j \quad \text{for } i = 1, 2, 3 \quad (3.3.10)$$

where  $H_{ii} = n_i \mathbf{H} \cdot n_i$  for  $i = 1, 2, 3$  and where  $\delta_{ij}$  is the Kronecker delta. This equation can be interpreted as a first requirement on the tensor  $\mathbf{H}$ . It follows from this equation that the diagonal components  $H_{ii}$  of  $\mathbf{H}$  must be proportional to the diagonal components  $e_i$  of  $\mathbf{D}$ . To fulfil this requirement,  $\mathbf{H}$  has been composed by a part proportional to  $\mathbf{D}$ , and by a part which diagonal components equal to zero:

$$\mathbf{H} = \beta \mathbf{D} - \gamma \text{tr}(\mathbf{D}) + \bar{\mathbf{H}} \quad ; \quad n_i \bar{\mathbf{H}} \cdot n_i = 0 \quad \text{for } i = 1, 2, 3 \quad (3.3.11)$$

Substitution of 3.3.11 into 3.3.10 gives:

$$\sum_{j=1}^3 \left( \frac{\partial \sigma_i}{\partial e_j} - (\mu_1 + 2\beta\sigma_i)\delta_{ij} - \mu_2 + 2\gamma\sigma_i \right) \dot{e}_j = 0 \quad \text{for } i = 1, 2, 3 \quad (3.3.12)$$

and since these equations must hold for every  $\dot{e}_j$  it follows that:

$$\frac{\partial \sigma_i}{\partial e_j} = (\mu_1 + 2\beta\sigma_i)\delta_{ij} + \mu_2 - 2\gamma\sigma_i \quad \text{for } i = 1, 2, 3 \quad (3.3.13)$$

For the commonly used objective stress rates the factors  $\beta$  and  $\gamma$  are constant. If this property is assumed for  $\beta$  and  $\gamma$  it can be shown that the set of nine differential equations 3.3.13 for the principle stresses  $\sigma_1, \sigma_2$  and  $\sigma_3$  has a solution, if  $\mu_1$  and  $\mu_2$  satisfy certain requirements: there exists a function  $f = f(J)$ , such that (see Appendix D and Van Wijngaarden and Veldpaus, 1986):

$$\mu_1 = \frac{2}{J} (G_0 - \beta f(J)) \quad ; \quad \mu_2 = \frac{df(J)}{dJ} \quad ; \quad f(1) = 0 \quad (3.3.14)$$

Here,  $G_0$  is a constant, which can be interpreted as the shear modulus of the material.

In the derivation of relationships 3.3.14, the following result has been used. It can be easily deduced from equation 2.4.7, which expresses the relationship between the principle stresses and the free energy  $\psi$ , that:

$$\gamma = \frac{1}{2} \quad (3.3.15)$$



With 3.3.14 and 3.3.15 the solution of 3.3.13 can be determined and is given in tensor form by:

$$\sigma = \frac{1}{J} (f(J)\mathbf{I} + \frac{G_0}{\beta} (\mathbf{B}^\beta - \mathbf{I})) \quad (3.3.16)$$

where the strain tensor  $\mathbf{B}^\beta$  is a symmetrical tensor with the same eigenvectors and eigenvalues as  $\mathbf{B}$ :

$$\mathbf{B}^\beta = \sum_{i=1}^3 \lambda_i^{2\beta} n_i n_i \quad (3.3.17)$$

This result means that the diagonal components of equation 3.3.7 completely determine the solution for the Cauchy stress  $\sigma$ , on the assumption that  $\beta$  and  $\gamma$  are constants. The only tensor still unknown is  $\bar{\mathbf{H}}$ . From equation 3.3.7 it follows that only three independent linear equations are left for the six unknown components  $\bar{H}_{ij} = n_i \cdot \mathbf{H} \cdot n_j$  ( $i, j = 1, 2, 3$ ;  $i \neq j$ ). These equations can be interpreted as constraints to be put on  $\bar{\mathbf{H}}$ . For this reason, three components can be freely chosen. At this point, it is assumed that the tensor  $\bar{\mathbf{H}}$  is skew-symmetric, which turns out also to be the case for the commonly used objective rates. Substitution of 3.3.16 and 3.3.11 into 3.3.7 then yields after some reorganisation:

$$\bar{\mathbf{H}} \cdot \mathbf{B}^\beta - \mathbf{B}^\beta \cdot \bar{\mathbf{H}} = (\dot{\mathbf{B}}^\beta) - (\Omega + \beta \mathbf{D}) \cdot \mathbf{B}^\beta - \mathbf{B}^\beta (\Omega + \beta \mathbf{D})^T ; \quad \bar{\mathbf{H}} = -\bar{\mathbf{H}}^T \quad (3.3.18)$$

and this equation completely determines the tensor  $\bar{\mathbf{H}}$ .

To summarize, it can be stated that the rate type constitutive equation 3.3.7 results in a correct stress-strain relationship for isotropic elastic behaviour, if  $\mu_1$  and  $\mu_2$  satisfy 3.3.14 and the tensor  $\mathbf{H}$  satisfies 3.3.11 with constant  $\beta$  and  $\gamma = \frac{1}{2}$ . The tensor  $\bar{\mathbf{H}}$  may be chosen as skew-symmetric, in order to arrive at an unique solution. This skew-symmetric tensor has to satisfy 3.3.18. For the Cauchy stress, an infinite number of constitutive relationships has been derived in 3.3.16: each  $\beta$  and each  $f=f(J)$  define their own stress-strain relationships

### 3.4 Some properties of elastic rate type relationships

In this subparagraph some special topics of rate-type constitutive equations for isotropic elastic behaviour are discussed. First of all it is noted that  $\bar{\mathbf{H}} = 0$  for  $\beta = \pm 1$

This follows easily from 3.3.18. In 3.3.6, it can be seen that, in this case, the objective rate equals that Truesdell rate for  $\beta = 1$  and the Cotter-Rivlin rate for  $\beta = -1$ . This means that the use of these objective rates, in the rate-type constitutive equations, leads to a correct description of isotropic elastic behaviour. The associated stress-strain relationships follow from 3.3.16 and are given by:

$$\sigma = \frac{1}{J} (f(J)I + G_\alpha(\mathbf{B} - I)) \quad \text{for } \beta = 1 \quad (3.4.1)$$

$$\sigma = \frac{1}{J} (f(J)I + G_\alpha(I - \mathbf{B}^{-1})) \quad \text{for } \beta = -1 \quad (3.4.2)$$

Next, the Jaumann rate and the Dienes rate are considered. The Jaumann rate is found for  $\beta = 0$  and  $\bar{\mathbf{H}} = 0$ , while the Dienes rate is found for  $\beta = 0$  and  $\Omega + \bar{\mathbf{H}} = \dot{\mathbf{R}} \cdot \mathbf{R}^T$ . However, for  $\beta = 0$  the relevant relationships of subparagraph 3.3 become:

$$\gamma = \frac{1}{2} ; \quad \mu_1 = 2 \frac{G_0}{J} ; \quad \mu_2 = \frac{df}{dJ} ; \quad f(1) = 0 \quad (3.4.3)$$

$$\sigma = \frac{1}{J} (f(J) + G_0 \ln(\mathbf{B})) \quad (3.4.4)$$

$$(\Omega + \bar{\mathbf{H}}) \cdot \ln(\mathbf{B}) - \ln(\mathbf{B}) \cdot (\Omega + \bar{\mathbf{H}}) = \ln(\dot{\mathbf{B}}) - 2\mathbf{D} \quad (3.4.5)$$

where the logarithmic strain tensor  $\ln(\mathbf{B})$  is defined by:

$$\ln(\mathbf{B}) = \sum_{i=1}^3 \ln(\lambda_i^2) n_i n_i = 2 \sum_{i=1}^3 e_i n_i n_i \quad (3.4.6)$$

Relationship 3.4.5 must be satisfied for each  $\mathbf{B}$ . It can be seen after a straightforward calculation that this will not hold for the Jaumann and for the Dienes rates. The use of these rates in the rate-type constitutive equations of the subparagraph 3.3 does not lead to a correct description of elastic behaviour. Dienes (1979), however, tried to use kinematical arguments about the use of the objective rate, which is called after him. But from the results obtained in this chapter, it is clear that the Dienes' arguments have to be rejected. Thermodynamical rather than kinematical arguments dictate what objective rate must be used in the case of elasticity.

In the subparagraph 3.3 the analysis was based on the rate-type constitutive equation 3.3.7. There is a second way of solving the stress tensor  $\sigma$  from this constitutive equation, which is based on the relationship between the objective stress rates in the equations 3.3.4 and 3.3.5. From 3.3.4 and from 3.3.7 it then follows that:

$$\overset{\vee}{\sigma} = \mathbf{A}^{-T} \cdot (\mathbf{A}^T \cdot \sigma \cdot \mathbf{A}) \cdot \mathbf{A}^{-1} = \mu_1 \mathbf{D} + \mu_2 \text{tr}(\mathbf{D}) \mathbf{I} \quad (3.4.7)$$

and therefore  $\sigma$  will be given by:

$$\sigma = \mathbf{A}^{-T} \left( \int_0^t \mu_1 \mathbf{A}^T \cdot \mathbf{D} \cdot \mathbf{A} \, dt + \int_0^t \mu_2 \text{tr}(\mathbf{D}) \mathbf{A}^T \cdot \mathbf{A} \, dt \right) \cdot \mathbf{A}^{-1} \quad (3.4.8)$$

This method which obtains an explicit relationship for  $\sigma$  will be used in chapter 5 as a starting point for the numerical treatment of constitutive equations, which contain objective rates.

If relationship 3.4.8 describes elastic behaviour it follows from 3.3.4, 3.3.5, 3.3.11 and 3.3.15 that:

$$(\dot{\mathbf{A}} \cdot \mathbf{A}^{-1})^T = -(\Omega + \mathbf{H}) = -(\Omega + \bar{\mathbf{H}} + \beta \mathbf{D}) + \frac{1}{2} \text{tr}(\mathbf{D}) \mathbf{I} \quad (3.4.9)$$

Substitution of this relationship into equation 3.3.8 yields:

$$(\dot{\mathbf{B}}^\beta) - (\dot{\mathbf{A}} \cdot \mathbf{A}^{-1})^T \cdot \mathbf{B}^\beta - \mathbf{B}^\beta \cdot \dot{\mathbf{A}} \cdot \mathbf{A}^{-1} - \text{tr}(\mathbf{D}) \mathbf{B}^\beta = 0 \quad (3.4.10)$$

Integration of this equation gives the following result:

$$\mathbf{A} \cdot \mathbf{A}^T = J \cdot \mathbf{B}^{-\beta} \quad (3.4.11)$$

This relationship means that if the tensor  $\mathbf{A}$  is defined by relationship 3.4.9, then  $\mathbf{A}$  can be expressed by:

$$\mathbf{A} = \sqrt{J} \mathbf{V}^{-\beta} \cdot \mathbf{Q} \quad ; \quad \mathbf{Q}^{-1} = \mathbf{Q}^T \quad (3.4.12)$$

where the rotation tensor  $\mathbf{Q}$  can be obtained by substituting this result in relationship 3.4.9.

### 3.5 The Oldroyd model

In subparagraph 2.6 the Oldroyd model was obtained using the thermodynamical theory with one tensorial hidden tensor. For incompressible materials this resulted in constitutive equations 2.6.27 and 2.6.28. Similar models can be obtained by the decomposition of the stress tensor  $\sigma$  in three tensors  $-p\mathbf{I}$ ,  $\tau_1$  and  $\tau_2$  and the decomposition of the deformation rate tensor  $\mathbf{D}$  in an elastic and viscous part  $\mathbf{D}_e$  and  $\mathbf{D}_v$ :

$$\sigma = -p\mathbf{I} + \tau_1 + \tau_2 \quad ; \quad \mathbf{D} = \mathbf{D}_e + \mathbf{D}_v \quad (3.5.1)$$

For these tensors the following constitutive relationships are assumed:

$$\overset{\nabla}{\tau}_1 = E D_e ; \quad \tau_1 = \lambda_1 D_v ; \quad \tau_2 = \lambda_2 D \quad (3.5.2)$$

Combination of these equations in 3.5.1 and 3.5.2 result in an Oldroyd model, which has been described in, for example Crochet, Davies and Crochet:

$$\sigma = -pI + \tau ; \quad \text{tr}(D) = 0 \quad (3.5.3)$$

$$\frac{1}{\lambda_1} \tau + \frac{1}{E} \overset{\nabla}{\tau} = \left(1 + \frac{\lambda_2}{\lambda_1} + \frac{\dot{\lambda}_2}{E}\right) D + \frac{\lambda_2}{E} \overset{\nabla}{D} \quad (3.5.4)$$

Of course the objective rates, used in 3.5.4, have to belong to one of the rate forms, that were discussed in subparagraph 3.3 and 3.4. In the Oldroyd model, obtained in subparagraph 2.6, the tensor  $\tau$  was expressed by the following equation (see 2.6.28):

$$\frac{1}{\lambda} \tau + \frac{1}{E_1} \overset{\Delta}{\tau} = \left(1 + \frac{\mu}{\lambda} + \frac{\dot{\mu}}{E_1}\right) D + \frac{\mu}{E_1} \overset{\Delta}{D} \quad (3.5.5)$$

where the objective rates of  $\tau$  and  $D$  are denoted by  $\overset{\Delta}{\tau}$  and  $\overset{\Delta}{D}$ , instead of  $\overset{\nabla}{\tau}$  and  $\overset{\nabla}{D}$ , to emphasize that this rate may differ from the objective rates discussed in subparagraph 3.3 and 3.4.

The Oldroyd models, obtained in 3.5.4 and 3.5.5, can be compared. This comparison leads to some very interesting results:

- The difference between these two Oldroyd models can be the use of the objective rates. In chapter 2 the objective rate was obtained by eliminating the tensor  $A$ , and in this chapter by making requirements on the elastic part of the deformation. Only in the case, where  $\beta$  equals zero, can these two models equal:

$$\overset{\nabla}{\tau} = \overset{\Delta}{\tau} = \dot{\tau} - (\Omega + \bar{H}) \cdot \tau + \tau \cdot (\Omega + \bar{H}) \quad (3.5.6)$$

$$\overset{\nabla}{D} = \overset{\Delta}{D} = \dot{D} - (\Omega + \bar{H}) \cdot D + D \cdot (\Omega + \bar{H}) \quad (3.5.7)$$

$$(\Omega + \bar{H}) \cdot \ln(B) - \ln(B) \cdot (\Omega + \bar{H}) = \overset{\Delta}{\ln(B)} - 2D \quad (3.5.8)$$

- From this result it follows directly, that the use of the Jaumann or the Dienes rate in the Oldroyd model, leads to a model in which the deformation rate can't be decomposed into an elastic and a viscous part as was done in this chapter. On the other hand, thermodynamically speaking no objections can be made against the use of these rate

forms. It just depends on the starting point of the constitutive model whether one accepts the use of these rates.

If the use of the rate forms, that were deduced in subparagraph 3.3, is thermodynamically spoken allowed, in the sense that the models obtained obey the Clausius-Duhem inequality, is still an open question for those cases where  $\beta \neq 0$ . This question can't be answered by the theory of the previous chapter, and must be investigated in a different way. In this work, no further attention will be given to this question.

### 3.6 The Maxwell model

The Maxwell model is obtained by the decomposition of the deformation rate tensor  $\mathbf{D}$  into a viscous and an elastic part, and by the assumption that these parts obey the following constitutive models:

$$\overset{\nabla}{\boldsymbol{\sigma}} = {}^4\mathbf{E}:\mathbf{D}_e \quad ; \quad \boldsymbol{\sigma}^d = \lambda \mathbf{D}_v \quad (3.6.1)$$

This model has become very popular in the field of metal plasticity, where the viscous part of the deformation rate  $\mathbf{D}_v$  is often referred to as the plastic part  $\mathbf{D}_p$ . Elimination of  $\mathbf{D}_e$  and  $\mathbf{D}_v$  in relationship 3.6.1 yields:

$$\frac{1}{\lambda} \boldsymbol{\sigma}^d + {}^{-4}\mathbf{E}:\overset{\nabla}{\boldsymbol{\sigma}} = \mathbf{D} \quad (3.6.2)$$

For metals the viscosity  $\lambda$  is not determined by the current state only, but also by the past. This history dependency is called hardening. In order to take hardening into account the so-called equivalent plastic strain  $\bar{\varepsilon}$  is introduced and is defined by:

$$\dot{\bar{\varepsilon}} = \sqrt{\frac{2}{3} \mathbf{D}_v:\mathbf{D}_v} \quad (3.6.3)$$

where  $\bar{\varepsilon}$  is zero in the absence of plastic deformation. With the equivalent or Von Mises stress  $\sigma_v$ , defined by:

$$\sigma_v = \sqrt{\frac{3}{2} \boldsymbol{\sigma}^d:\boldsymbol{\sigma}^d} \quad (3.6.4)$$

the constitutive equation 3.6.2 becomes:

$$-4 \mathbf{E} : \overset{\vee}{\sigma} + \frac{3}{2} \frac{\dot{\bar{\epsilon}}}{\sigma_v} \sigma^\sigma = \mathbf{D} \quad (3.6.5)$$

It is noted that the definitions of  $\bar{\epsilon}$ ,  $\sigma_v$  and the constitutive equation 3.6.5 correspond to the definitions and constitutive model in subparagraph 2.7. In a case where the same requirements are made for the objective rates as in subparagraph 3.5, an equality can be obtained for these quantities and the model.

In metal plasticity the history dependency is taken into account by postulating that the Von Mises stress depends on the equivalent plastic strain and the equivalent plastic strain rate:

$$\sigma_v = \sigma_v(\bar{\epsilon}, \dot{\bar{\epsilon}}) \quad (3.6.6)$$

The model obtained, represented by 3.6.5 and 3.6.6, is known as the Prantl-Reuss model (see Hill 1950). If all elastic effects are neglected, this model can be simplified to the so-called Levy-Von Mises model:

$$\frac{3}{2} \frac{\dot{\bar{\epsilon}}}{\sigma_v} \sigma^\sigma = \mathbf{D} \quad (3.6.7)$$

In the field of rheology, this model is often referred to as a special case of a non-Newtonian fluid.

It is known from experiments that the dependency of  $\sigma_v$  on  $\dot{\bar{\epsilon}}$  can be neglected for metals at relatively low temperature and, besides, that the dependency of  $\sigma_v$  on  $\bar{\epsilon}$  can be neglected for relative high temperatures. In order to obtain a constitutive model, most experimental work on metals is focussed on the hardening equation 3.6.6. In the next chapter three experimental set-ups will be discussed.

### 3.7 The Kelvin model

In this subparagraph another special version of the Oldroyd model is discussed. This version, known as the Kelvin model, is described by:

$$\text{tr}(\mathbf{D}) = 0 ; \quad \sigma = -p\mathbf{I} + \tau ; \quad \overset{\vee}{\tau} = E\mathbf{D} + \lambda \overset{\vee}{\mathbf{D}} \quad (3.7.1)$$

This model can be used to describe purely plastic behaviour of metals with kinematical hardening. As Prager (1956) pointed out this model can be derived from some simple assumptions:

- The material is incompressible, so

$$\text{tr}(\mathbf{D}) = 0 \quad ; \quad \boldsymbol{\sigma} = -p\mathbf{I} + \boldsymbol{\tau} \quad (3.7.2)$$

- there exists a yield surface  $f$ , where  $f$  is given by:

$$f = (\boldsymbol{\tau} - \boldsymbol{\alpha}) : (\boldsymbol{\tau} - \boldsymbol{\alpha}) - \frac{2}{3} \sigma_0^2 \quad (3.7.3)$$

Here the tensor  $\boldsymbol{\alpha}$  is the so-called shift tensor and  $\sqrt{\frac{2}{3}} \sigma_0$  is the radius of the yield surface. The stress tensor  $\boldsymbol{\tau}$  either lies on the yield surface ( $f=0$ ), or inside the yield surface ( $f < 0$ ).

- If the tensor  $\boldsymbol{\tau}$  is inside the yield surface no deformation takes place. If  $\boldsymbol{\tau}$  is on the yield surface,  $\mathbf{D}$  is perpendicular to the yield surface:

$$\mathbf{D} = 0 \text{ for } f < 0 \quad ; \quad \mathbf{D} = \eta(\boldsymbol{\tau} - \boldsymbol{\alpha}) \text{ for } f = 0 \quad (3.7.4)$$

This relationship for  $\mathbf{D}$  is called the associated flow rule.

The radius of the yield surface can depend on the equivalent plastic strain  $\bar{\varepsilon}$  and on the equivalent strain rate  $\dot{\bar{\varepsilon}}$ :

$$\sigma_0 = \sigma_0(\bar{\varepsilon}, \dot{\bar{\varepsilon}}) \quad ; \quad \dot{\bar{\varepsilon}} = \sqrt{\frac{2}{3} \mathbf{D} : \mathbf{D}} \quad (3.7.5)$$

- the objective rate  $\overset{\nabla}{\boldsymbol{\alpha}}$  of the shift tensor is proportional to  $\mathbf{D}$ :

$$\overset{\nabla}{\boldsymbol{\alpha}} = h\mathbf{D} \quad ; \quad h = h(\varepsilon, \dot{\varepsilon}) \quad (3.7.6)$$

where  $\boldsymbol{\alpha} = 0$  in the absence of plastic deformation.

From 3.7.4 and 3.7.5 it is evident that:

$$\dot{\bar{\varepsilon}} = 0 \text{ for } f < 0 \quad ; \quad \dot{\bar{\varepsilon}} = \frac{2}{3} \eta \sigma_0 \text{ for } f = 0 \quad (3.7.7)$$

and therefore 3.7.4 can be written as:

$$\mathbf{D} = 0 \text{ for } f < 0 \quad ; \quad \boldsymbol{\tau} = \boldsymbol{\alpha} + \frac{2}{3} \frac{\sigma_0}{\dot{\bar{\varepsilon}}} \mathbf{D} \text{ for } f = 0 \quad (3.7.8)$$

Elimination of the shift tensor finally yields:

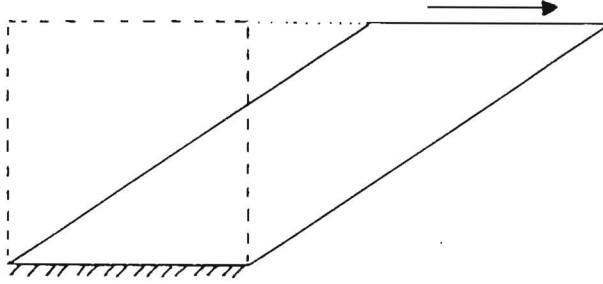


Figure 1. The simple shear test

$$\mathbf{D} = \mathbf{0} \text{ for } f < 0 ; \quad \overset{\nabla}{\boldsymbol{\tau}} = h\mathbf{D} + \frac{2}{3} \left( \frac{\sigma_0}{\dot{\epsilon}} \mathbf{D} \right) \text{ for } f = 0 \quad (3.7.9)$$

The choice of the objective rate has been the subject of much discussion lately (see, for example Nagtegaal and De Jong (1982), Lee, Mallet and Wertheimer (1983), Dafalias (1985), Atluri (1984)). It is striking to see that, in these discussions, only objective rates of the form:

$$\overset{\nabla}{\boldsymbol{\alpha}} = \dot{\boldsymbol{\alpha}} - (\boldsymbol{\Omega} + \mathbf{H})\boldsymbol{\alpha} + \boldsymbol{\alpha}(\boldsymbol{\Omega} + \mathbf{H}) ; \quad \mathbf{H}^T = -\mathbf{H} \quad (3.7.10)$$

are considered. Probably the reason for this choice is that, with this rate form,

$\overset{\nabla}{(\boldsymbol{\alpha})^d} = \overset{\nabla}{(\boldsymbol{\alpha}^d)}$  and therefore  $\boldsymbol{\alpha} = \boldsymbol{\alpha}^d$  and so  $\boldsymbol{\tau} = \boldsymbol{\tau}^d$ , i.e.  $\text{tr}(\boldsymbol{\tau}) = \text{tr}(\boldsymbol{\alpha}) = 0$ . Then for  $f=0$  the constitutive equation can also be written as:

$$\boldsymbol{\sigma}^d = \boldsymbol{\alpha} + \frac{2}{3} \frac{\sigma_0}{\dot{\epsilon}} \mathbf{D} ; \quad \overset{\nabla}{\boldsymbol{\alpha}} = h\mathbf{D} ; \quad \text{tr}(\mathbf{D}) = 0 \quad (3.7.11)$$

Furthermore it is worth noting that the proposed objective rates are evaluated in these discussions by analysing what is known as the simple shear test (see figure 1): a proposed objective rate is accepted if no oscillations occur in the shear stress as a function of the deformation. It turns out that, as a result, the Jaumann rate fails to pass the test.



## 4 The determination of material properties

### 4.1 Introduction

In the previous chapters specific constitutive equations for classes of material behaviour were obtained. These equations contain a number of material parameters, which have to be determined experimentally.

The choice of a suitable experiment largely depends on the class of material behaviour to be investigated. Here, only so-called Maxwell materials with constitutive equations of the type:

$$\frac{1}{\eta} \sigma^d + {}^{-4}\mathbf{E}:\overset{\nabla}{\sigma} = \mathbf{D} \quad (4.1.1)$$

will be considered (see subparagraph 3.6). The behaviour of many metals can be described with sufficient accuracy by a constitutive equation of this type. In this chapter

only large deformations will be considered. The elastic part  ${}^{-4}\mathbf{E}:\overset{\nabla}{\sigma}$  can then be ignored, and the constitutive equation reduces to:

$$\sigma^d = \eta \mathbf{D} \quad (4.1.2)$$

As a consequence  $\text{tr}(\mathbf{D})$  will be equal to zero, so the material is assumed to be incompressible. The constitutive equations can then be reduced to:

$$\sigma = -p\mathbf{I} + \tau \quad ; \quad \tau = \eta \mathbf{D} \quad (4.1.3)$$

The material property to be determined experimentally is, in this case, the 'viscosity'  $\eta$ . From 3.6.3, 3.6.4 and 3.6.5 it can be seen that:

$$\eta = \frac{2\sigma_v}{3\dot{\epsilon}} \quad ; \quad \sigma_v = \sqrt{\frac{3}{2} \sigma^d:\sigma^d} \quad ; \quad \dot{\epsilon} = \sqrt{\frac{2}{3} \mathbf{D}:\mathbf{D}} \quad (4.1.4)$$

where  $\sigma_v$  is the Von Mises stress and  $\dot{\epsilon}$  is the equivalent strain rate. Then the relevant constitutive equation can be written as:

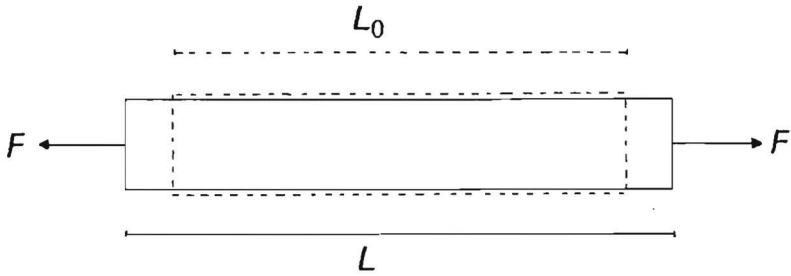


**Figure 2. The tension test**

$$\tau = \frac{2}{3} \frac{\sigma_v}{\dot{\epsilon}} \mathbf{D} \quad (4.1.5)$$

where  $\sigma_v$  is now the material property to be determined as a function of  $\bar{\epsilon}$  and  $\dot{\bar{\epsilon}}$  (see 3.6.6):

$$\sigma_v = \sigma_v(\bar{\epsilon}, \dot{\bar{\epsilon}}) \quad (4.1.6)$$

In the next subparagraphs 4.2-4.4 the tension test, the torsion test and the compression test are discussed. Unless otherwise stated, temperature effects will be ignored.

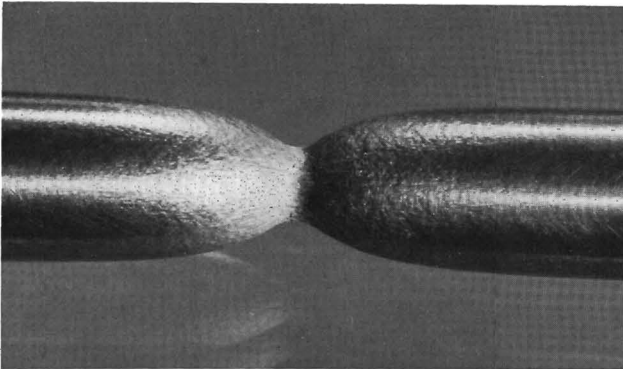


**Figure 3. Necking of an aluminium bar**

## 4.2 The tension test

In the tension test an attempt is made to achieve an uniform, one-dimensional stress situation in the test specimen, i.e. a stress situation such that, in each point of the specimen:

$$\sigma = s \underline{e}\underline{e} \quad ; \quad \tau = s \left( -\frac{1}{3} I + \underline{e}\underline{e} \right) \quad (4.2.1)$$

where  $\underline{e}$  is a given unit vector. From 4.1.5, it follows that  $D$  must be equal to:

$$D = \frac{3}{2} \frac{\dot{\bar{\epsilon}}}{\sigma_v} s \left( -\frac{1}{3} I + \underline{e}\underline{e} \right) \quad (4.2.2)$$

A deformation of this kind can be approximated by elongating a solid, slender bar, with a constant cross section. To eliminate end effects, only the middle section of the bar is considered. During the experiment, the current length,  $L$ , of this section and the applied force  $F$  are measured (see figure 2). A simple kinematical analysis yields that the axial component  $\underline{e} \cdot D \cdot \underline{e}$  of the tensor  $D$  will be equal to  $\frac{\dot{L}}{L}$  and, because of the incompressibility,  $D$  can therefore be expressed by:

$$D = \frac{3}{2} \dot{\epsilon} \left( -\frac{1}{3} I + \underline{e}\underline{e} \right) \quad ; \quad \epsilon = \ln \left( \frac{L}{L_0} \right) \quad (4.2.3)$$

Here,  $L_0$  is the length of the middle section of the unstressed bar and  $\epsilon$  is what is known as the logarithmic strain of that section. From this relationship for  $D$  and from the definition of the equivalent strain rate  $\dot{\bar{\epsilon}}$  in 4.1.4 it is apparent that, in this case, the equivalent strain  $\bar{\epsilon}$  is equal to the logarithmic strain  $\epsilon$ :

$$\bar{\epsilon} = \epsilon = \ln \left( \frac{L}{L_0} \right) \quad (4.2.4)$$

Substitution of this result in 4.2.2 yields  $\sigma_v = s$ , where the current stress is related to the measured force  $F$  and the current area  $A$  of the cross section by  $s = \frac{F}{A}$ . Due to the assumed incompressibility of the bar, the current volume  $A \cdot L$  of the middle section is equal to the volume  $A_0 \cdot L_0$  of the unstressed bar. So the material quantity  $\sigma_v$  can be determined from the measured quantities  $F$  and  $\bar{\epsilon}$  by using:

$$\sigma_v = \frac{F}{A} = \frac{FL}{A_0 L_0} = \frac{F}{A_0} e^{\bar{\epsilon}} \quad (4.2.5)$$

Usually a constant strain rate is chosen for the tension tests. By repeating the test on identical specimens with different strain rates, it is possible to determine  $\sigma_v$ , as a function of  $\bar{\epsilon}$  and  $\dot{\bar{\epsilon}}$ .

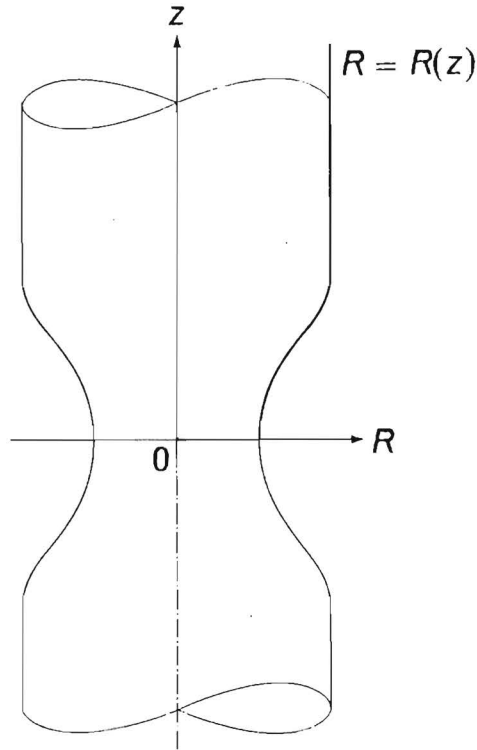
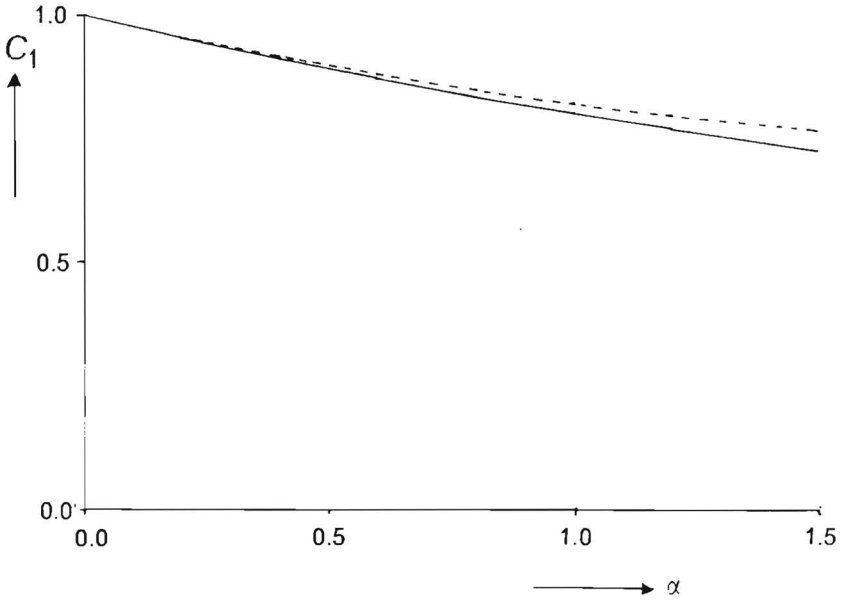


Figure 4. The necking zone of a cylindrical bar

If  $\sigma_v$  turns out to depend only on  $\bar{\epsilon}$  or  $\dot{\bar{\epsilon}}$  the material is known as a strain hardening, or strain rate hardening material respectively. At relatively low temperatures, metals are strain hardening materials, due to the dislocation density growth and the lack of recrystallisation. At relatively high temperatures recrystallization occurs. This stops the dislocation density growth, but makes the metal strain rate dependent. Sometimes, it is assumed that  $\sigma_v$  doesn't depend on  $\bar{\epsilon}$  and  $\dot{\bar{\epsilon}}$ , but on the energy rate and the total energy needed for deformation of the bar. Hill (1950) showed that there is no difference between purely strain hardening and purely work hardening. This doesn't apply to strain rate and work rate hardening metals!

The main disadvantages of the tension test is that necking occurs: if the force  $F$  reaches a maximum value, then, due to bifurcation, flow localisation will be observed (figure 3) and the stress tensor  $\sigma$  and the deformation rate tensor  $D$  no longer satisfy 4.2.1 and 4.2.2 . As a consequence, relationship 4.2.5, between the axial force  $F$  and the equiv-



**Figure 5. Correction factor:** C1 according to Siebel (—) and Bridgman (-----)

alent stress, no longer holds. Flow localisation occurs for a strain hardening metal, in a constant strain rate tension test, when the axial force reaches its maximum value, i.e., when:

$$\frac{dF}{d\bar{\epsilon}} = 0 \rightarrow \frac{1}{\sigma_v} \frac{d\sigma_v}{d\bar{\epsilon}} = 1 \quad (4.2.6)$$

If the stress-strain curve 4.2.5 is given by Ludwick's hardening rule:

$$\sigma_v = C(\bar{\epsilon} + \bar{\epsilon}_0)^n \quad (4.2.7)$$

then necking occurs when:

$$\bar{\epsilon} = n - \bar{\epsilon}_0 \quad (4.2.8)$$

This means that for low values of the strain, only, experimental data can be obtained using a standard tension test. It is evident that, for strain rate hardening materials the situation is even worse: in that case the bar begins to neck almost immediately.

In the necking zone, the stress situation is much more complex than that given by 4.2.1. For cylindrical bars, however, several authors found corrections for relationship 4.2.5.

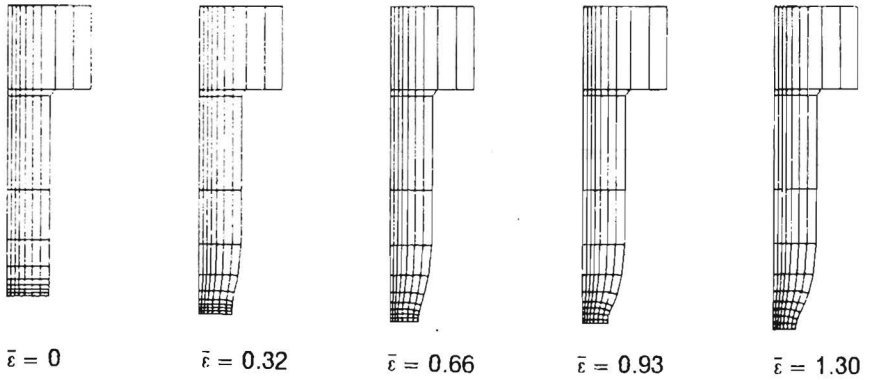


Figure 6. Several stages of a finite element analysis of the necking of a cylindrical bar

They all found that, in the neighbourhood of the smallest cross section,  $\sigma_v$  and  $\epsilon$  can be approximated by:

$$\sigma_v = C_1 \frac{F}{A} \quad ; \quad \bar{\epsilon} = \ln\left(\frac{A_0}{A}\right) \quad (4.2.9)$$

where  $A$  is the area of the smallest cross section. Furthermore  $C_1$  can be regarded as a correction factor. Different formulae are given for  $C_1$  in literature. An important quantity in these formulae is the scalar  $\alpha$ , defined by:

$$\alpha = \left(R \frac{d^2 R}{dz^2}\right)_{z=0} \quad (4.2.10)$$

Here,  $R$  is the radius of the neck and  $z$  is the axial coordinate, such that  $z=0$  in the middle of the neck (figure 4).

Two well-known proposals for  $C_1$  are the following:

- Siebel (1925) and Davidenkov and Spiridonova (1946) found that:

$$C_1 = \frac{4}{4 + \alpha} \quad (4.2.11)$$

- Bridgman (1952) found that:

$$C_1 = \frac{1}{\left(1 + \frac{2}{\alpha}\right) \ln\left(1 + \frac{\alpha}{2}\right)} \quad (4.2.12)$$

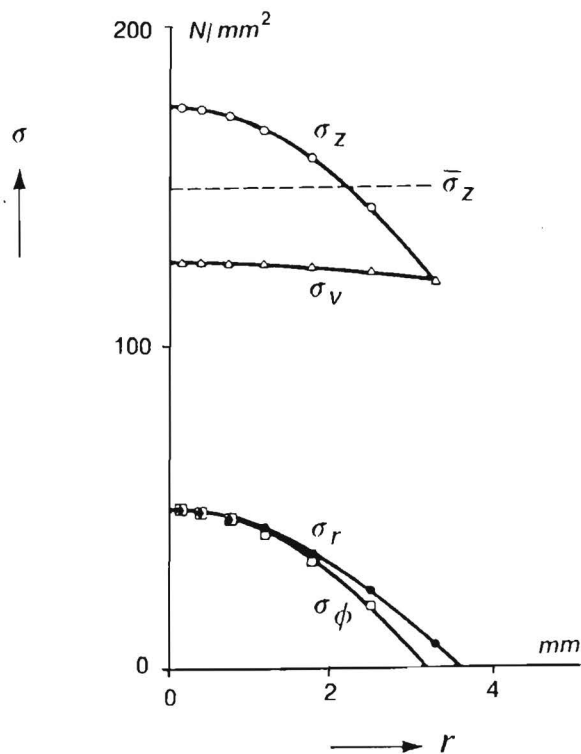


Figure 7. The stress components in the necking zone ( $z=0$ )

In figure 5,  $C_1$  is drawn for both cases as a function of  $\alpha$ . From this figure and also from 4.2.11 and 4.2.12 it is apparent that for small values of  $\alpha$ , the correction factors are almost the same.

Davidenko and Spiridonova found relationship 4.2.11 for the correction factor in a complete experimental way by measuring on the crystals in the necking area. In Appendix E, this relationship is derived by assuming that the radial velocity  $u_r$ , in the neighbourhood of the smallest cross section can be approximated by:

$$u_r = r f(z) \quad (4.2.13)$$

such that:

$$\left| \frac{df}{dz} \right| \ll |f(z)| \quad (4.2.14)$$

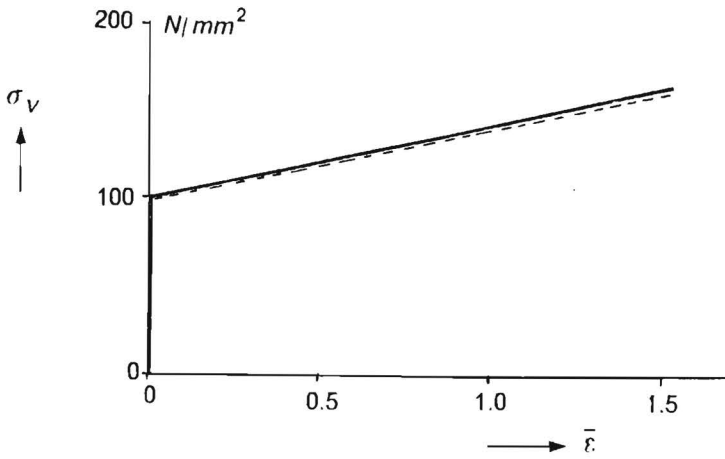


**Figure 8. Stress-strain curves:** One curve (—) is used as the input for the finite element analysis and the other (----) is reconstructed from the results of this analysis

Before necking, 4.2.13 and 4.2.14 are fulfilled. A consequence of 4.2.13 is that  $\sigma_r = \sigma_\phi$  and a consequence of 4.2.13 and 4.2.14 is that the Von Mises stress is almost constant in every cross section near  $z=0$ , i.e. it is not a function of  $r$ . This consequence can be checked by a finite element analysis of a cylindrical tensile bar. In figure 6, some of

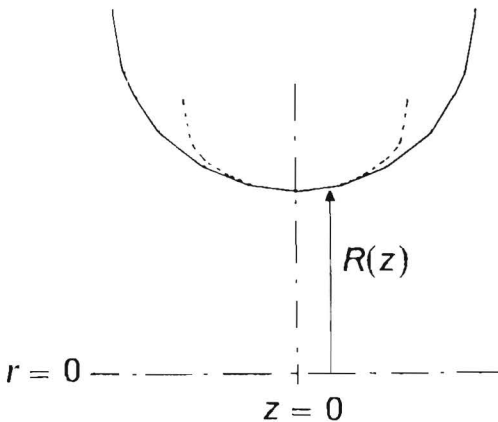


**Figure 9. Predicted shapes of the necking zone:** Prediction by Siebel (----) and Bridgman (—)



the steps of such an analysis are given. Here, a linear strain hardening model is used, which means that the Von Mises stress depends linearly on the equivalent strain. In figure 7, various stress components have been drawn, for the case where  $\bar{\epsilon} \approx 0.7$ . Clearly, the two previously mentioned consequences are fulfilled. Another check for the correction factor in relationship 4.2.11 for the correction factor can be made by determining the stress-strain curve with 4.2.13 and the calculated shape of the neck (figure 6). This curve must be the same as the linear stress-strain curve, that was used as an input for the calculations. From figure 8, it can be seen that the two curves are almost the same, even for very large values of  $\bar{\epsilon}$ .

From 4.1.13 and 4.1.14, the shape of the neck can be determined (see Appendix E). In the derivation of 4.1.12, Bridgman made an assumption about this shape: it should be a part of a torus. It turns out that both shapes are almost the same in the vicinity of the smallest cross section. These shapes have been drawn in figure 9.

In practice it doesn't make much difference which of these relationships for the correction factor is used, when determining the stress-strain curve from experimental results. The problem that remains is how to measure the shape of the neck since this shape must be known to determine first  $\alpha$  and  $A$ , and then the Von Mises stress and the equivalent strain. One way is to elongate the bar, bit by bit, and measure the shape of the bar in between times. This method has two disadvantages: it will take a long time before one experiment is completed and, more seriously only strain hardening can be determined.

Galenkamp (1984) developed an experimental set-up to measure the shape of the bar during the tensile test. This set-up is shown in figure 10. On the left handside of the bar, a homogeneous lightsource LS is mounted. The shadow image of the tensile bar TB is projected via a mirror M and a lens L into a linear array camera DA. The camera has 2048 light sensitive diodes, which detect a light-shadow-light line of the shadow image. The shadow part of the line, which is indicated by the number of diodes that haven't been lit, is a measurement of the diameter of the bar at a position  $z$ . By rotating the mirror this position can be changed. This change of position takes about 30 milliseconds, and a measurement of the diameter takes about 20. So, about 20 measurements on different positions  $z$  can be done in one second. This is fast enough to obtain a quasi-stationary result.

Figure 11 is a photo of the total set-up. From this picture another advantage of this measurement technique can be seen: it can be used in nearly all traditional experimental set-ups, without basic changes to the original one.

A result obtained with this set-up for an aluminium tensile bar, is shown in figure 12. In this figure two curves have been drawn: one for the average tensile stress  $\bar{\sigma}_z$  in the

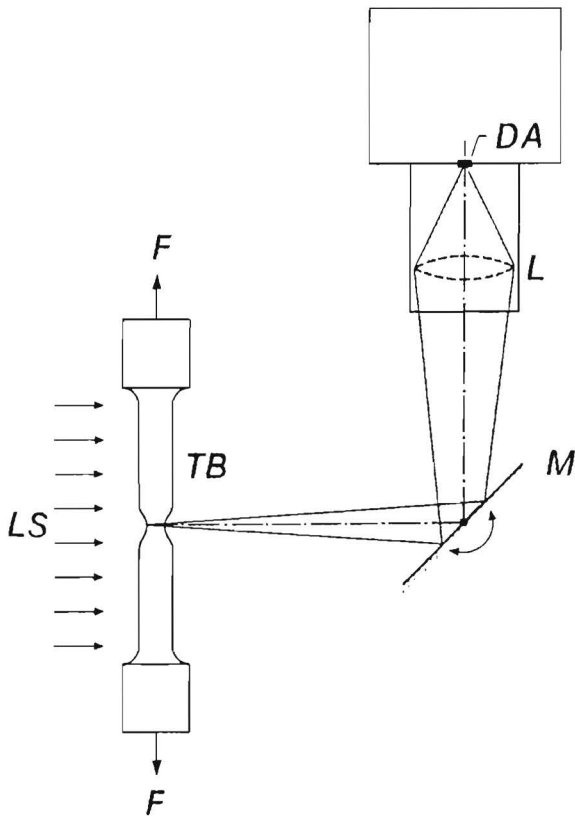


**Figure 10. Cross-section of the experimental set-up of Galenkamp**

smallest cross section and one for the Von Mises stress, which was obtained by multiplying  $\bar{\sigma}_z$  with the correction factor in 4.2.11. For  $\bar{\epsilon} = 1.5$ , fracture in the bar occurs. At this point  $\alpha = 1.0$ . This is a value that still gives nearly the same correction factor value in the relationships 4.2.11 and 4.2.12.

To summarise it can be stated that the Galenkamp's experimental set-up is an extension of the standard set-ups, which makes it possible to obtain experimental data for strain and strain rate hardening materials until fracture occurs. A basic assumption in both the standard set-ups and Galenkamp's is that the cross sections in the bar remain circular. This is not always the case for example it is not so for lead, at room temper-

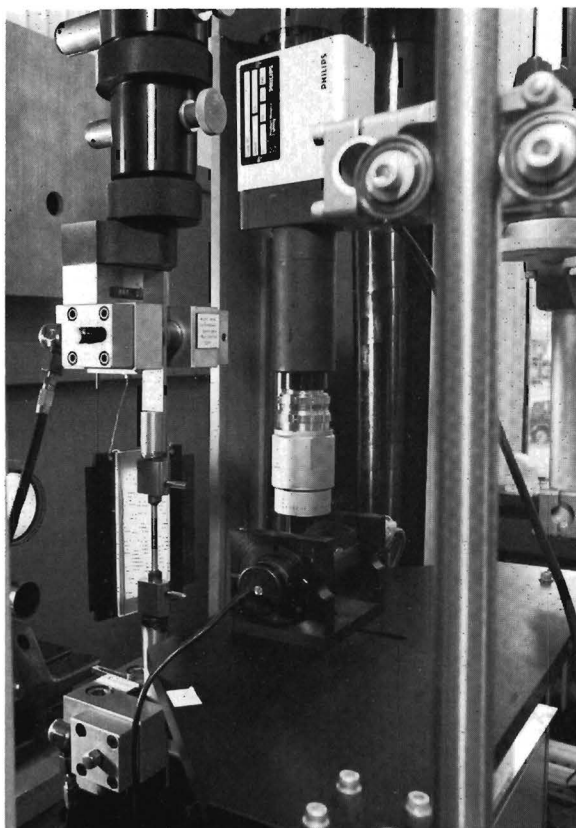


Figure 11. Photo of the set-up of Galenkamp

ature. Extension of Galenkamp's set-up for experiments at high temperatures is rather difficult, as one then has to combine the optical measurement technique with the heating system.

### ***4.3 The torsion-tension test***

In the combined torsion-tension test long cylindrical bars are used, loaded by a twisting torque  $M$  and a possible axial force  $F$  at the ends of the bar (see figure 13). In this test it is tried to achieve a velocity field of the type:

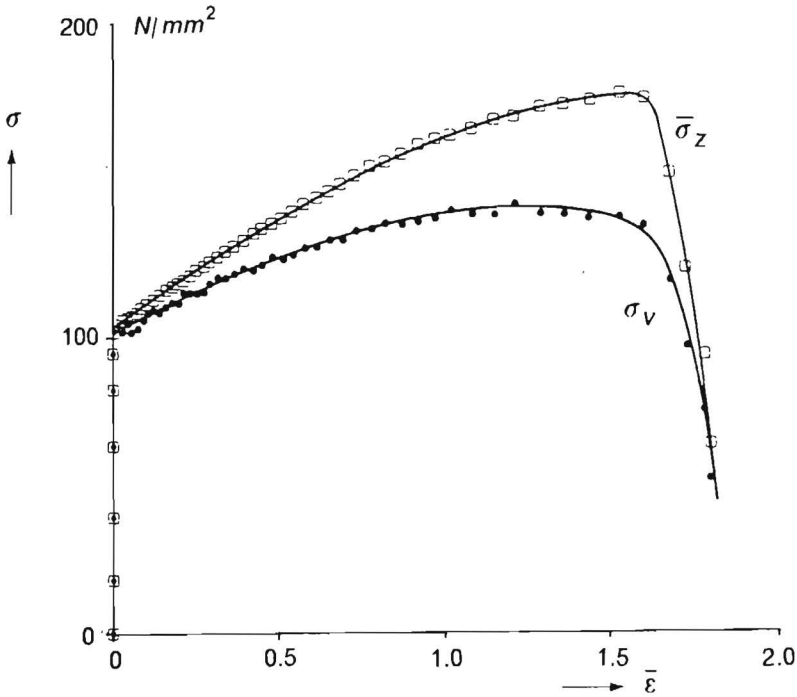


Figure 12. Results of a tension test for an aluminium bar

$$u = u_r(r, t)e_r(t) + r\omega(z, t)e_\phi(t) + u_z(z, t)e_z \quad (4.3.1)$$

where  $e_r$ ,  $e_\phi$  and  $e_z$  are the base vectors of the polar coordinate system  $(r, \phi, z)$ ,  $\omega(z, t)$  is the current angular velocity of the cross section at axial position  $z$  and the radial velocity  $u_r$  and the axial velocity  $u_z$  are given by:

$$u_r = u_r(r, t) \quad ; \quad u_z = u_z(z, t) \quad (4.3.2)$$

which means that the bar retains its cylindrical shape, during deformation. The corresponding deformation rate tensor  $\mathbf{D}$  is given by:

$$\mathbf{D} = \frac{\partial u_r}{\partial r} e_r e_r + \frac{u_r}{r} e_\phi e_\phi + \frac{\partial u_z}{\partial z} e_z e_z + \frac{1}{2} r \frac{\partial \omega}{\partial z} (e_\phi e_z + e_z e_\phi) \quad (4.3.3)$$

From the assumed incompressibility, i.e.  $\text{tr}(\mathbf{D}) = 0$ , it is evident that:

$$u_z(z, t) = \dot{\epsilon}(t)z \quad ; \quad u_r = -\frac{1}{2} \dot{\epsilon}(t)r \quad (4.3.4)$$

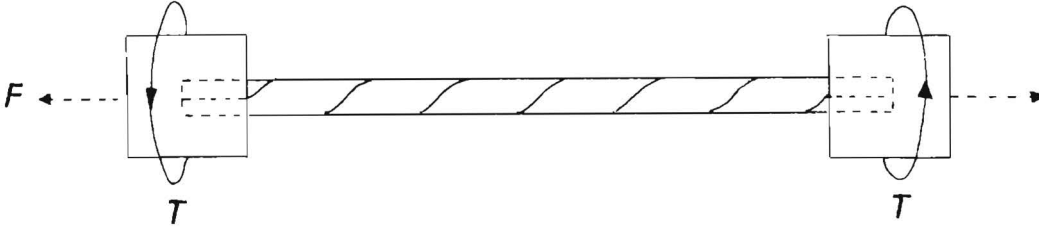


Figure 13. The torsion-tension test

where  $\dot{\epsilon}(t)$  is the current logarithmic axial strain. Substitution of these results in 4.3.3 yields for  $\mathbf{D}$ :

$$\mathbf{D} = -\frac{1}{2} \dot{\epsilon} \mathbf{I} + \frac{3}{2} \dot{\epsilon} e_z e_z + \frac{1}{2} r \frac{\partial \omega}{\partial z} (e_\phi e_z + e_z e_\phi) \quad (4.3.5)$$

Hence the equivalent strain rate can be determined:

$$\dot{\bar{\epsilon}} = \sqrt{\frac{2}{3} \mathbf{D} : \mathbf{D}} = \sqrt{\dot{\epsilon}^2 + \frac{1}{3} \left( r \frac{\partial \omega}{\partial z} \right)^2} \quad (4.3.6)$$

Furthermore, with  $\boldsymbol{\sigma} = -p\mathbf{I} + \eta\mathbf{D}$  it follows that the Cauchy stress tensor  $\boldsymbol{\sigma}$  is given by:

$$\boldsymbol{\sigma} = -\left(p + \frac{1}{2} \dot{\epsilon}\right) \mathbf{I} + \frac{3}{2} \eta \dot{\epsilon} e_z e_z + \frac{1}{2} \eta r \frac{\partial \omega}{\partial z} (e_\phi e_z + e_z e_\phi) \quad (4.3.7)$$

This stress tensor has to satisfy the balance equation of momentum. A lengthy but straightforward elaboration of this condition finally results in:

$$p = -\frac{1}{2} \eta \dot{\epsilon} \quad ; \quad \omega(z, t) = \dot{\alpha}(t) z \quad (4.3.8)$$

and therefore  $\boldsymbol{\sigma}$  becomes:

$$\boldsymbol{\sigma} = \frac{3}{2} \eta \dot{\epsilon} e_z e_z + \frac{1}{2} \eta \dot{\alpha} r (e_\phi e_z + e_z e_\phi) \quad (4.3.9)$$

Besides, from 4.3.6 it is apparent that the equivalent strain rate  $\dot{\bar{\epsilon}}$  will depend on  $r$  and  $t$  only:

$$\dot{\bar{\epsilon}} = \sqrt{\dot{\epsilon}^2 + \frac{1}{3} (r \dot{\alpha})^2} \quad (4.3.10)$$

Finally, the twisting torque  $M$  and the axial force  $F$  at the ends of the bar are given by:

$$M = 2\pi \int_{r=0}^R \sigma_z r^2 dr = \pi \dot{\alpha} \int_{r=0}^R \eta r^3 dr \quad (4.3.11)$$

$$F = 2\pi \int_{r=0}^R \sigma_z r dr = 3\pi \dot{\epsilon} \int_{r=0}^R \eta r dr \quad (4.3.12)$$

where  $R$  is the current radius of the bar. From 4.3.4, it follows that  $R$  is related to the radius  $R_0$  of the unstressed bar by:

$$R = R_0 e^{-\frac{1}{2} \epsilon} \quad (4.3.13)$$

The assumed velocity field can be approximately reached in the middle section of long cylindrical bars. To decrease the influence of end effects the ratio of the radius  $R_0$  and the length  $L_0$  should be small, which means that very long thin bars have to be used as test specimens.

Of special interest is the case in which the axial force  $F$  is absent. From 4.3.12 it follows that:

$$\dot{\epsilon} = 0 ; \quad z(t) = z_0 ; \quad r(t) = r_0 \quad (4.3.14)$$

which implies that the length of the bar remains unchanged if the specimen is not loaded in axial direction. In reality the metal bars will lengthen or shorten in such case. This can be explained by considering elastic and anisotropic effects in the bar. Some examples of this phenomenon will be given below. As will be apparent, the deformation due to the elongation or shortening is negligible compared with the deformation due to twisting.

With  $\dot{\epsilon} = 0$  the relationships for  $\dot{\bar{\epsilon}}$  and  $\bar{\epsilon}$  reduce to:

$$\dot{\bar{\epsilon}} = \frac{1}{3} r \dot{\alpha} \sqrt{3} ; \quad \bar{\epsilon} = \frac{1}{3} r \alpha \sqrt{3} \quad (4.3.15)$$

where  $\alpha$  and  $\dot{\alpha}$  are assumed to be positive. The relationship for the twisting torque becomes:

$$M = \pi \dot{\alpha} \int_{r=0}^R \eta r^3 dr = \frac{2}{3} \sqrt{3} \pi \int_{r=0}^R \sigma_v r^2 dr \quad (4.3.16)$$

Here the parameter  $\eta$  is replaced by  $\sigma_v = \frac{3}{2} \eta \dot{\bar{\epsilon}}$ , as mentioned earlier in this chapter.

In a torsion test of this type both the twisting torque  $M(t)$  and the rotation  $\alpha(t)$  of the ends of the specimen are registered for a constant value of  $\dot{\alpha}$ . The final problem is to deter-

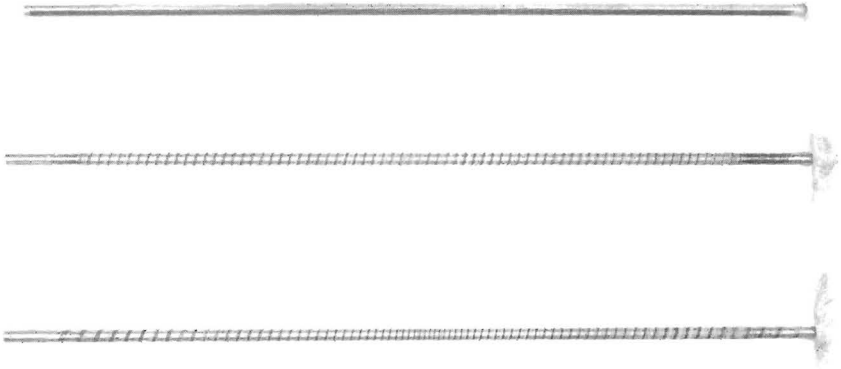


**Figure 14. Photo of three torsion bars:** The upper bar is a undeformed bar, the middle bar has been slowly deformed and the lower bar has been quickly deformed

mine the stress-strain relationship  $\sigma_v = \sigma_v(\bar{\varepsilon}, \dot{\bar{\varepsilon}}) = \sigma_v\left(\frac{1}{3} r\dot{\alpha}\sqrt{3}, \frac{1}{3} r\alpha\sqrt{3}\right)$  from the measured values because 4.3.16 does not give an explicit relationship for  $\sigma_v$ . Differentiating the torque  $M$  in 4.3.16 to the parameters  $\alpha$  and  $\dot{\alpha}$ , the following relationship for  $\sigma_v$  on one the hand and  $M$ ,  $\alpha$  and  $\dot{\alpha}$  on the other is obtained after a straightforward calculation:

$$\sigma_v|_{r=R} = \frac{\sqrt{3}}{2\pi R^3} \left( 3M + \dot{\alpha} \frac{\partial M}{\partial \dot{\alpha}} + \alpha \frac{\partial M}{\partial \alpha} \right) |_{r=R} \quad (4.3.17)$$

This means that an analytical expression has been obtained for the Von Mises stress on the outer radius of the bar. The corresponding values of  $\bar{\varepsilon}$  and  $\dot{\bar{\varepsilon}}$ , in this position, can easily be deduced from relationship 4.3.15:

$$\dot{\bar{\varepsilon}}|_{r=R} = \frac{1}{3} \dot{\alpha} R \sqrt{3} \quad ; \quad \bar{\varepsilon}|_{r=R} = \frac{1}{3} \alpha R \sqrt{3} \quad (4.3.18)$$

As in to the tension test, localisation of the deformation can be observed in the torsion test. In figure 14, three copper bars are shown. The radius of these bars is 2 mm and the length 200 mm. The upper bar is an undeformed bar with a straight black line drawn on it. The middle bar is a deformed bar, where the deformation has been reached with a rotation velocity of 1 rotation per minute. The lowest bar has been rotated with a velocity of 1 rotation per second. It can be clearly seen that the deformation of the middle bar is uniform and that localisation occurred in the lowest bar. The reason for this localisation is that the torsion bar can become very hot due to dissipation. For a low rotation velocity, the dissipated energy can easily be conducted to the ends of the bar. If the velocity is high, the thermal resistance is too great. It was observed, for the lowest bar, that the temperature rise in the middle of the bar was at least 100°C . To obtain this result, experiments were done with a infra-red camera.

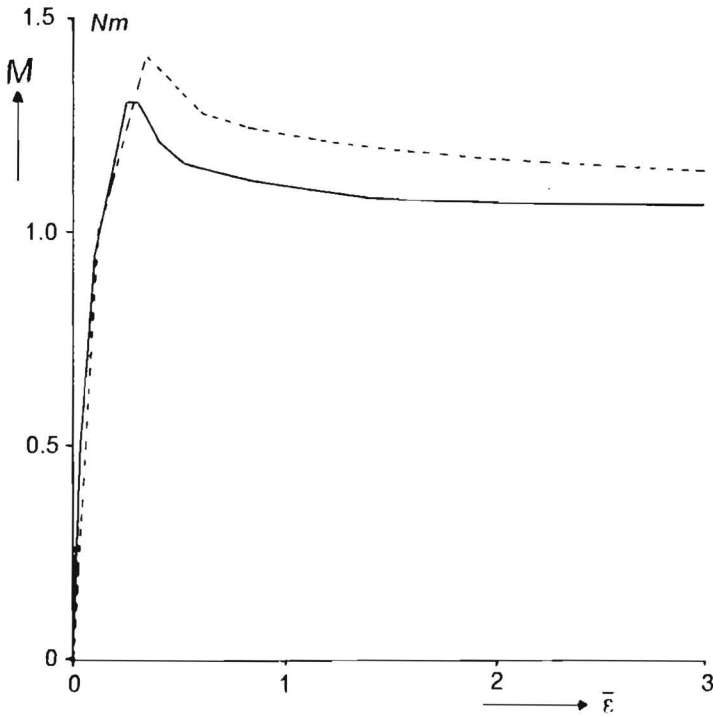


**Figure 15.** Results obtained from two torsion tests of lead: Torque versus strain at a strain rate of 0.016 1/s (—) and at a strain rate of 0.048 1/s (-----)

As the yield stress of metals decreases as the temperature increases, one can expect that the torque  $M$  will reach a maximum for the lowest bar, after which the deformation localises. In other words, one can postulate that localisation occurs during a torsion test if the torque reaches a maximum. Such a postulation is similar to the tension test, where localisation occurs if the applied force reaches a maximum. However, this postulation is not true for the torsion test. To show this, the results obtained from the torsion of lead bars are considered. In figure 15 it can be seen that for every rotation velocity (or deformation rate) the torque  $M$  reaches a maximum. Observation of the deformations of these bars, however, didn't show any localisation. This contradicts the postulation. The fact that the torque reaches a maximum for lead bars, is due to metallurgical effects. For all metals at relatively high temperatures (i.e. temperatures at which no hardening due to recrystallisation is observed) these effects can be seen. For some of these metals, even oscillations of the torque can be observed. Rauch, Canova, Jonas and Semiatin (1984) gave some theoretical explanation for this non-



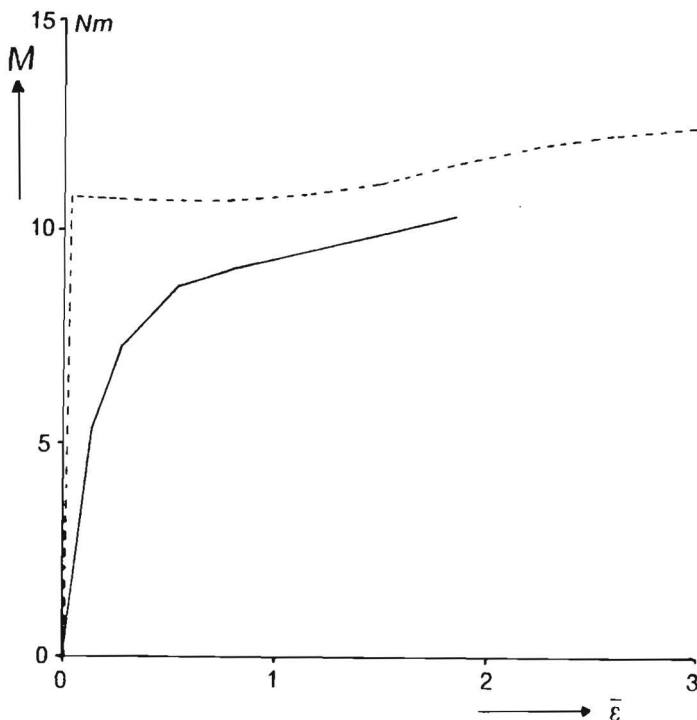


**Figure 16. Results obtained from two torsion tests of copper:** Torque versus strain for copper bars with (—) and without (-----) a heat treatment

localisation effect, caused by metallurgical effects. They also predicted the moment, at which localisation will occur, due to temperature effects.

The measurement of the axial force (no axial deformation) or the axial deformation (no axial force) or a combination of these two gives an impression of the non-isotropic effects, such as kinematic hardening. In figure 16, the results of two torsion tests are illustrated: one for a copper bar with no heat treatment (dotted line) and the other for a copper bar with a heat treatment (solid line). Because of the heat treatment, there is a difference in the crystalline structure of the bars, which leads to this difference in the torque response. Taking into account the elongation of these bars, a much larger difference is obtained (see figure 17). In figure 18, the radius of the bar during torsion of lead bars has been drawn, for different deformation rates. Apparently, the anisotropic effects are only influenced by the total deformation. It is strongly recommended that these phenomena be investigated in relation to the constitutive models, obtained in

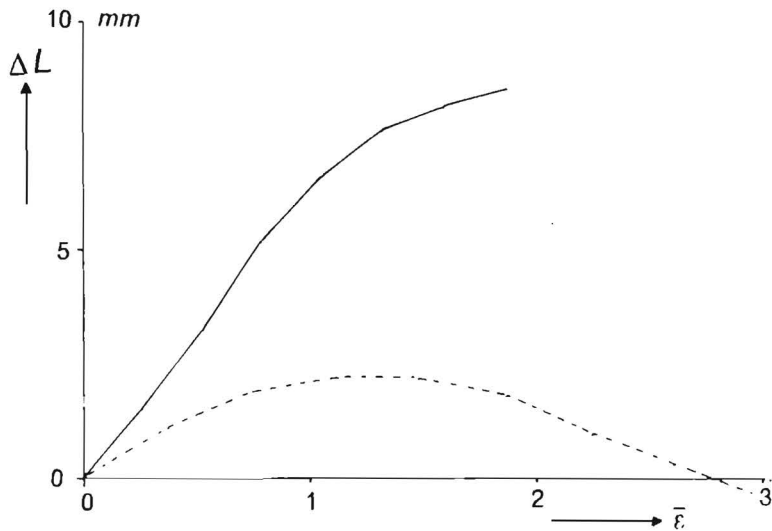
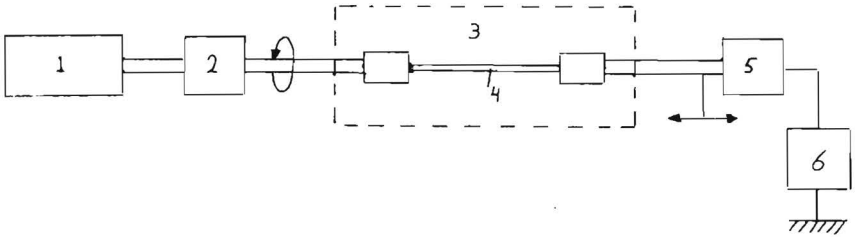


**Figure 17. Elongation during a torsion test of two copper bars:** Elongation versus strain for copper bars with (—) and without (-----) a heat treatment

subparagraph 3.7. Montheillet, Cohen and Jonas (1984) did some torsion experiments on the development of axial stresses, when the elongation of the bars is suppressed. They succeeded in relating the axial force to the texture development in the bar.

Besides the advantages that at a relatively low deformation rate, no localisation occurs, and that model studies can be made of non-isotropic effects, the main advantage of the torsion test, compared with the tension test, is that measurements can easily be done for different temperatures, by putting an oven around the bar. In figure 19 the results are given for a torsion test on lead bars at different temperatures. Due to the temperature increase an enormous decrease of the torque can be observed. The results obtained at 300°C will be used in chapter 5.

The total set-up for a torsion bank can be as follows:



- 1) drive for the rotation of the bar
- 2) element for the measurement of the total angle
- 3) oven
- 4) bar
- 5) element for the measurement of the torque  $M$
- 6) element for the measurement of the elongation or the axial force

In figure 20 a photo is given of such a set-up developed and built by Meershoek (1988).

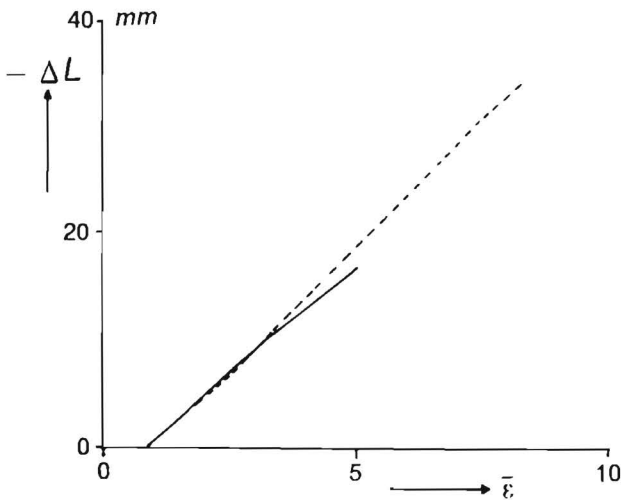


**Figure 18.** Shortening during a torsion test of two lead bars: Shortening versus strain for lead bars at a strain rate of 0.016 1/s (—) and 0.024 1/s (-----)

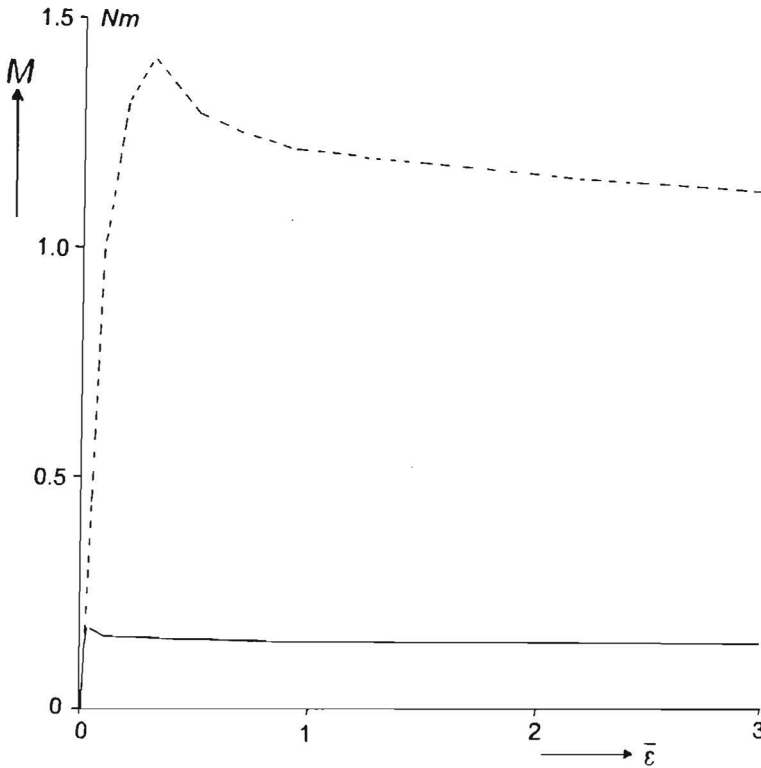


**Figure 19.** Results obtained from two torsion tests of lead: Torque versus strain at a temperature of 20°C (—) and 300°C (-----)

In summary it can be stated that some of the disadvantages of the tension test (instabilities for small deformations and the difficulties of taking measurements at different temperatures) can be avoided, by doing torsion tests. Further, non-isotropic effects can be studied with the torsion test. A disadvantage of the torsion test is that the ratio between the radius and the length of the bar has to be small and the rotation velocity can't be too large, because of thermal instabilities. Hence, large values of the strain rate can not be achieved. For strain hardening materials, experimental data for large strain rates can be obtained from the tension test. For metals at relatively high temperatures, however, this is not possible, because of the non-uniform necking. For these metals, the compression test can be an alternative.

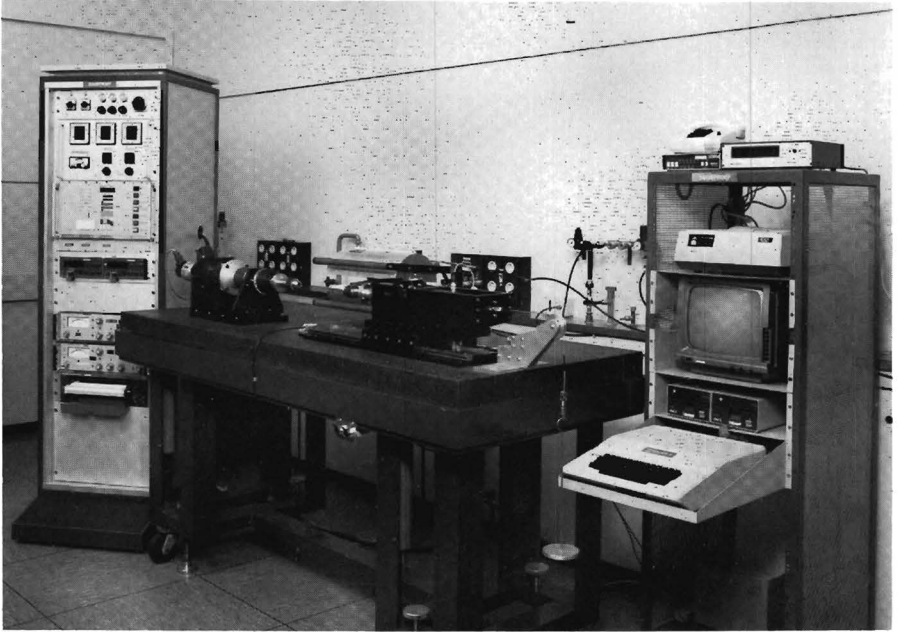


Figure 20. Photo of the experimental set-up for torsion tests

## 4.4 The compression test

In this subparagraph the compression test will be discussed. Using this test, material properties can be determined at large deformation rates and at different temperatures. A condition for this test is that the Von Mises stress  $\sigma_v$  only depends on the equivalent strain rate  $\dot{\epsilon}$  and the temperature.

Figure 21 gives an idea of the experimental set-up. A cylindrical pallet, whose height  $h$  is much smaller than its radius  $R$ , is compressed with a velocity  $\dot{h}$ , where  $\dot{h} < 0$ . The surface of the upper and lower stamps is such, that sticking occurs on the interfaces between the pallet and the stamps. The temperature in the pallet can be controlled by the temperature in the stamps, whose surfaces have to be almost isothermal. As the energy losses near the outer radius of the pallet will be small, due to the small height,

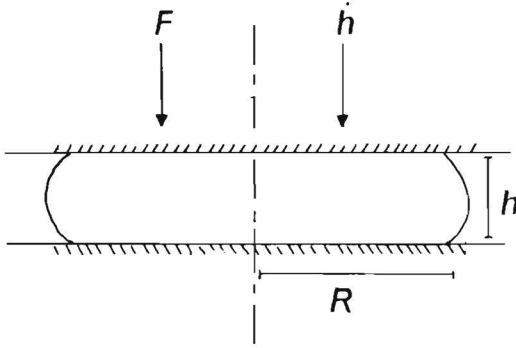


Figure 21. The compression test

near isothermal conditions will be reached in the pallet. During the experiment, the pressure force  $F$ , the height  $h$  and the (compression) velocity  $\dot{h}$  are measured.

In order to obtain a relationship between the Von Mises stress  $\sigma_v$  and the equivalent strain  $\dot{\epsilon}$  on the one hand and the pressure force  $F$ , the height  $h$  and the velocity  $\dot{h}$  on the other, use will be made of the ratio between the height and the radius. As this ratio is very small, the ratio between the axial coordinate  $z$  and the radial coordinate  $r$  will also be small, in most parts of the pallet. The same will hold good for the axial and radial velocity, and the derivatives in radial and axial direction (see Van Wijngaarden, Dijksman and Wesseling, 1982) :

$$\frac{h}{R} = \delta ; \quad \frac{u_z}{u_r} = O(\delta) ; \quad \frac{\frac{\partial}{\partial r}}{\frac{\partial}{\partial z}} = O(\delta) \quad (4.4.1)$$

where  $O(\delta)/\delta$  remains finite when  $\delta \rightarrow 0$ . The parameter delta is much smaller than 1, for the pallets under consideration. It is now easy to deduce that the deformation rate tensor  $\mathbf{D}$  is reduced to:

$$\mathbf{D} = \frac{1}{2} \frac{\partial u_r}{\partial z} (\mathbf{e}_r \mathbf{e}_z + \mathbf{e}_z \mathbf{e}_r) + O(\delta) \quad (4.4.2)$$

From relationship 4.1.6 between the stresses and the strain rates and from 4.4.2 it follows that the Cauchy stress can be expressed by:

$$\boldsymbol{\sigma} = -p(\mathbf{e}_r \mathbf{e}_r + \mathbf{e}_\phi \mathbf{e}_\phi + \mathbf{e}_z \mathbf{e}_z) + \sigma_{rz}(\mathbf{e}_r \mathbf{e}_z + \mathbf{e}_z \mathbf{e}_r) + O(\delta) \quad (4.4.3)$$

Hence, the definitions of the Von Mises stress and the equivalent strain rate yield:

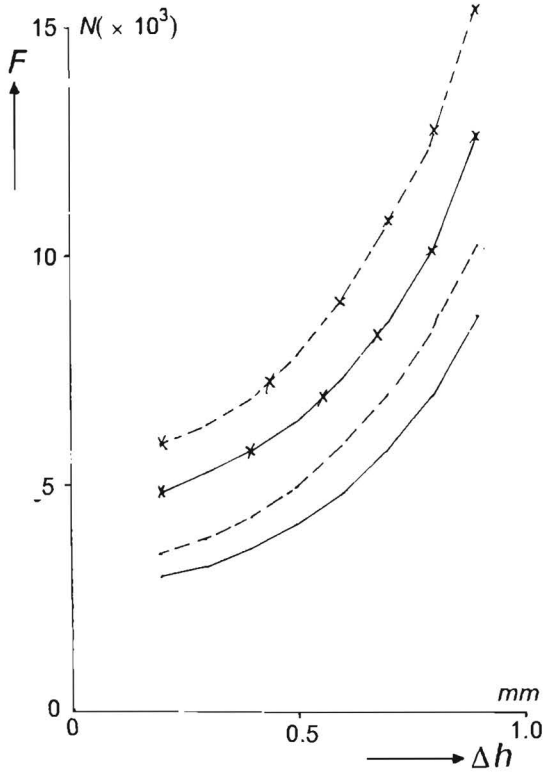


Figure 22. Results obtained from four compression tests of lead: Compression force versus height reduction at two temperatures and two compression velocities (— 300°C, 3 mm/s ; x—x 300°C, 30 mm/s ; ..... 275°C, 3 mm/s ; x---x 275°C, 30 mm/s )

$$\sigma_v = \sqrt{3} |\sigma_{rz}| + O(\delta^2) ; \quad \dot{\epsilon} = \frac{1}{\sqrt{3}} \left| \frac{\partial u_r}{\partial z} \right| + O(\delta^2) \quad (4.4.4)$$

Taking incompressibility into account, the balance equation of mass becomes:

$$\frac{\partial u_r}{\partial r} + \frac{u_r}{r} + \frac{\partial u_z}{\partial z} = 0 \quad (4.4.5)$$

and the neglecting of body forces and inertia terms in the balance equation of momentum leads to:

$$\frac{\partial p}{\partial r} = \frac{\partial \sigma_{rz}}{\partial z} + O(\delta^2) ; \quad \frac{\partial p}{\partial z} = O(\delta^2) \quad (4.4.6)$$

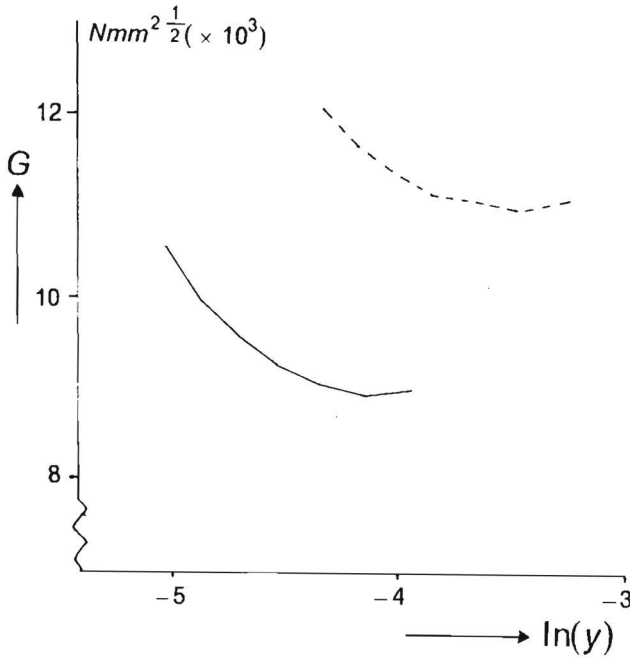


**Figure 23.** Results obtained from two compression tests of lead:  $G$  versus  $\ln(y)$  at a compression velocity of  $-1.5$  mm/s (—) and  $-3$  mm/s (-----)

For  $\delta \rightarrow 0$ , a set of equations is found from which the desired relationship between  $\sigma_v$  and  $\dot{\epsilon}$  on one the hand and  $F$ ,  $h$  and  $\dot{h}$  on the other can be deduced (see Appendix F). It is similar to the deduction, made by Doustens and Laquerbe (1987) for compression flows of liquids between parallel circular plates with constant radius.

Let  $G$  and  $y$  be defined by:

$$G = h^2 \sqrt{\dot{h}} F \quad ; \quad y = \frac{|\dot{h}|R}{h^2} = - \frac{\dot{h}R}{h^2} \quad (4.4.7)$$

A direct consequence of the assumption that the Von Mises stress  $\sigma_v$  only depends on the equivalent strain rate  $\dot{\epsilon}$  and the temperature  $\theta$ , is that  $G$  is a function of  $y$  and  $\theta$  only:

$$G = G(y, \theta) \quad (4.4.8)$$

On the outer radius and the interface between the pallet and the stamps an analytical expression can be found for  $\sigma_v$  and  $\dot{\epsilon}$  in terms of the quantities  $G$  and  $y$  (see Appendix G):



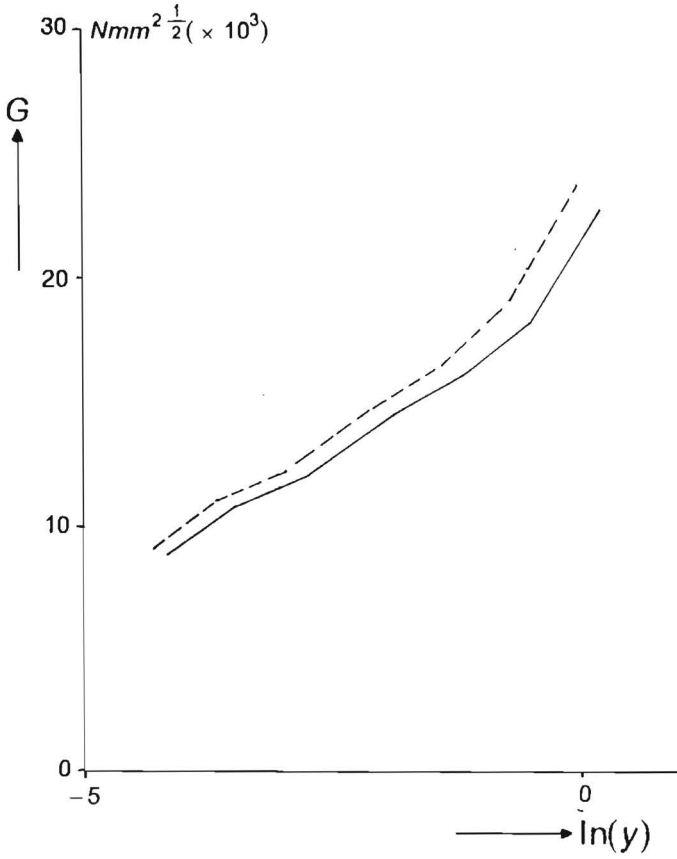


Figure 24. Results obtained from two compression tests of lead: G versus  $\ln(y)$  at a height of 1.2 mm (—) and 1.3 mm (-----)

$$\sigma_v = \frac{\sqrt{3\pi}}{2V_0\sqrt{V_0}} \left( 3G + y \frac{\partial G}{\partial y} \right) \quad (4.4.9)$$

$$\dot{\epsilon} = \frac{1}{\sqrt{3}} \left( 2y + \sigma_v \left( \frac{\partial \sigma_v}{\partial y} \right)^{-1} \right) \quad (4.4.10)$$

where  $V_0$  is the volume of the pallet.

As an example, the compression of pallets of lead is discussed. The pallets have an initial height of 2 mm and a radius of 10 mm. They were compressed to a height of 1 mm for various compression velocities ( $0.025 \text{ mm/s} \leq |\dot{h}| \leq 2 \text{ mm/s}$ ) and at a temperature of 275°C and 300°C. In figure 22, some of the curves obtained for the force as

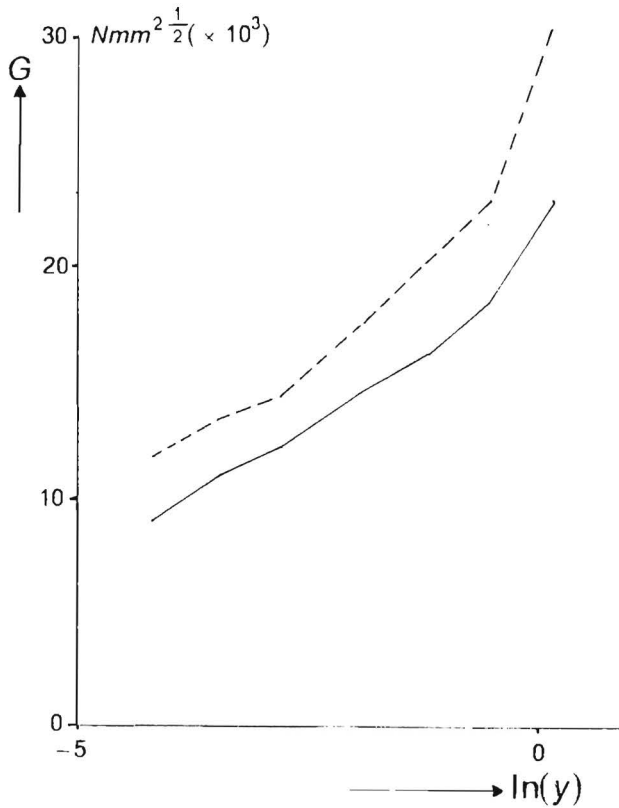


Figure 25. Results obtained from two compression tests of lead:  $G$  versus  $\ln(y)$  at a temperature of 300°C (—) and 275°C (-----)

a function of the height reduction  $\Delta h$  have been drawn. During each test the compression velocity and the temperature remained constant. It can be clearly seen that the force increases for increasing height reduction and compression velocity and for decreasing temperature.

In the previous subparagraph it was observed that during a torsion test the Von Mises stress increased to a maximum and then decreased to a constant value which only depended on the strain rate and the temperature. The same phenomena can be observed from the results obtained with the compression test. If the Von Mises stress of lead only depends on the strain rate at constant temperature, then  $G$  is a function of  $y$ . The curves in figure 23 are based on the measurements of  $F$  and  $h$  in experiments with constant compression velocity  $\dot{h} = -1.5\text{mm/s}$  and  $\dot{h} = -3\text{mm/s}$ . It is apparent that

by increasing  $y$ ,  $G$  first decreases, then slightly increases. The curves in figure 24 represent the results of a number of experiments in which  $F$  is measured as a function of  $\dot{h}$ , at constant height reduction. From these curves it can be seen that  $G$  increases by increasing  $y$ . In evaluating of these results, to get a relationship between the Von Mises stress and the equivalent strain rate, it is assumed that the most reliable results are obtained at large deformation, which means at large height reduction.

In figure 25, two curves for  $G$  have been drawn for two different temperatures. It can be clearly seen that  $G$  increases as temperature decreases. In the next chapter, the results obtained at a temperature of  $300^{\circ}\text{C}$  are used for the derivation of a relationship between  $\sigma_v$  and  $\dot{\epsilon}$ . Relationships 4.4.9 and 4.4.10 have been used for this purpose.

## **5 The extrusion of lead**

### **5.1 Introduction**

In this chapter the application of some of the theories in the previous chapters will be discussed. Most of the subjects in this chapter have already been published by Van Wijngaarden, Van Bakel, Verwey and Meershoek (1986). The application is adapted from the thermocompression bonding technique, where lead is deformed between two substrates. The next subparagraph gives a short review of the thermocompression technique and the mechanical problems that arise from it. In subparagraph 5.3 the mechanical model that has been used until now, of the thermocompression process is discussed and some statements are given about the choices, that have been made to obtain a constitutive model for lead. In the set-up of the program future extensions have been taken into account for better material models for lead. Instead of the used Maxwell model, Oldroyd models and even combinations of Maxwell models and the Kelvin model can be easily brought into the program. Some statements about the way, this can be done, are made. In order to solve the relevant balance equations, a finite element technique has been used, in which special attention has been given to substitution of the constitutive equations into the balance equations. The choice of the elements will be motivated, as well as the iteration technique, used to solve the non-linear equations.

In the first instance, results were obtained with a Maxwell model, whose viscous part had been fitted into the results of the torsion test. These results were mainly used for the investigation of the convergence of the iteration scheme. Only recently, an update has been made for the viscous part of the Maxwell model. In this case, the experimental data obtained from the compression test and creep tests, which have been published in literature, have also been taken into account. Only the first results can be presented, because the project is still going on. In future, comparisons will be made between the results of the calculations and the experimental observations of the thermocompression technique.

## **5.2 Thermocompression bonding**

Thermocompression is a technique, in which a bonding metal is deformed between two substrates. The process is performed at about 90 % of the melting temperature (Kelvin) of the metal. Due to compressive stresses close contact is established between the bonding metal and the substrates, to be bonded. During the deformation the oxidised surface of the bonding metal is broken. The high temperature ensures a high rate of physical and chemical interaction between the pure lead and the substrates. As the temperature is always below the melting temperature of the bonding metal and the two substrates, bonding is carried out in the solid state. This technique is suitable for substrates of oxides (ceramic materials or glasses), metals and alloys. An advantage of this technique is that bonding can be done very quickly, even within 5 milliseconds.

A large range of bonding materials can be used from indium at 20°C to niobium at 1750°C. When one of the substrates is glass, the bonding temperature may not be higher than the softening temperature of glass, which is about 550°C. This means that the bonding materials used must be reactive below 550°C. The only three alternatives for glass are therefore indium, lead and aluminium.

Indium is a good bonding metal, but often it cannot be used in further steps of the process, due to its relatively low melting temperature of 157°C. Aluminium has a higher melting point (660°C), but shows insufficient stress relaxation during cooling. Using lead (melting temperature of 326°C) as a bonding metal, it is necessary to heat the substrates up to about 300°C, before bonding.

Lead, however shows sufficient stress relaxation for stresses built up after bonding. This can be seen in figure 26, which shows a thermocompression bond between glass and steel, where the substrates have a big difference in thermal expansion. After cooling to 20°C, the bond made with lead is still intact, but the glass substrate used for the aluminium bond, is broken. The cooling phase is therefore not considered in this chapter.

Considering the bonding process of lead between glass and steel one of the main problems that arise, is the failure of the bond, due to the fact, that the surface of one or both substrates is not completely plain. After the compression of lead unloading takes place, which can result in elastic relaxation of the substrates. It is then possible that large tensile stresses occur in the lead, which can cause a failure of the bond. In the following subparagraphs a mechanical model will be discussed, which describes the compression and unloading phases of the thermocompression process.

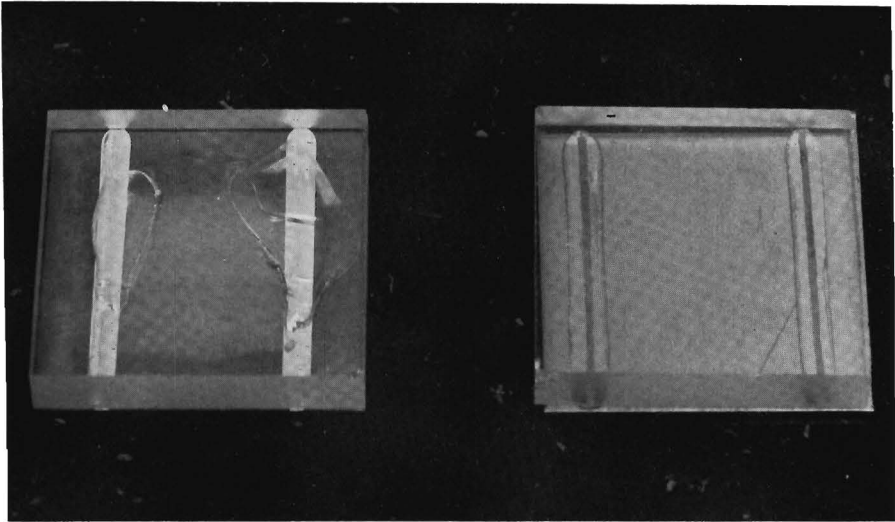


Figure 26. A thermocompression bond of lead (right) and aluminium (left) between glass and steel

At the time of writing this thesis, the first results of the model analyses have been obtained, like it has already been mentioned in the subparagraph 5.1. These and future results will be used to obtain an insight into the thermocompression process, perhaps leading to further improvements.

### ***5.3 A model for thermocompression***

In this subparagraph thermocompression of rings of lead are considered. First, the ring is compressed between the two substrates, after which unloading takes place (see figure 27). The initial radius of a cross section of the ring is about 2 mm. During compression the height between the two substrates is reduced to about 0.3 mm, a height reduction of more than 90 %. This means that very large deformations will take place. The whole process of compression and unloading takes place at a temperature of 300°C, and isothermal conditions are assumed. Because lead is very soft at this temperature, it is assumed that the substrates can be considered rigid. During the compression phase the eventually not plain substrates are deformed elastically. After unloading, the elastic deformations cause initially a loading to the bond which, in turn, is relaxed, due to the relaxation capability of lead.

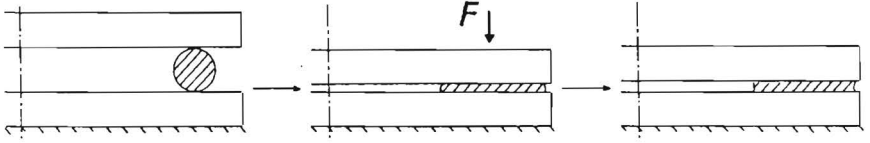


Figure 27. Compression and unloading of a ring

The balance of mass and momentum have to be fulfilled during the process. These equations are:

$$\frac{\dot{\rho}}{\rho} + \frac{\partial u_r}{\partial r} + \frac{u_r}{r} + \frac{\partial u_z}{\partial z} = 0 \quad (5.3.1)$$

$$\frac{\partial \sigma_r}{\partial r} + \frac{\sigma_r - \sigma_\phi}{r} + \frac{\partial \sigma_{rz}}{\partial z} = 0 \quad (5.3.2)$$

$$\frac{\partial \sigma_{rz}}{\partial r} + \frac{\sigma_{rz}}{r} + \frac{\partial \sigma_z}{\partial z} = 0 \quad (5.3.3)$$

The boundary conditions for this set of partial differential equations are the following (see figure 28). On the symmetry plane,  $z=0$ , the symmetry conditions  $\sigma_{rz} = 0$  and  $u_z = 0$  will hold. On the interface between lead and substrate, ( $z=h$ ), sticking is assumed, which indicates that  $u_r = 0$  and  $u_z = \dot{h}$ . This assumption seems valid, because on these two interfaces the substrates are bonded to lead. On the free boundaries ( $r = R_1(z, t)$  and  $r = R_2(z, t)$ ), no stress is applied. The position of these free boundaries can be obtained by solving the the following equations:

$$(r - R_i(z, t)) = 0 \rightarrow \frac{\partial R_i}{\partial t} - u_r + u_z \frac{\partial R_i}{\partial z} = 0 \text{ for } i = 1, 2 \quad (5.3.4)$$

This model is completed by the constitutive equations for lead. In the previous chapter some results obtained from experiments, have already been discussed. From these results it can be concluded that the viscous behaviour of lead is mainly influenced by the strain rate and the temperature. But the temperature dependency is irrelevant, because it is assumed that the process is isothermal. Secondary effects, such as the increase of the torque at the beginning of the deformation and the shortening of the torsion bars (see subparagraphs 4.3 and 4.4), are negligible. In that case it is assumed, that the constitutive behaviour can be described with a Maxwell model (see subparagraph 3.6). This model, where the deformation rate is decomposed into an elastic and a viscous part, is usually used for metals. The elastic part, which will be very small compared with the total deformation, is taken into account, so as to be able

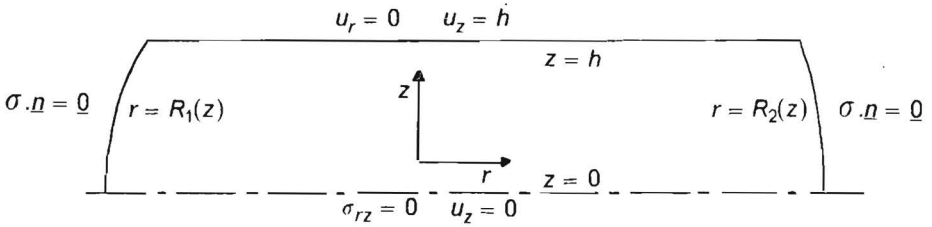


Figure 28. Cross section of the upper half of the ring

to describe relaxation effects that may occur during the unloading phase of the ring. The secondary effects could be taken into account by considering an Oldroyd model, for instance (see subparagraphs 2.6 and 3.5) or a Maxwell model, in combination with kinematical hardening (see section 3.6 and 3.7). How these models work out, with respect to the experiments in chapter 4, and whether these models are able to describe these secondary effects, hasn't been investigated yet, although it is easy to show that these models lead to elongations in, or shortening of torsion bars, when no axial force is applied to the bar. Further investigation is required in order to bring the secondary effects into account. However, in the discussion of the numerical approximation of the Maxwell model in Appendix G (and the next subparagraph), a possible numerical treatment of the Oldroyd model and of the Maxwell model with kinematical hardening is given as well.

Finally lead is considered to be incompressible. For the viscous part of the deformation this can be shown by experiment. For the elastic part this is probably not true. This part, however, is very small with respect to the total deformation, and so the assumption about the incompressibility can be made. Then the balance equations of mass reduce to:

$$\text{tr}(\mathbf{D}) = \frac{\partial u_r}{\partial r} + \frac{u_r}{r} + \frac{\partial u_z}{\partial z} = 0 \quad (5.3.5)$$

The constitutive equations for lead then become:

$$\sigma = -p\mathbf{I} + \tau \quad (5.3.6)$$

$$\frac{1}{\eta(\dot{\bar{\epsilon}})} \tau + \frac{1}{E} \overset{\vee}{\tau} = \mathbf{D} \quad (5.3.7)$$



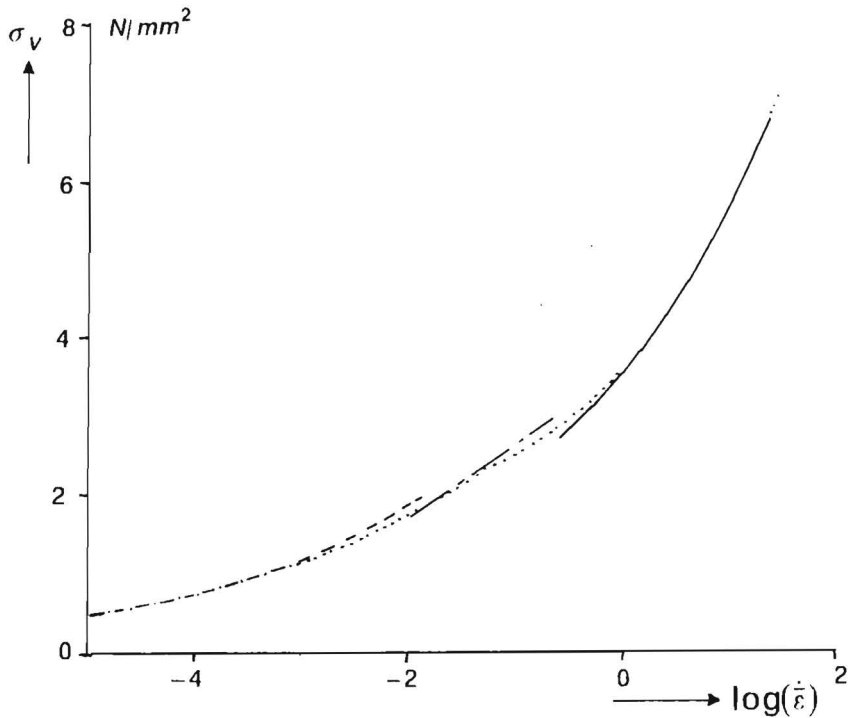


**Figure 29. Several stress-strain rate curves:** Von Mises stress versus strain rate obtained from a creep test (-----), a torsion test (---), a compression test (—) and a fit (.....)

where the objective stress rate still has to be defined. In the next subparagraph a solution method is discussed for this constitutive relationship, which is valid for every rate, defined in chapters 2 and 3. In the final subparagraph results obtained using the Truesdell rate, will be discussed. There was no particular reason for this choice. It is doubtful whether in this case, the choice would make much difference, because the elastic part of the deformation is very small.

In subparagraph 4.3 and 4.4 results were given on tests on the torsion and compression of lead, obtained at a temperature of 300, °C. Frost and Ashbey (1982) have also published results, obtained from several tests on lead. In figure 29, where the Von Mises stress is drawn as a function of the equivalent strain rate, all these results have been assembled. Frost and Ashbey gave results for very low equivalent strain rates ( $\dot{\epsilon} \leq 0.01$ ). In fact these authors were mainly interested in creep experiments. For the torsion test results were obtained for  $0.01 \leq \dot{\epsilon} \leq 0.5$ . The fact that results could be ob-

tained for only relatively small values of the equivalent strain rate, has already been mentioned in subparagraph 4.3. For  $\dot{\epsilon} \geq 1$  the compression test gave some results, which have been discussed in subparagraph 4.4. One of the most striking results is, that these test are complementary. From the results obtained the viscosity  $\eta$  has been described, in terms of  $\sigma_v$ , in the following way:

$$\frac{1}{\eta} = C_1 \sigma_v^n \quad \text{for } \sigma_v \leq \sigma_0 \quad (5.3.8)$$

$$\frac{1}{\eta} = C_1 \sigma_v^n + C_2 \frac{(\sigma_v - \sigma_0)^m}{\sigma_v} \quad \text{for } \sigma_v > \sigma_0 \quad (5.3.9)$$

This relationship has also been reproduced in figure 29. The following values have been used:

$$C_1 = 5.10^{-4} mm^{2+2n} / N^{1+n} s ; \quad C_2 = 0.25 mm^{2m} / N^m s ; \quad \sigma_0 = 2.13 N / mm^2$$

$$n = 4.56 ; \quad m = 2.27 \quad (5.3.10)$$

For the property E, in relationship 5.3.7, a value is given in Frost and Ashbey (1982). The value is at 300°C:

$$E = 9500 N / mm^2 \quad (5.3.11)$$

In the next subparagraph a solution method will be discussed for both these constitutive equations and the balance equations.

## 5.4 The solution procedure

In order to solve the balance equations 5.3.2, 5.3.3 and 5.3.5 Galerkin's method is used. Let the pressure  $p$  be approximated by the base functions  $\psi_i$  for  $i = 1, \dots, M$  and the velocity  $u$  by the base functions  $\phi_j$  for  $i = 1, \dots, N$ . Then, the weighted formulae become:

$$\int_V \text{tr}(\mathbf{D}) \psi_i dV = 0 \quad (5.4.1)$$

$$\int_V (-p\mathbf{I} + \boldsymbol{\tau}) : (\nabla \phi_j) dV = \int_{\delta V} \phi_j \cdot \boldsymbol{\sigma} \cdot \mathbf{n} ds \quad (5.4.2)$$

The right-hand side of equation 5.4.2 is equal to zero, due to the boundary conditions: either  $\boldsymbol{\sigma} \cdot \mathbf{n} = 0$  or  $\phi = 0$ .

Direct substitution of the constitutive equation 5.3.6 in order to eliminate the stress tensor  $\boldsymbol{\tau}$  in 5.4.2, is not possible. This equation is therefore transformed into the following equations, which are a numerical approximation of the original constitutive equations:

$$\boldsymbol{\tau} = \kappa \mathbf{D} + \mathbf{G} \quad (5.4.3)$$

$$\kappa = \eta \frac{\Delta t E}{\eta + \Delta t E} \quad (5.4.4)$$

$$\mathbf{G} = \frac{\eta}{\eta + \Delta t E} \mathbf{P} \cdot \boldsymbol{\tau}_0 \cdot \mathbf{P}^T \quad (5.4.5)$$

$$\mathbf{P} = \mathbf{I} + \Delta t (\boldsymbol{\Omega} + \mathbf{H}) \quad (5.4.6)$$

where  $\boldsymbol{\tau}_0$  is the value of this stress tensor at the previous point of time of the material point under consideration and where the tensor  $\mathbf{H}$  is given by equation 3.3.11 and 3.3.18. This numerical approximation is derived in Appendix G.

In this chapter the tensor  $\mathbf{H}$  is chosen as equal to the deformation rate tensor  $\mathbf{D}$ , which is obtained for  $\beta = 1$  in 3.3.18. This choice of  $\mathbf{H}$  results in a non-linear relationship between the stress on one the hand and the velocity and previous values of the stress on the other. Choices for  $\beta^2 \neq 1$  will lead to much more complicated relationships between the stress and velocity: in that case the main problem would be to obtain a relationship for  $\mathbf{H}$  in terms of the velocity. This problem hasn't been investigated in this thesis.

Substitution of 5.4.3 into 5.4.2 yields:

$$\int_V (-p\mathbf{I} + \kappa \mathbf{D}) : (\nabla \phi_i) dV = - \int_V \mathbf{G} : (\nabla \phi_i) dV \quad (5.4.7)$$

Because the quantity  $\kappa$  and the tensor  $\mathbf{G}$  are non-linear in terms of the velocity, this weighted relationship 5.4.7 is also non-linear. There are several numerical techniques, which deal with non-linearities. Damsteegt, Segal and Van der Zanden (1986) showed that for these kind of constitutive relationships a relative simple Picard iteration scheme can lead to a converging solution strategy. In this case the Picard scheme is given by:

$$\int_V (-p\mathbf{I} + \bar{\kappa} \mathbf{D}) : (\nabla \phi_i) dV = - \int_V \bar{\mathbf{G}} : (\nabla \phi_i) dV \quad (5.4.8)$$

where  $\bar{\kappa}$  and  $\bar{\mathbf{G}}$  are the values of  $\kappa$  and  $\mathbf{G}$ , obtained from the values of the velocity at the previous iteration step.

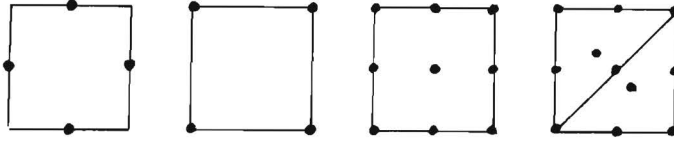


Figure 30. Several elements with their nodal points for the velocity

Except for the pressure and the velocity, the only unknown in relationship 5.4.8 is the volume  $V$ . This volume is obtained by an explicit numerical integration of relationship 5.3.4.

For the choice of elements several elements have been considered: three quadrangular elements and one triangular (see figure 30). These elements have been tested for accuracy and on their numerical smoothing in the vicinity of singular points. This has been done, because in the actual problem, two singular points can be considered, due to sticking on the lead substrate interface. As a test case the compression of a ring with a rectangular cross-section has been chosen (see figure 31). The height of the ring was be much smaller than the radial thickness of the ring. Therefore, the numerical solutions could be compared with the so called Reynolds solution (see Ap-

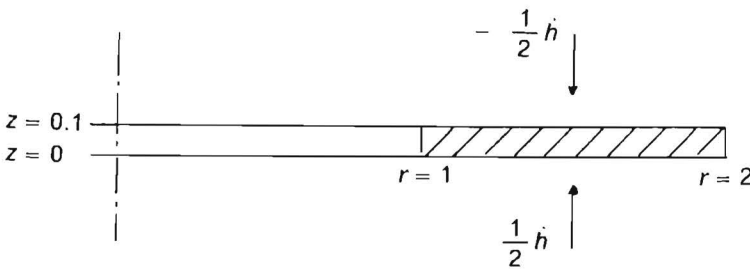


Figure 31. Compression of a ring with a rectangular cross-section

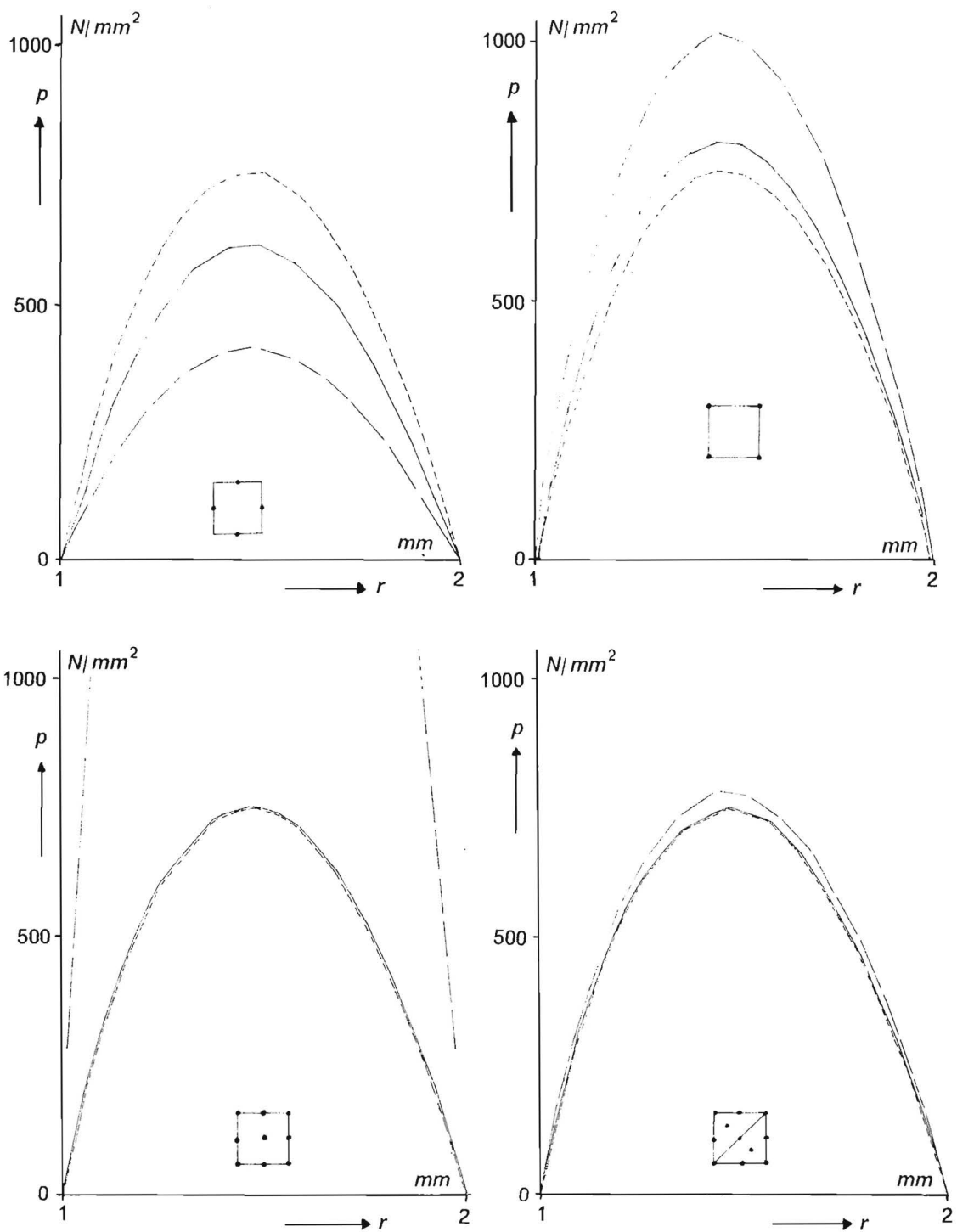


Figure 32. Numerical and analytical results of the compression of a ring: Pressure versus radius obtained from a coarse mesh (—), a mesh that is twice as fine (---) and the analytical solution (— · —)

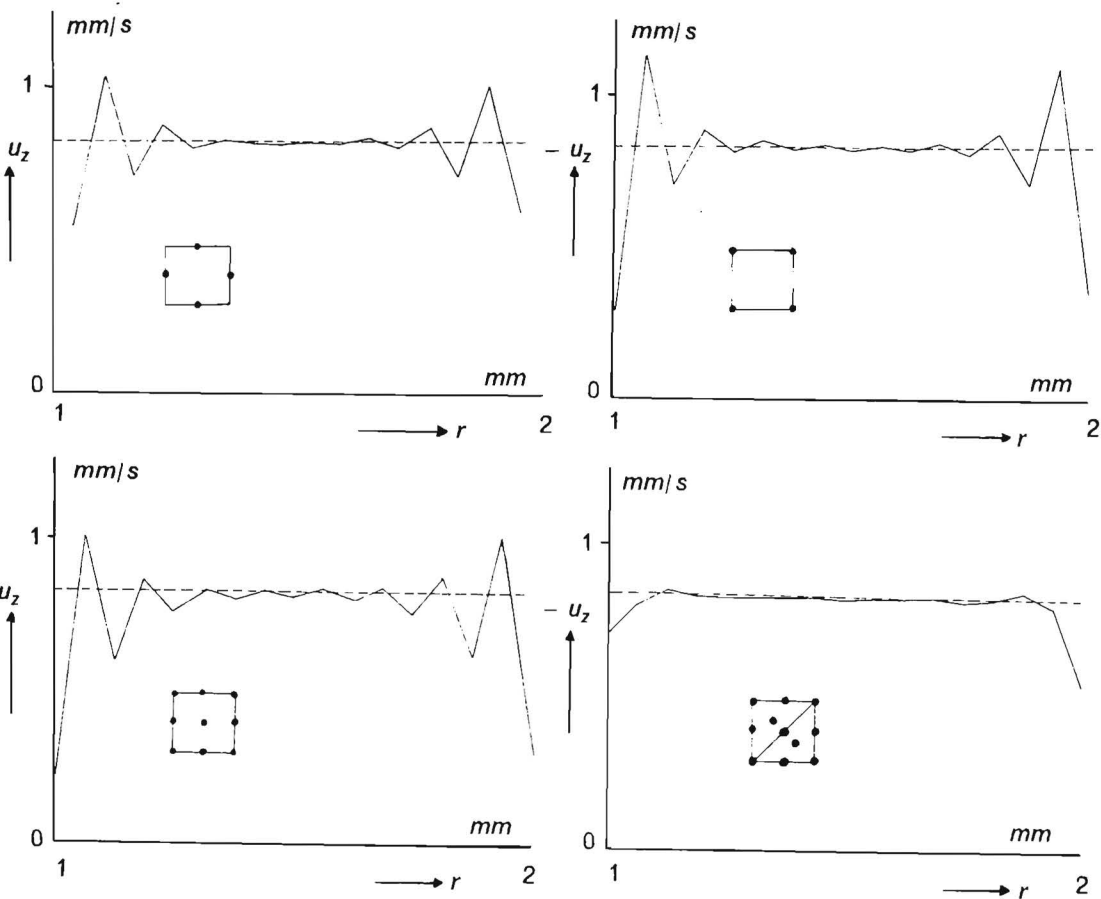
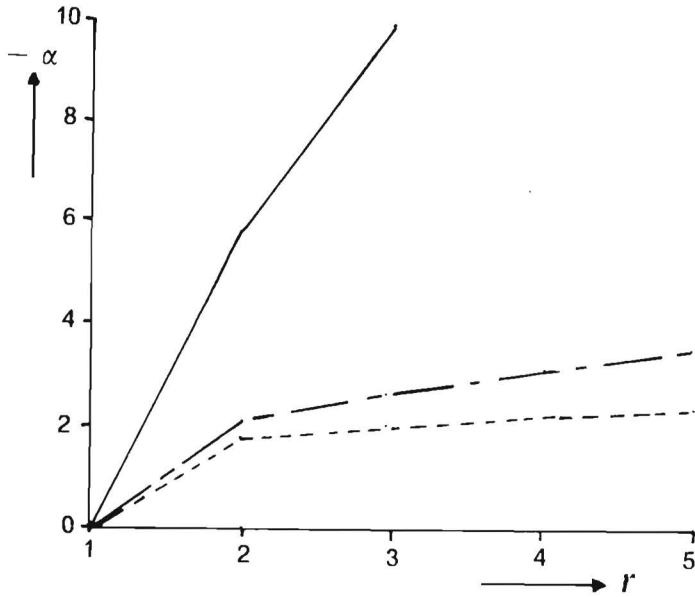


Figure 33. Numerical and analytical results of the compression of a ring: Axial velocity versus radius obtained from a finite element analysis (-----) and the analytical solution (-----)

pendix H). The results of the pressure have been drawn in figure 32. To obtain these results, two meshes were used for each element: 2 or 4 elements respectively in the height direction and 16 or 32 elements respectively in the radial direction for the quadrangular elements with four nodes. The two other element meshes were twice as coarse, so as to obtain a good comparison. From these results, it can be seen that the triangle and the nine-node quadrangle give the best results. For the axial velocity component, which has been considered in the vicinity of the interface between lead and substrate, only the triangle gives acceptable results (see figure 33): the other ele-



**Figure 34. Convergence for different material properties:** C2 is equal to 0.006 (—), 60 (---) and 600000 (----)

ments show much larger oscillations, due to the singularities. Dhait and Hubert (1986) found similar superior numerical results for this triangular element.

Because of these results the triangle element, which is often called the bubble element, has been chosen for numerical analysis of the compression of the lead ring. This element was developed by Crouzeix and Raviart (1973). Griffith (1979) showed how the total number of unknowns can be decreased enormously, which makes the use of this accurate element very attractive, with respect to calculation time. All the results, shown in the next section, have been obtained with this element.

### 5.5 Preliminary results

The computer program, used for acquiring results of the compression and unloading of lead, was developed by Van Bakel (1988). This program is based on the theories discussed in the previous section.

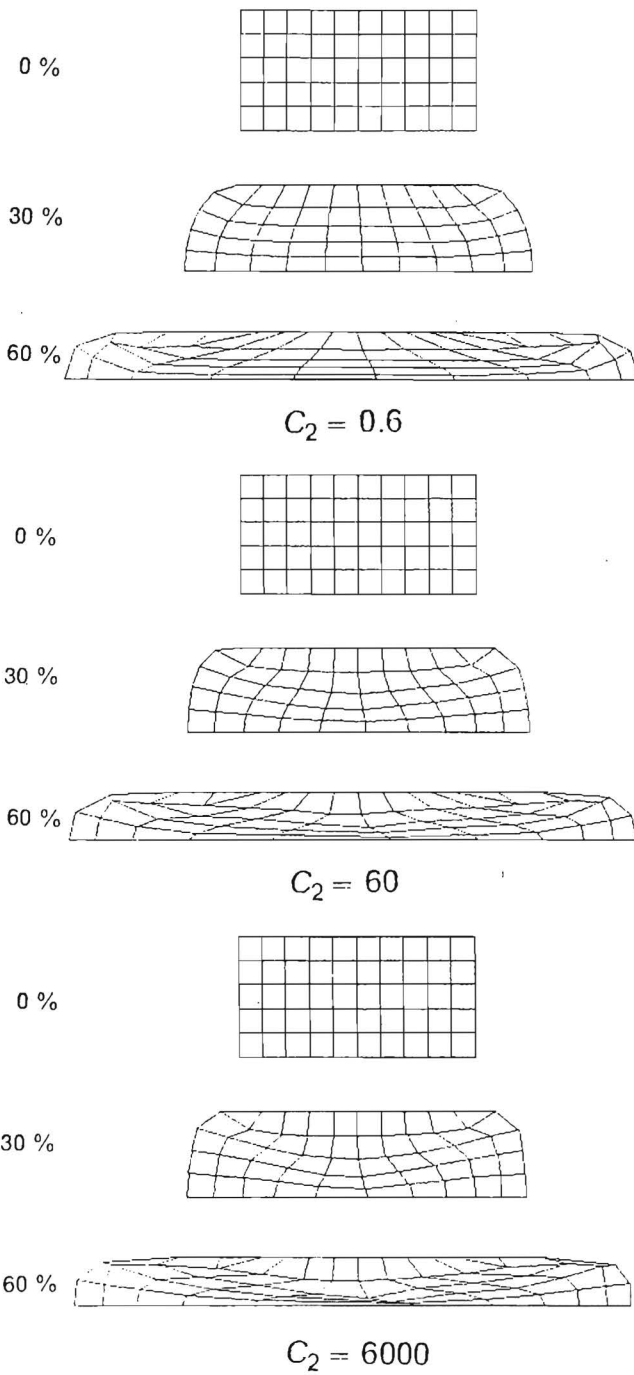


Figure 35. : Deformation pattern at different height reductions for different material properties



The first results obtained concern the compression phase, where attention is given to the influence of the material parameter  $C_2$  (see 5.3.9). The other material properties in models 5.3.8 and 5.3.9 were slightly different from the properties given in 5.3.10. At the time that these investigations were made, the data for the creep tests (Frost and Ashbey 1982) and the compression test (subparagraph 4.4) had not been taken into account. The other properties had the following values:

$$C_1 = 10^{-4} \text{ mm}^2/\text{Ns}; \sigma_v = 2.13 \text{ N/mm}^2; n = 0; m = 1; E = 10^4 \text{ N/mm}^2 \quad (5.5.1)$$

The property  $C_2$  varied between  $6 \cdot 10^{-3}$  and  $6 \cdot 10^5$ . Besides the slight difference in material properties, the first results have been obtained for an initial rectangular cross section of the ring, instead of the more realistic circular cross section.

In figure 34, the convergence of the Picard iteration scheme is shown for three different values of  $C_2$ , on a height reduction of 60 %. On the vertical axis in this figure, the quantity  $\delta$  has been drawn, which is defined by:

$$\delta = \log \left( \left| \frac{n_r - n_{r-1}}{n_1} \right| \right) \quad (5.5.2)$$

where  $n_r$  is the norm for the solution vector of the finite element analysis, obtained after the  $r$ -th iteration. It can be clearly observed that, for increasing values of  $C_2$  more iterations are needed, in order to obtain equally accurate answers. However, the Picard iteration scheme always converges. For large values of  $C_2$ , the material becomes an almost ideal plastic. If  $C_2 \rightarrow \infty$ , then it follows from 5.3.9 that  $\sigma_v \rightarrow \sigma_0$ . In figure 35 the deformed material grid has been drawn for various values of  $C_2$ . It can be seen that due to increasing values of  $C_2$ , the deformation pattern localises. This localisation is probably the cause of the worse convergence of the Picard scheme. In figure 36, the compression force has been drawn, as a function of the parameter  $C_2$ . From this figure, it can be concluded that the force is very sensitive for variations of  $C_2$ , if  $C_2$  is of the order 1. In 5.3.10, it can be seen that  $C_2 \approx 0.25$ , which means that the process conditions have to be tightly controlled in order to obtain a reproducible bonding technique.

Recently, some numerical experiments have been done with the material properties, given in 5.3.10. The ring has an initial radius of 20 mm and a circular cross section with a radius of 2 mm. Figure 37 shows the results, that have been obtained for the axial stress on the interface of lead and the substrate, during the compression phase. The increase of the area on the interface can be observed. As input for these calculations, a measured force versus time curve was used. The boundary value for the axial velocity on the interface can then be obtained iteratively. In figure 38, some vector plots have been drawn for various phases during compression. In figure 39, the axial stress on the interface has been given, during unloading. If the ring is completely unloaded,

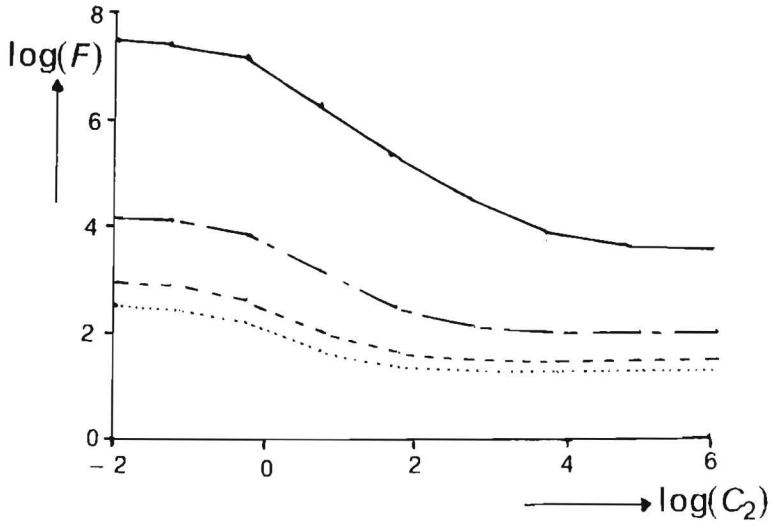


Figure 36. Compression force for different material properties:  $F$  versus  $C_2$  at a height reduction of 0 % (.....), 30 % (-----), 60 % (-.-) and 90 % (—)

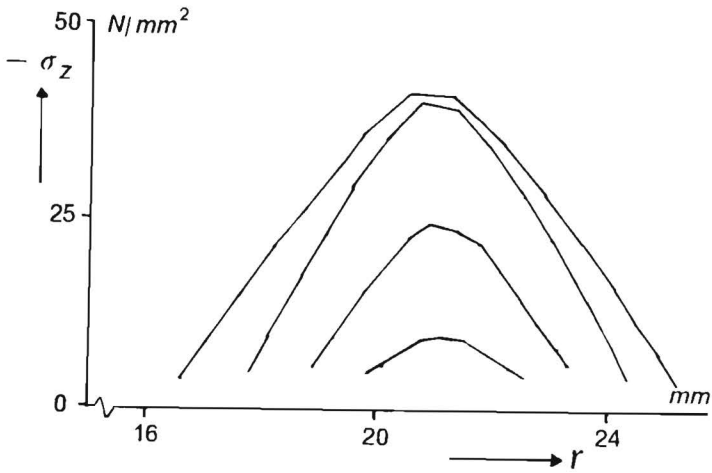
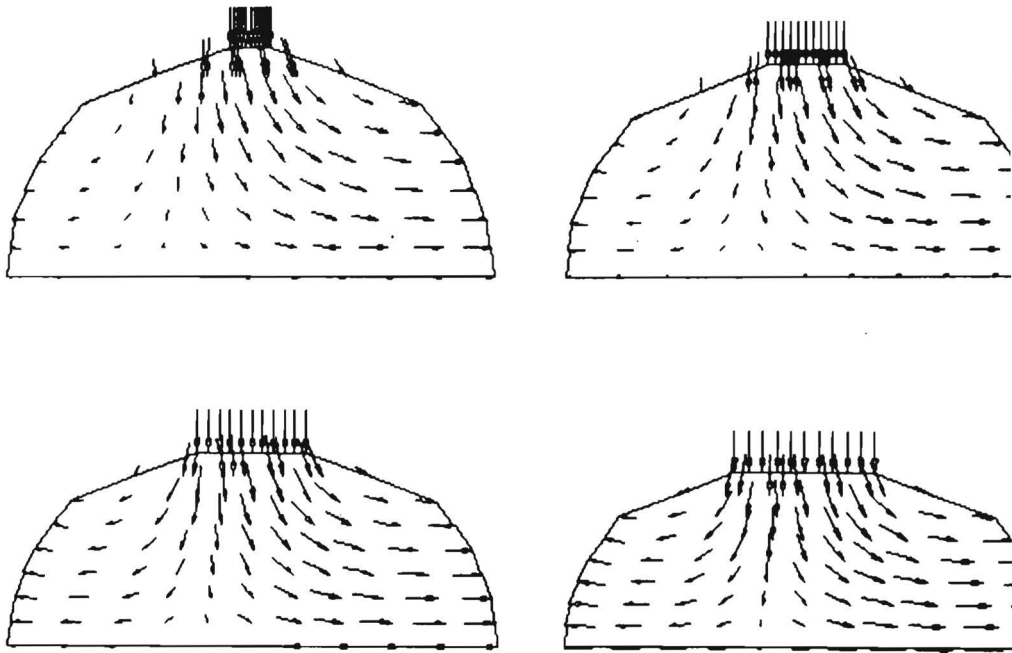


Figure 37. Axial stress during several stages of the compression phase on the interface between lead and substrate



**Figure 38. Vector plots during several stages of the compression phase**

then there are two areas, where tension can be observed. It is known from experiments that, in the same areas the bond can fail. This failure mechanism can be influenced by the interval of time, in which unloading takes place. The calculated residual tension stresses might correspond with the observed failing of the bonds. This is even now an open question. In future numerical as well as bonding experiments will have to provide the answer.

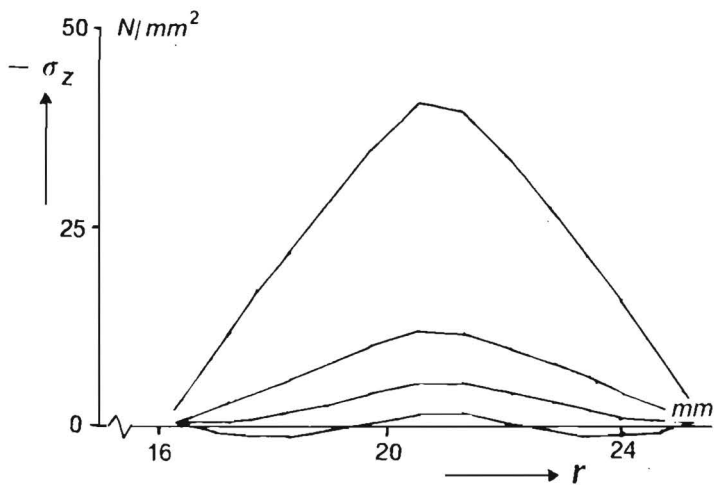


Figure 39. Axial stress during several stages of the unloading phase on the interface between lead and substrate

## 6 Discussion

In chapters 2 and 3 two different theories were discussed, both of which yield constitutive equations for metals. It was pointed out that the two theories only coincide once, in the case of the Oldroyd and Maxwell models. The latter, especially, is often applied in the field of plasticity. Also, the theory of the decomposition of the deformation rate, as discussed in chapter 3, is usually used in this field. However, it was shown that from the hidden tensors theory constitutive models for metals can be also obtained. Chapter 4 then shows that a simple Maxwell model can only describe the primary effects observed from experiments. Phenomena, such as the overshoot of the torque or shortening of lead during torsion, can't be predicted with a Maxwell model. It is still an open question whether the Oldroyd or Kelvin models in combination with a Maxwell model, are able to describe these phenomena, as was suggested in subparagraph 5.3. A good alternative, however, seems to be the theory of hidden variables. If a better physical understanding is obtained from these phenomena, then hidden variables might be found, whose evaluation can be described in terms of the state and hidden variables. This approach, for instance, seems to be a good alternative for describing kinematical hardening. A better understanding is needed of this hardening phenomenon, but pointless discussions about what rate should be used, considering the shear test (figure 1), can be avoided in this way.

The combined tension-torsion test seems to be a good start for further investigation points of some of the secondary effects. In particular a lot of information can be obtained from the elongation or shortening of the specimen, which can be easily measured. In the compression test too some non-viscous and non-elastic phenomena were observed. Understanding the results of this test, however, is much harder, because the deformation pattern is more complicated than the deformation field of the torsion-tension test. In literature, some work has already been reported, relating the secondary effects, such as those can be observed during a torsion test, to metallurgical quantities. These relationships can help to obtain constitutive equations in the way, just discussed: the metallurgical quantities may be related to some hidden variables.

In future, the need for accurate constitutive equations will increase. The reason for this increase is not only, that with modern computers and numerical techniques, more and

more problems, arising from continuum mechanics, can be solved. Also the requirements, of many processes, such as thermocompression, will increase, in order to obtain a better reproducibility of these processes. Particularly in the field of precision engineering, where processes such as extrusion, grinding, cutting, etc., are considered, a good understanding of the mechanical process is indispensable.

## References

- S.A.Atluri - On the constitutive relationships at finite strain: hypo-elasticity and elasto-plasticity with isotropic or kinematical hardening. - *Comp. Meth. in Appl. Mech. and Eng.*, Vol.43 (1984) 137-171
- B.I.M.van Bakel - CFT Report (1987) - to appear
- J.F.Besseling - A thermodynamic approach to rheology - *Proc. IUTAM symp. on Irreversible Aspects of Continuum Mechanics*, Vienna (1966), Springer Verlag
- M.A.Biot - Theory of Stress-Strain relationships in anisotropic viscoelastic and relaxation phenomena - *J. of Appl. Physics*, Vol.25 (1954) 1385-1391
- S.R.Bodner and Y.Partom - Constitutive equations for elastic- viscoplastic strain hardening materials- *J. of Appl. Mech.*, Vol.42 (1975) 385-389
- P.W.Bridgman - *Studies in large plastic flow and fracture* - McGraw-Hill, New York (1952)
- M.J.Crochet,A.R.Davies and K.Walters - *Numerical Simulation of Non-Newtonian Flow*, Elsevier (1984)
- J.Damsteegt,A.Segal and J.van der Zanden - On the convergence of numerical computations of the flow of a power-law and a Carreau liquid - *Delft University of technology,WTHD 184* (1986)
- N.N.Davidenkov and N.I.Spiridonova - Mechanical methods of testing; analysis of the state of stress in the neck of a tensile test specimen - *Proc. ASTM*, Vol.46 (1946) 1147-1158
- Y.F.Defalias - The plastic spin - *J.of Appl. Mech.*, Vol.52 (1985) 865-871
- G.Dhatt and G.Hubert - A study of penalty elements for incompressible laminar flows - *Int. J. for Num. Meth. in Fl.*, Vol.6 (1986) 1-19

J.K.Dienes - On the analysis of rotation and stress rate in deforming bodies - Acta Mech., Vol.32 (1979) 217-232

A.Doustens and M.Laquerbe - Exploitation rheometrique du test d'écrasement entre plateaux paralleles - J. de Mecan. Theor. et Appl., Vol.6 (1987) 315-332

J.D.Fast - Entropy - Philips Technical Library (1962)

H.J.Frost and M.F.Ashby - Deformation-Mechanism maps - Pergamon Press (1982)

A.C.Eringen - Mechanics of Continua - John Wiley and Sons (1967)

H.Galenkamp en H.van Wijngaarden - Bepaling van de Von Mises spanning uit de insnoering bij de trekstaaf - Philips Technisch Tijdschrift, Vol.42 (1984) 11-19

D.F.Griffiths - Finite elements for incompressible flow - Math. Meth. in the Appl. Sci., Vol.1 (1979) 16-33

S.R.de Groot - Thermodynamics of Irreversible Processes - North Holland Publishing Company (1951)

S.R.de Groot and P.Mazur - Non-Equilibrium Thermodynamics - North Holland Publishing Company (1962)

A.M.A.van der Heyden and J.F.Besseling - A large strain plasticity theory and the symmetry properties of its constitutive equations - Comp. and Struct., Vol.19 (1984) 271

R.Hill - The mathematical Theory of Plasticity - Clarendon Press (1950)

S.J.Kim and J.T.Oden - Generalized potentials in finite elastoplasticity - Int. J. of Engng. Sci., Vol.22 (1984) 1235-1257

S.J.Kim and J.T.Oden - Generalized flow potentials in finite elastoplasticity,II. Examples - Int. J. of Engng. Sci., Vol.23 (1985) 515-530

S.J.Kim and J.T.Oden - Finite analysis of a class of problems in finite elastoplasticity based on the thermodynamical theory of materials of type N - Comp. Meth. in Appl. Mech. and Engng., Vol.53 (1985) 277-302

E.H.Lee - Elastic-plastic deformation at finite strains - J. of Appl. Mech., Vol.36 (1969) 1:6

E.H.Lee - Some comments on elastic-plastic analysis - Int. J. of Sol. and Struc., Vol.17 (1981) 859-872



E.H.Lee, R.L.Mallet and T.B.Wertheimer - Stress analysis for anisotropic hardening in finite deformation plasticity - J. of Appl. Mech., Vol.50 (1983) 554-560

J.E.A.Meershoek - Nat.Lab. Report (1988) - to appear

F.Montheillet, M.Cohen and J.J.Jonas - Axial stresses and texture development during the torsion testing of Al, Cu and  $\alpha$ -Fe - Acta Metall., Vol 32 (1984) 2077-2089

J.Muller - Thermodynamics - Pitman (1985)

J.C.Nagtegaal and J.E.de Jong - Some aspects of non-isotropic work hardening in finite strain plasticity, in: E.H.Lee and R.L.Mallet eds., Plasticity of metals at finite strain: theory, experiment and computation - Div. Appl. Mech., Stanford Univ. and Dept. Mech. Engng., RPI., Stanford (1982) 65-102

S.Nemat-Nasser - Decomposition of strain measures and their rates in finite deformation elastoplasticity - Int. J. of Sol. and Struc., Vol.15 (1979) 155-166

S.Nemat-Nasser - On finite deformation elastoplasticity - Int. J. of Sol. and Struc., Vol.18 (1982) 857-872

W.Prager - A new method of analyzing stresses and strains in work hardening plastic solids - J. of Appl. Mech., Vol 23 (1956) 493-496

E.Rauch, G.R.Canova, J.J.Jonas and S.L.Semiatin - An analysis of flow localization during torsion testing - Acta Metall., Vol.33 (1985) 465-476

R.A.Schapery - Application of thermodynamics to thermomechanical, fracture and birefringent phenomena in viscoelastic media - J. of Appl. Physics, Vol.35 (1964) 1451-1465

E.Siebel - Formanderungsfestigkeit und Spannungsverteilung im eingeschnurten Stabe - Bericht des Werkstoffausschusses des Vereins deutscher Eisenhüttenleute, Vol 71 (1925)

C.Truesdell - Rational Thermodynamics - Mc.Graw-Hill Book Company (1968)

H. van Wijngaarden, J.F.Dijksman and P.Wesseling - Non-isothermal flow of a molten polymer in a narrow rectangular cavity - J. of Non-Newt. Fl. Mech., Vol.11 (1982) 175-199

H.van Wijngaarden, B.L.M. van Bakel, A.D.Verwey and J.E.A.Meershoek - Numerical simulation of thermocompression bonding - Proc. of NUMIFORM '86, Gothenburg (1986)

H.van Wijngaarden en F.E.Veldpaus - On the correct form of rate type constitutive equations for elastic behaviour - Technical University of Eindhoven, Report nr. WFW 86.038 (1986)

## Appendix A

Due to a rigid body rotation, represented by the tensor  $\mathbf{Q}$ , the position vector  $\mathbf{x}$  is transformed into the vector  $\bar{\mathbf{x}}$  in the following way:

$$\bar{\mathbf{x}} = \mathbf{Q} \cdot \mathbf{x} \quad (\text{A.1})$$

where the rotation tensor  $\mathbf{Q}$  can only depend on time. By definition, it then follows that the position vector  $\mathbf{x}$  is objective. Because the position vector  $\mathbf{X}$  of the original state is not transformed by the rigid body rotation of the current state,  $\mathbf{X}$  is invariant. From the definition of the deformation tensor  $\mathbf{F}$ , it is evident that:

$$\bar{\mathbf{F}} = \frac{d\bar{\mathbf{x}}}{d\mathbf{X}} = \frac{d(\mathbf{Q} \cdot \mathbf{x})}{d\mathbf{X}} = \mathbf{Q} \cdot \frac{d\mathbf{x}}{d\mathbf{X}} = \mathbf{Q} \cdot \mathbf{F} \quad (\text{A.2})$$

which means that  $\bar{\mathbf{F}}$  is neither objective nor invariant. Because of the uniqueness of the polar decomposition of  $\mathbf{F}$ , it directly follows from A.2 and 1.2.5 that:

$$\bar{\mathbf{R}} = \mathbf{Q} \cdot \mathbf{R} ; \mathbf{U} = \mathbf{U} ; \bar{\mathbf{V}} = \mathbf{Q} \cdot \mathbf{V} \cdot \mathbf{Q}^T \quad (\text{A.3})$$

Consequently  $\mathbf{U}$  and  $\mathbf{C}$  (see 1.2.7) are invariant, and  $\mathbf{V}$  and  $\mathbf{B}$  (see 1.2.7) objective.

Differentiation of  $\bar{\mathbf{x}}$  gives:

$$\dot{\bar{\mathbf{x}}} = \dot{\bar{\mathbf{u}}} = \dot{\mathbf{Q}} \cdot \mathbf{x} + \mathbf{Q} \cdot \dot{\mathbf{x}} = \dot{\mathbf{Q}} \cdot \mathbf{x} + \mathbf{Q} \cdot \mathbf{u} \quad (\text{A.4})$$

which means that the velocity vector is neither invariant nor objective. From the differentiation of  $\bar{\mathbf{F}}$ , it is apparent that:

$$\dot{\bar{\mathbf{F}}} \cdot \bar{\mathbf{F}}^{-1} = \dot{\mathbf{Q}} \cdot \mathbf{Q}^T + \mathbf{Q} \cdot \dot{\mathbf{F}} \cdot \mathbf{F}^{-1} \cdot \mathbf{Q}^T \quad (\text{A.5})$$

So the symmetric part of this expression, which is equal to the deformation rate tensor  $\mathbf{D}$ , is objective, because  $\dot{\mathbf{Q}} \cdot \mathbf{Q}^T$  is skew-symmetric. The skew-symmetric part of A.5, which is equal to the spin tensor  $\Omega$ , is then neither objective nor invariant:

$$\dot{\Omega} = \dot{\mathbf{Q}} \cdot \mathbf{Q}^T + \mathbf{Q} \cdot \Omega \cdot \mathbf{Q}^T \quad (\text{A.6})$$

Let  $p$  be some invariant ( and thus objective) scalar function of  $x$  . The gradient of  $p$ , i.e.  $\nabla p$ , is defined by:

$$p(x + \Delta x) - p(x) = \nabla p \cdot \Delta x \quad (A.7)$$

for each infinitesimally small vector  $\Delta x$ . After a rigid body rotation the following solution is obtained:

$$\bar{p}(\bar{x} + \Delta \bar{x}) - \bar{p}(\bar{x}) = p(x + \Delta x) - p(x) = \nabla p \cdot \Delta x = \nabla \bar{p} \cdot \mathbf{Q} \Delta x \quad (A.8)$$

which means that the gradient of  $p$  is objective. As the constitutive quantities  $\underline{h}$  and  $\sigma$  enter the second law of thermodynamics (relationship 1.3.7), the scalar expressions  $\sigma : \underline{D}$  and  $\underline{h} \cdot \nabla \theta$  may have to be objective:

$$\bar{\sigma} : \bar{D} = \sigma : D \quad \text{and} \quad \bar{h} \cdot \nabla \bar{\theta} = h \cdot \nabla \theta \quad (A.9)$$

From the objectivity of  $D$  and  $\nabla \theta$  it follows that  $\sigma$  and  $h$  are objective too. It is obvious from the definition of the tensor  $A$  that the tensors  $\bar{S}$  and  $\bar{C}$  are invariant.

By definition the time derivatives of invariant quantities are invariant too. However, for an objective vector  $p$  and a tensor  $P$  it can be seen that:

$$\dot{\bar{p}} = \dot{Q} \cdot p + Q \cdot \dot{p} \quad (A.10)$$

$$\dot{\bar{P}} = \dot{Q} \cdot P \cdot Q^T + Q \cdot \dot{P} \cdot Q^T + Q \cdot P \cdot \dot{Q}^T \quad (A.11)$$

From relationship A.6 it can be derived that the following expressions are objective:

$$\dot{\bar{p}} - \Omega \cdot \bar{p} = Q \cdot (\dot{p} - \Omega \cdot p) \quad (A.12)$$

$$\dot{\bar{P}} - \Omega \cdot \bar{P} + \bar{P} \cdot \Omega = Q \cdot (\dot{P} - \Omega \cdot P + P \cdot \Omega) \cdot Q^T \quad (A.13)$$

The latter expression is known as the Jaumann rate of  $P$ . In chapter 2 and 3 several other similar objective rates of tensors are discussed.

## Appendix B

If the free energy  $\psi$  can be expressed by:

$$\psi = \psi(\bar{\mathbf{C}}, \theta) \quad (B.1)$$

then it follows directly from 2.2.9 and 2.2.14 that:

$$\dot{\psi} = \frac{\partial \psi}{\partial \bar{\mathbf{C}}} : \dot{\bar{\mathbf{C}}} + \frac{\partial \psi}{\partial \theta} \dot{\theta} = \frac{1}{\rho_0} \bar{\mathbf{S}} : \dot{\bar{\mathbf{C}}} - \eta \dot{\theta} \quad (B.2)$$

By introducing the second Piola Kirchoff stress  $\mathbf{S}$ , which is equal to  $\mathbf{J} \cdot \mathbf{F}^{-1} \cdot \boldsymbol{\sigma} \cdot \mathbf{F}^{-T}$ , and the tensor  $\mathbf{C}$  (see 1.2.7), evaluation of the free energy can also be expressed by:

$$\dot{\psi} = \frac{1}{2\rho_0} \mathbf{S} : \dot{\mathbf{C}} - \eta \dot{\theta} \quad (B.3)$$

Finally the relationships 1.4.4 and 1.4.5 together with B.2 yield:

$$\dot{\psi} = \frac{1}{\rho} \boldsymbol{\sigma} : \mathbf{D} - \eta \dot{\theta} \quad (B.4)$$

If the free energy only depends on the Cauchy strain tensor  $\mathbf{C}$  and the temperature  $\theta$  as is the case for elastic materials, then due to isotropy this relationship reduces to:

$$\psi = \psi(I:\mathbf{C}, I:\mathbf{C}^2, I:\mathbf{C}^3, \theta) = \psi(J_1, J_2, J_3, \theta) \quad (B.5)$$

Substitution of B.5 into B.3 gives the following constitutive relationship for elastic materials:

$$\begin{aligned} \mathbf{S} &= \beta_0 \mathbf{I} + \beta_1 \mathbf{C} + \beta_2 \mathbf{C}^2 \\ \beta_0 &= 2\rho_0 \frac{\partial \psi}{\partial J_1} ; \beta_1 = 4\rho_0 \frac{\partial \psi}{\partial J_2} ; \beta_2 = 6\rho_0 \frac{\partial \psi}{\partial J_3} \end{aligned} \quad (B.6)$$

It can easily be seen from 1.2.7, that the invariants  $J_1$ ,  $J_2$  and  $J_3$  can be expressed in terms of the tensor  $\mathbf{B}$ . In the same way, the invariants are expressed in terms of the tensor  $\mathbf{C}$ :

$$J_1 = I:C = I:\mathbf{B} ; J_2 = I:C^2 = I:\mathbf{B}^2 ; J_3 = I:C^3 = I:\mathbf{B}^3 \quad (B.7)$$

Replacement of the tensors  $\mathbf{S}$  and  $\mathbf{C}$  by the tensors  $\boldsymbol{\sigma}$  and  $\mathbf{B}$  in B.6 yields:

$$\boldsymbol{\sigma} = \frac{1}{J} (\beta_0 \mathbf{B} + \beta_1 \mathbf{B}^2 + \beta_2 \mathbf{B}^3) \quad (B.8)$$

where  $\beta_0, \beta_1$ , and  $\beta_2$  can be expressed in terms of the invariants of  $\mathbf{B}$ , because of B.6 and B.7. Substitution of the Cayley-Hamilton relationship which is:

$$\mathbf{B}^3 - J_1 \mathbf{B}^2 + \frac{1}{2} (J_1^2 - J_2) \mathbf{B} - \frac{1}{6} (2J_3 - 3J_1 J_2 + J_1^3) \mathbf{I} = 0 \quad (B.9)$$

finally gives the following result:

$$\boldsymbol{\sigma} = a_0 \mathbf{I} + a_1 \mathbf{B} + a_2 \mathbf{B}^2 \quad (B.10)$$

where, after a straightforward calculation,  $a_0, a_1$  and  $a_2$  are expressed by:

$$a_0 = \rho (3J_1 J_2 - 2J_3 - J_1^3) \frac{\partial \psi}{\partial J_1} ; a_1 = \rho (2 \frac{\partial \psi}{\partial J_1} + 3(J_1^2 - J_2) \frac{\partial \psi}{\partial J_3})$$

$$a_2 = 2\rho (2 \frac{\partial \psi}{\partial J_2} - 3J_1 \frac{\partial \psi}{\partial J_3}) \quad (B.11)$$

Because of B.5 and B.8 the free energy and the eigenvalues of  $\boldsymbol{\sigma}$  which are better known as the main stresses  $\sigma_i$ , can be expressed in terms of the eigenvalues of  $\mathbf{B}$ :

$$\psi = \psi(e_1, e_2, e_3, \theta) ; \sigma_i = \sigma_i(e_1, e_2, e_3, \theta) \text{ for } i = 1, 2, 3 ; e_i = \ln(\lambda_i) \quad (B.12)$$

where  $\lambda_1^2, \lambda_2^2$  and  $\lambda_3^2$  are the eigenvalues of  $\mathbf{B}$ . Using this result, relationship B.4 becomes:

$$\dot{\psi} = \frac{1}{\rho} \boldsymbol{\sigma} : \mathbf{D} - \eta \dot{\theta} = \frac{1}{\rho} \sum_{i=1}^3 \sigma_i \dot{e}_i - \eta \dot{\theta} \quad (B.13)$$

from which it follows that:

$$\sigma_i = \rho \frac{\partial \psi}{\partial e_i} \quad (B.14)$$

## Appendix C

In this Appendix a solution is deduced for equation 2.6.3. This equation can be expressed in the following way:

$${}^4\mathbf{A}:\dot{\mathbf{Q}} + {}^4\mathbf{B}:\mathbf{Q} = \mathbf{H} \quad (\text{C.1})$$

All the tensors in C.1 are symmetric, and  ${}^4\mathbf{A}$  is regular. The solution procedure for this equation is similar to the procedure Biot (1954) proposed for the same kind of equation.

First, a solution for the homogeneous equation, i.e.  $\mathbf{H} = 0$ , is obtained. Suppose:

$$\mathbf{Q} = e^{-\lambda t} \mathbf{V} \quad (\text{C.2})$$

where  $\mathbf{V}$  is symmetric and doesn't depend on time. Substitution in C.1 yields:

$$(-\lambda {}^4\mathbf{A} + {}^4\mathbf{B}):\mathbf{V} = 0 \quad (\text{C.3})$$

This means that  $\mathbf{V}$  is a  ${}^4\mathbf{A}$ -eigenvector of  ${}^4\mathbf{B}$  with corresponding eigenvalue  $\lambda$ . Because of the symmetrical property of  ${}^4\mathbf{A}$ ,  ${}^4\mathbf{B}$  and  $\mathbf{V}$  there are six eigenvectors  $\mathbf{V}_i$  and eigenvalues  $\lambda_i$  ( $i = 1, \dots, 6$ ). From these definitions of  $\mathbf{V}_i$  and  $\lambda_i$  it follows that:

$$\lambda_i \mathbf{V}_i : ({}^4\mathbf{B}:\mathbf{V}_j) = -\lambda_i \bar{\lambda}_j \mathbf{V}_i : ({}^4\mathbf{A}:\mathbf{V}_j) = -\lambda_i \bar{\lambda}_j (\mathbf{V}_i : {}^4\mathbf{A}) : \mathbf{V}_j = \bar{\lambda}_j (\mathbf{V}_i : {}^4\mathbf{B}) : \mathbf{V}_j \quad (\text{C.4})$$

This means that  $\lambda_i$  has to be real ( $i = j$ ) instead of complex, and that:

$$\mathbf{V}_i : {}^4\mathbf{B}:\mathbf{V}_j = 0 \text{ for } i \neq j \quad (\text{C.5})$$

Due to the regularity property of  ${}^4\mathbf{A}$  and relationship C.4 the eigenvectors can be chosen in such way that:

$$\mathbf{V}_i : {}^4\mathbf{A}:\mathbf{V}_j = \delta_{ij} \quad (\text{C.6})$$

where  $\delta_{ij}$  is the Kronecker delta. Suppose:

$$\mathbf{Q} = \sum_{i=1}^6 \rho_i \mathbf{V}_i \quad (\text{C.7})$$

Substitution in C.1 gives:

$$\sum_{i=1}^6 ({}^4\mathbf{A}: \mathbf{V}_i \dot{p}_i + {}^4\mathbf{B}: \mathbf{V}_i p_i) = \mathbf{H} \quad (\text{C.8})$$

Pre-multiplying this relationship with  $\mathbf{V}_j$ , the following equation is obtained for  $p_j$ :

$$\dot{p}_j + \lambda_j p_j = \mathbf{V}_j: \mathbf{H} \quad (\text{C.9})$$

The solution of this equation and relationship C.7 finally yield:

$$\mathbf{Q} = \sum_{j=1}^6 {}^4\mathbf{V}_j: \int_0^t e^{-\lambda_j(t-\tau)} \mathbf{H}(\tau) d\tau \quad (\text{C.10})$$

where:

$$\mathbf{Q}(0) = 0 \quad \text{and} \quad {}^4\mathbf{V}_j = \mathbf{V}_j \mathbf{V}_j \quad (\text{C.11})$$



## Appendix D

In this Appendix a solution is deduced for equation 3.3.13. This equation is:

$$\frac{\partial \sigma_i}{\partial e_j} = (\mu_1 + 2\beta\sigma_i)\delta_{ij} + \mu_2 - 2\gamma\sigma_i \quad (D.1)$$

which is valid for  $i, j = 1, 2, 3$ . From  $\sigma_i = \sigma(e_1, e_2, e_3)$  (see 3.3.9) it follows for  $i \neq j \neq k$  that:

$$\frac{\partial \sigma_i}{\partial e_j} - \frac{\partial \sigma_i}{\partial e_k} = 0 \quad (D.2)$$

From this equation it is obvious that  $\sigma_i = \sigma_i(e, J)$ , because  $\ln(J) = e_1 + e_2 + e_3$ . The nine equations in D.1 can then be reduced to six:

$$\frac{\partial \sigma_i}{\partial e_i} + J \frac{\partial \sigma_i}{\partial J} = \mu_1 + 2\beta\sigma_i + \mu_2 - 2\gamma\sigma_i \quad \text{for } i = 1, 2, 3 \quad (D.3)$$

$$J \frac{\partial \sigma_i}{\partial J} = \mu_2 - 2\gamma\sigma_i \quad \text{for } i = 1, 2, 3 \quad (D.4)$$

From these equations it directly follows that:

$$\mu_1 = \mu_1(e_i, J) \quad \text{and} \quad \mu_2 = \mu_2(e_i, J) \quad (D.5)$$

This equation must be valid for every  $i$ , so:

$$\mu_1 = \mu_1(J) \quad \text{and} \quad \mu_2 = \mu_2(J) \quad (D.6)$$

Differentiating equation 2.4.7 to  $e_j$  the following relationship is obtained:

$$\rho_0 \frac{\partial^2 \psi}{\partial e_i \partial e_j} = J \left( \sigma_i + \frac{\partial \sigma_i}{\partial e_j} \right) = J \left( \sigma_j + \frac{\partial \sigma_j}{\partial e_i} \right) \quad (D.7)$$

Substitution of equation D.1 into this relationship, leads to the requirement that  $\gamma = \frac{1}{2}$ . By defining the function  $f = f(J)$  with  $f(1) = 0$ , in such a way that:

$$\frac{df(J)}{dJ} = \mu_2 \quad (D.8)$$

equation D.4 yields:

$$J\sigma_i = f(J) + \bar{\sigma}_i(e_i) \quad (D.9)$$

The combination of D.3, D.6 and D.9 finally gives:

$$J\mu_1 = 2(G_0 - \beta f(J)) \quad (D.10)$$

$$\bar{\sigma}_i = \frac{G_0}{\beta} (e^{2\beta e_i} - 1) = \frac{G_0}{\beta} (\lambda_i^{2\beta} - 1) \quad (D.11)$$

This means that the Cauchy stress tensor can be expressed by:

$$\sigma = \frac{1}{J} (f(J)\mathbf{I} + \frac{G_0}{\beta} (\mathbf{B}^\beta - \mathbf{I})) \quad (D.12)$$

## Appendix E

The tension bar has to obey the following equations during necking:

$$\frac{\partial \sigma_r}{\partial r} + \frac{\sigma_r - \sigma_\phi}{r} + \frac{\partial \sigma_{rz}}{\partial z} = 0 \quad (E.1)$$

$$\frac{\partial \sigma_{rz}}{\partial r} + \frac{\sigma_{rz}}{r} + \frac{\partial \sigma_z}{\partial z} = 0 \quad (E.2)$$

where the following boundary conditions have to be met in the vicinity of the neck:

$$u_z = \sigma_{rz} = 0 \quad \text{on} \quad z = 0 \quad (E.3)$$

$$u_r = \sigma_{rz} = 0 \quad \text{on} \quad r = 0 \quad (E.4)$$

$$\sigma \cdot \underline{n} = 0 \quad \text{on} \quad r = R(z) \quad (E.5)$$

where  $R(z)$  is the outer radius of the bar and where  $\underline{n}$  is the normal on the surface of the bar. The boundary condition E.5 can therefore be written as:

$$\sigma_r - \sigma_{rz} \frac{dR}{dz} = 0 \quad \text{and} \quad \sigma_{rz} - \sigma_z \frac{dR}{dz} = 0 \quad (E.6)$$

In chapter 4, it is assumed that the constitutive relationships can be expressed by:

$$\sigma^d = \frac{2\sigma \sqrt{\dot{\bar{\epsilon}}, \dot{\bar{\epsilon}}}}{3\dot{\bar{\epsilon}}} \mathbf{D} \quad (E.7)$$

In relationships 4.2.13 and 4.2.14 the following assumptions were made about the radial velocity in the vicinity of the smallest cross section:

$$u_r = rf(z, t) \quad \text{with} \quad \left| \frac{\partial f}{\partial z} \right| \ll \left| f(z, t) \right| \quad (E.8)$$

From boundary condition E.3 and the fact that  $\text{tr}(\mathbf{D}) = 0$ , it follows that the axial velocity  $u_z$  can be expressed by:

$$u_z = -2 \int_0^z f(z, t) dz \quad (E.9)$$

and the deformation rate tensor  $\mathbf{D}$  by:

$$\mathbf{D} = f(z, t)(\mathbf{e}_r \mathbf{e}_r + \mathbf{e}_\phi \mathbf{e}_\phi - 2\mathbf{e}_z \mathbf{e}_z) + \frac{1}{2} r \frac{\partial f}{\partial z} (\mathbf{e}_r \mathbf{e}_z + \mathbf{e}_z \mathbf{e}_r) \quad (E.10)$$

Due to E.8 the equivalent strain rate  $\dot{\bar{\epsilon}}$  can be approximated by:

$$\dot{\bar{\epsilon}} = \sqrt{\frac{2}{3} \mathbf{D}:\mathbf{D}} \simeq 2|f(z, t)| \quad (E.11)$$

Integration of this equation yields that the equivalent strain  $\bar{\epsilon}$  doesn't also depend on the radial position. The same can therefore be concluded for the Von Mises stress  $\sigma_v$ . Consequently from E.7 and E.10 it follows directly that  $\sigma_{rz}$  is proportional to  $r$ , and  $\sigma_r = \sigma_\phi$  is a parabolic function of  $r$ , due to E.1:

$$\sigma_r = A(z, t)r^2 + B(z, t) \quad ; \quad \sigma_{rz} = -2A(z, t)rz \quad (E.12)$$

Following the definition of the Von Mises stress the axial stress  $\sigma_z$  can be expressed in the vicinity of the smallest cross section by:

$$\sigma_z = A(z, t)r^2 + B(z, t) + \sigma_v(z, t) \quad (E.13)$$

Then, equation E.2 requires that:

$$A = A(t) \quad \text{and} \quad B + \sigma_v = 2A(t)z^2 + C(t) \quad (E.14)$$

The force  $F$  can be expressed by:

$$F = 2\pi \int_0^{R(z)} \sigma_z r dr \quad (E.15)$$

Substitution of E.13 into E.15 gives:

$$B + \sigma_v = \frac{F}{\pi R^2} - \frac{1}{2} AR^2 \quad (E.16)$$

From the boundary condition E.6, the following requirement is obtained for  $B$ :

$$B = -AR^2 - 2AzR \frac{dR}{dz} \quad (E.17)$$

Eliminating  $A$ ,  $B$  and  $C$  from E.14, E.16 and E.17, the required correction factor  $C_1$  is found:

$$\sigma_v(z=0) = C_1 \frac{F}{\pi R^2} = \frac{4}{4+\alpha} \frac{F}{\pi R^2} \quad (E.18)$$

where  $\alpha$  is defined by:

$$\alpha = \left( R \frac{d^2 R}{dz^2} \right)_{z=0} \quad (E.19)$$

The other boundary condition on the outer radius (see E.6) gives:

$$B + \sigma_v = -AR \left( 2z + R \frac{dR}{dz} \right) \left( \frac{dR}{dz} \right)^{-1} \quad (E.20)$$

Relationship E.14 and E.20 lead to the equation for the outer radius, which after a straightforward calculation gives:

$$\bar{R}^4 + (4\bar{z}^2 - 2 - \frac{4}{\alpha})\bar{R}^2 + 1 + \frac{4}{\alpha} = 0 \quad (E.21)$$

where  $\bar{R} = \frac{R}{R(z=0)}$  and  $\bar{z} = \frac{z}{R(z=0)}$ . Bridgman (1952) assumed that the radius could be expressed by:

$$\bar{R} = 1 + \frac{1}{\alpha} - \frac{1}{\alpha} \sqrt{1 - \alpha^2 \bar{z}^2} \quad (E.22)$$

These two functions for  $\bar{R}$  have been drawn in figure 9.

## Appendix F

In this Appendix the compression of the upper half of the cylindrical pallet ( $0 \leq z \leq \frac{1}{2}h$ ) is considered. In this part the shear rate  $\frac{\partial u_r}{\partial z}$  is negative, which means that equations 4.4.4 and 4.4.6 yield:

$$\frac{\partial u_r}{\partial z} = -\sqrt{3}\dot{\epsilon} \quad \text{and} \quad \sigma_{rz} = z \frac{\partial p(r, t)}{\partial r} = -\frac{1}{3}\sqrt{3}\sigma_v \quad (F.1)$$

The Von Mises stress  $\sigma_v$  only depends on the equivalent strain rate, and possibly also on the temperature. It is assumed that the inverse of this relationship exists with respect to  $\dot{\epsilon}$ :

$$\sigma_v = \phi(\dot{\epsilon}) \quad \text{and} \quad \dot{\epsilon} = \phi^{-1}(\sigma_v) \quad (F.2)$$

where the temperature dependence is not mentioned, because only isothermal compression tests are considered. From F.1 and F.2 it follows that on  $z = \frac{1}{2}h$  and  $r = R$ :

$$\sigma_v = \frac{\sqrt{3}}{2}h\left(-\frac{\partial p}{\partial r}\right)_{r=R} \quad \text{and} \quad \dot{\epsilon} = \phi^{-1}\left(\frac{\sqrt{3}}{2}h\left(-\frac{\partial p}{\partial r}\right)_{r=R}\right) \quad (F.3)$$

Integration of relationship 4.4.5 (balance of mass) yields

$$\int_0^{\frac{1}{2}h} u_r dz = -\int_0^{\frac{1}{2}h} \frac{\partial u_r}{\partial z} z dz = -\frac{hr}{4} \quad (F.4)$$

By the introduction of the quantity  $y = -\frac{hr}{h^2}$ , F.1, F.2 and F.4 lead to the following equation:

$$\int_0^{\frac{1}{2}} \phi^{-1}(\sqrt{3}(-h\frac{\partial p}{\partial r})x) x dx = \frac{yr}{4\sqrt{3}R} \quad (F.5)$$

If the inverse of this equation exists, a function  $\psi = \psi(y)$  can be introduced such that on  $z = \frac{1}{2}h$  and  $r = R$  (see F.3):

$$\left(-h\frac{\partial p}{\partial r}\right) = \psi(y) ; \quad \sigma_v = \frac{\sqrt{3}}{2}\psi(y) ; \quad \dot{\epsilon} = \psi^{-1}\left(\frac{\sqrt{3}}{2}\psi(y)\right) \quad (F.6)$$

The force  $F$  can therefore be expressed by:

$$F = \pi \int_0^R \left( -\frac{\partial p}{\partial r} \right) r^2 dr = \frac{\pi R^3}{hy^3} \int_0^y \psi(x) x^2 dx \quad (F.7)$$

The volume  $V_0$  of the pallet remains constant and equals to  $\pi hR^2$ . A quantity  $G$  can therefore be introduced such that:

$$G = h^2 \sqrt{h} F = \frac{V_0 \sqrt{V_0}}{\sqrt{\pi} y^3} \int_0^y \psi(x) x^2 dx \quad (F.8)$$

from which it directly follows that  $G = G(y)$

Differentiating  $G$  with respect to  $y$  and substituting in F.6 gives at co-ordinates  $z = \frac{1}{2} h$  and  $r = R$ :

$$\sigma_v = \frac{\sqrt{3\pi}}{2V_0 \sqrt{V_0}} \left( 3G + y \frac{dG}{dy} \right) \quad (F.9)$$

From equation F.5 it directly follows that on  $r = R$ :

$$\int_0^{\frac{\sqrt{3}}{2} \psi(y)} \phi^{-1}(x) x dx = \frac{\sqrt{3}}{4} y \psi^2(y) \quad (F.10)$$

Differentiation of F.10 with respect to  $y$  and substitution of F.3 and F.6 in this equation finally gives at co-ordinates  $z = \frac{1}{2} h$  and  $r = R$ :

$$\dot{\varepsilon} = -\frac{1}{\sqrt{3}} \left( 2y + \sigma_v \left( \frac{d\sigma_v}{dy} \right)^{-1} \right) \quad (F.11)$$

## Appendix G

In this Appendix every objective tensor  $\mathbf{G}$  will be related to an invariant tensor  $\bar{\mathbf{G}}$  by:

$$\bar{\mathbf{G}} = \mathbf{A}^T \cdot \mathbf{G} \cdot \mathbf{A} \quad (\text{G.1})$$

The objective rate of  $\mathbf{G}$  is then related to  $\dot{\bar{\mathbf{G}}}$  (see 3.4.7) by

$$\dot{\bar{\mathbf{G}}} = \mathbf{A}^T \cdot \overset{\nabla}{\mathbf{G}} \cdot \mathbf{A} \quad (\text{G.2})$$

where  $\mathbf{A}$  is given by (see 3.4.9):

$$(\dot{\mathbf{A}} \cdot \mathbf{A}^{-1})^T = -(\boldsymbol{\Omega} + \mathbf{H}) \quad (\text{G.3})$$

The Oldroyd model (see 3.5.4) can be expressed by:

$$\frac{1}{\eta} \boldsymbol{\tau} + \frac{1}{E} \overset{\nabla}{\boldsymbol{\tau}} = \mathbf{D} + \lambda \overset{\nabla}{\mathbf{D}} \quad (\text{G.4})$$

The invariant form of this equation is:

$$\frac{1}{\eta} \bar{\boldsymbol{\tau}} + \frac{1}{E} \dot{\bar{\boldsymbol{\tau}}} = \bar{\mathbf{D}} + \lambda \dot{\bar{\mathbf{D}}} \quad (\text{G.5})$$

When an implicit Euler numerical integration scheme is used, the following expression is obtained:

$$\frac{1}{\eta} \bar{\boldsymbol{\tau}} + \frac{\bar{\boldsymbol{\tau}} - \bar{\boldsymbol{\tau}}_0}{\Lambda t E} = \bar{\mathbf{D}} + \lambda \frac{\bar{\mathbf{D}} - \bar{\mathbf{D}}_0}{\Lambda t} \quad (\text{G.6})$$

where the tensors  $\bar{\boldsymbol{\tau}}_0$  and  $\bar{\mathbf{D}}_0$  are the values of the tensors  $\bar{\boldsymbol{\tau}}$  and  $\bar{\mathbf{D}}$  at the point of time prior to the material point under consideration. This equation leads to the following expression for the original objective tensors:

$$\boldsymbol{\tau} = \eta \frac{E(\Lambda t + \lambda)}{\eta + \Lambda t E} \mathbf{D} + \frac{\eta}{\eta + \Lambda t E} \mathbf{P} \cdot (\boldsymbol{\tau}_0 - \lambda E \mathbf{D}_0) \cdot \mathbf{P}^T \quad (\text{G.7})$$



where  $\mathbf{P} = \mathbf{A}^{-T} \mathbf{A}_0^T$ . Numerical integration of equation G.3 leads to the following expression:

$$(\dot{\mathbf{A}} \mathbf{A}^{-1})^T \simeq \mathbf{A}^{-T} \cdot \frac{\mathbf{A}^T - \mathbf{A}_0^T}{\Delta t} = -(\boldsymbol{\Omega} + \mathbf{H}) \quad (\text{G.8})$$

Then for  $\mathbf{P}$  the following expression is found:

$$\mathbf{P} = \mathbf{I} + \Delta t (\boldsymbol{\Omega} + \mathbf{H}) \quad (\text{G.9})$$

For  $\lambda = 0$  the relationships 5.4.3, 5.4.4, 5.4.5 and 5.4.6 are easily obtained from G.7 and G.9.

If kinematical hardening is taken into account, the same numerical integration scheme can be used. Consider the following elastic-plastic model with kinematical hardening:

$$\frac{1}{\eta} (\boldsymbol{\tau} - \boldsymbol{\alpha}) + \frac{1}{E} \nabla \boldsymbol{\tau} = \mathbf{D} ; \quad \nabla \boldsymbol{\alpha} = h \mathbf{D} \quad (\text{G.10})$$

Numerical integration gives:

$$\boldsymbol{\tau} = \eta \frac{\Delta t E}{\eta + \Delta t E} \mathbf{D} + \frac{\Delta t E}{\eta + \Delta t E} \boldsymbol{\alpha} + \frac{\eta}{\eta + \Delta t E} \mathbf{P} \cdot \boldsymbol{\tau}_0 \cdot \mathbf{P}^T \quad (\text{G.11})$$

and for  $\boldsymbol{\alpha}$  the following expression is obtained:

$$\boldsymbol{\alpha} = \Delta t h \mathbf{D} + \mathbf{P} \cdot \boldsymbol{\alpha}_0 \cdot \mathbf{P}^T \quad (\text{G.12})$$

Substitution of G.12 into G.11 yields:

$$\boldsymbol{\tau} = (\eta + \Delta t h) \frac{\Delta t E}{\eta + \Delta t E} \mathbf{D} + \frac{1}{\eta + \Delta t E} \mathbf{P} \cdot (\eta \boldsymbol{\tau}_0 + \Delta t E \boldsymbol{\alpha}_0) \cdot \mathbf{P}^T \quad (\text{G.13})$$

This means that this constitutive model can be solved in a way similar to that in which the ordinary Maxwell model is solved. (see subparagraph 5.4).

## Appendix H

In subparagraph 4.4 an asymptotic approximation has been made for compression flows. In this case, i.e. the compression of a ring, the same approximation can be made because the height  $h$  of the ring is much smaller than the width  $R_2 - R_1$ . The appropriate balance equations for a viscous flow then reduce to (see 4.4.3 and 4.4.6):

$$\frac{\partial u_r}{\partial r} + \frac{u_r}{r} + \frac{\partial u_z}{\partial z} = 0 \quad (H.1)$$

$$\frac{\partial p}{\partial r} = \frac{1}{2} \frac{\partial}{\partial z} \left( \eta \frac{\partial u_r}{\partial z} \right) = 0 \quad ; \quad p = p(r, t) \quad (H.2)$$

The boundary conditions are:

$$z = 0 \quad u_r = 0 \quad u_z = 0 \quad (H.3)$$

$$z = h \quad u_r = 0 \quad u_z = \dot{h} \quad (H.4)$$

$$r = R_1 \quad p = 0 \quad (H.5)$$

$$R = R_2 \quad p = 0 \quad (H.6)$$

Integration of H.1 and H.2 in the axial direction yields:

$$\int_0^h u_r dz = \dots \frac{1}{2} \dot{h} r + \frac{C_0}{r} \quad (H.7)$$

$$u_r = \frac{1}{\eta} \frac{\partial p}{\partial r} z(z - h) \quad (H.8)$$

where  $C_0$  can only depend on time. Substitution of H.8 into H.7 gives:

$$\frac{h^3}{6\eta} \frac{\partial p}{\partial r} = \dots \frac{1}{2} \dot{h} r + \frac{C_0}{r} \quad (H.9)$$

Using the boundary conditions the following expressions for  $p$ ,  $u_r$  and  $u_z$  can be obtained:

$$p = \frac{3\eta\dot{h}}{2h^3} \left( \frac{\ln R_2 - \ln r}{\ln R_2 - \ln R_1} (R_2^2 - R_1^2) + r^2 - R_2^2 \right) \quad (H.10)$$

$$u_r = \frac{3\dot{h}}{2h^3} z(z-h) \left( 2r - \frac{R_2^2 - R_1^2}{\ln R_2 - \ln R_1} \frac{1}{r} \right) \quad (H.11)$$

$$u_z = \frac{\dot{h}}{h^3} z^2(3h - 2z) \quad (H.12)$$

In figure 32 and 33 the following data have been used:

$$h = 0.1mm ; \dot{h} = -1mm/s ; R_1 = 1mm ; R_2 = 2mm ; \eta = 1Ns/mm^2 \quad (H.13)$$

## Samenvatting

Dit proefschrift behandelt constitutieve relaties voor metalen. Twee theorieën, waarmee relaties tussen spanningen en rekken of reksnelheden verkregen kunnen worden, zullen worden besproken. De eerste theorie betreft de introductie van verborgen variabelen. Met name wordt aandacht besteed aan de voorwaarden, die volgen uit de Clausius-Duhem ongelijkheid. Deze laatste staat ook bekend als de tweede hoofdwet van de thermodynamica. Modellen voor metalen, die met deze theorie kunnen worden verkregen, staan bekend als modellen voor energie of rek verstevigende materialen en materialen van het type N. De tweede theorie behandelt de decompositie van de spanningen en de reksnelheden. Speciale aandacht wordt geschonken aan relaties tussen afgeleiden van spanningen en reksnelheden. Bewezen wordt dat slechts een speciale klasse van afgeleiden gebruikt kan worden voor dit doel. Een vergelijking wordt gemaakt tussen de modellen die met beide theorieën zijn verkregen. Ten slotte worden twee modellen, die volgen uit de tweede theorie, nader toegelicht: het Maxwell model voor elasto-plastische materialen en het Kelvin model voor materialen met kinematische versteviging. Drie experimenten, waarmee materiaaleigenschappen te verkrijgen zijn, worden beschreven: de trekproef inclusief insnoering, de gecombineerde torsie-trek proef met speciale aandacht voor pure torsie en de compressie proef. Enige experimentele resultaten zullen besproken worden. Tot slot wordt de opzet van een computerprogramma besproken, waarmee de extrusie van lood beschreven kan worden. Enige resultaten, die onlangs met behulp van dit programma verkregen zijn, zullen worden getoond.

## **Curriculum vitae**

22-8-1955

Born in Arnhem in the Netherlands

1974

Diploma V.W.O.

1974-1981

Study Mathematics at the Technical University of Delft, the 'ingenieurs' title was obtained "cum laude".

1981-1986

Employment at Philips Research Laboratories in Eindhoven.

1986-

Employment at the Centre For Manufacturing Technology of N.V. Philips Gloeilampen in Eindhoven.

# Nawoord

Het in deze dissertatie beschreven onderzoek is grotendeels verricht op het Natuurkundig Laboratorium van Philips, in de groep Mechanica en Tribologie van dr.ir.E.A.Muijderman.

Dit proefschrift is mede tot stand gekomen door de onvermoeibare inbreng van dr.ir.F.E.Veldpaus, van de Technische Universiteit te Eindhoven, faculteit werktuigbouwkunde. Frans, ik wil je niet alleen bedanken voor je inbreng, maar ook voor de bijzonder prettige samenwerking in de afgelopen jaren.

Tevens wil ik ook de promotie commissie met als eerste promotor prof.dr.ir. J.D. Janssen bedanken voor hun moeite dit proefschrift kritisch door te lezen.

Hans Galenkamp en John Meershoek wil ik bedanken voor hun inbreng en enthousiasme tijdens dit onderzoek op het Nat.Lab..

Daarnaast wil ik nog noemen mijn collega's op het Nat.Lab., de deelnemers aan het thermocompressie project, en de vele anderen die mij bij het schrijven van dit proefschrift geholpen hebben.

Monique, bedankt voor al het typewerk, het maken van de omslag en enige tekeningen, en met name voor al het geduld dat je hebt opgebracht, en de tijd die je mij gegund hebt bij het 'promofileren'.

***Stellingen***

*behorende bij het proefschrift*

***Constitutive Equations for Metals  
with an Application to the  
Extrusion of Lead***

*van*

***Hans van Wijngaarden***

1. De thermodynamische theorie met verborgen variabelen is een krachtig hulpmiddel bij het afleiden van constitutieve vergelijkingen.
  - hoofdstuk 2 van dit proefschrift
  - S.R.de Groot en P. Mazur - Non-Equilibrium Thermodynamics - North Holland Publishing Company (1962)
2. In de kinematica is de gradient van de snelheid de som van de symmetrische deformatiesnelheidstensor en de anti-symmetrische spintensor. De interpretatie van deze tensoren als een directe maat voor de verandering van de deformatie respectievelijk de rotatie van het materiaal is onjuist en kan leiden tot foutieve materiaal beschrijvingen.
  - J.C. Nagtegaal en F.E. Veldpaus - Analysis of metal forming problems with an improved finite strain plasticity formulation - Numerical Methods in Industrial Forming Processes, Ed. Pittman, Wood, Alexander and Zienkiewicz, Pineridge Press, Swansea, UK (1982)
3. De afschuifproef is een onzinnige test voor het bepalen van de te gebruiken objectieve tensor afgeleide in het geval van elasticiteit en kinematische versterking.
  - S.A. Atluri - On the constitutive relationship at finite strain: hypo-elasticity and elasto-plasticity with isotropic or kinematical hardening - Comp. Meth. in Appl. Mech. and Eng., Vol 43 (1984)
4. Voor het juist kunnen beschrijven van kinematische versterking is een beter fysisch inzicht nodig in dit fenomeen. Dit inzicht kan verkregen worden door het doen van gerichte experimenten.
  - E.H. Lee, R.L. Mallet and T.B. Wertheimer - Stress analysis for anisotropic hardening in finite deformation plasticity - J. of Appl. Mech., Vol 50 (1983)
5. Menig commercieel eindig elementen pakket zou kwalitatief sterk verbeteren als aan de elementen bibliotheek het 'bubble'-element zou worden toegevoegd.
  - hoofdstuk 5 van dit proefschrift



6. Eindige elementen en differentie methoden zijn er enkel en alleen voor het oplossen van integraal en differentiaal vergelijkingen. Vele fysische interpretaties van deze methoden zijn dan ook niet relevant en vaak verwarrend.
  - J. Blaauwendraat en A.W.M. Kok - Elementenmethode - Agon Elsevier, (1973)
7. Wetenschapsbeoefening krijgt een toenemend analytisch en daardoor projectmatig karakter. De interne organisatie van wetenschappelijke instellingen dient hierop aangepast te worden.
  - G. Holst - De tien geboden van het Nat.Lab. - NRC-Handelsblad, (12 juni 1985)
8. Het groepsresultaat, dat door goede interne samenwerking in positieve zin beïnvloed wordt, is in de praktijk vaak belangrijker dan het individuele resultaat. Naast formele individuele beoordelingen in bijvoorbeeld het onderwijs en het bedrijfsleven dienen groepsbeoordelingen daarom (veel vaker) toegepast te worden.
9. De ware informaticus herkent men aan zijn bureau.
10. In het ziekenhuis ben je gezegend met een non als afdelingshoofd.